Zeitschrift: IABSE reports = Rapports AIPC = IVBH Berichte
Band: 57/1/57/2 (1989)

Rubrik: Poster Session 2

POSTERS

Leere Seite
Blank page
Page vide

Zur Zeitfestigkeit der Verdübelung bei Verbundträgern mit Profilblechen

Fatigue Strength of Headed Stud Connections for Composite Beams with Profiled Steel Sheeting

Résistance à la fatigue des goujons dans des structures mixtes

H. BODE
Prof. Dr. -Ing.
Universität Kaiserslautern
Kaiserslautern, BR Deutschland

J. KRETZ
Dipl. -Ing.
Universität Kaiserslautern
Kaiserslautern, BR Deutschland

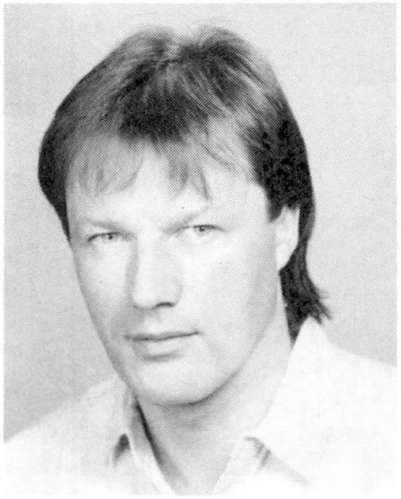

ZUSAMMENFASSUNG

Dieser Beitrag beschäftigt sich mit dem Trägerverbund zwischen Betongurten und Stahlträgern, der durch Verwendung von Stahlprofilblechen beeinflusst wird. Die Untersuchungen betreffen die Tragfähigkeit der Verdübelung unter nicht ruhender oder dynamischer Belastung. Die günstigen Zeitfestigkeiten bei Verwendung von Profilblechen lassen für Verbundträger einen grösseren Anwendungsbereich im Industriebau erwarten.

SUMMARY

This paper deals with the composite action between concrete flanges and steel sections, which is influenced by the use of profiled steel sheetings. The study concerns the connector strength in case of dynamic loading. The relatively high fatigue strengths even in case of profiled steel sheetings crossing the steel section form the basis for a wider use of composite beams for industrial buildings.

RÉSUMÉ

Cet article traite de la liaison entre la section de béton et la poutre métallique. Cette liaison est influencée par l'emploi de tôles profilées. Les essais concernent la résistance des goujons sous charge mobile ou dynamique. L'effet favorable de l'emploi de tôles sur la résistance à la fatigue de la structure mixte permet d'en prévoir une plus grande utilisation dans les bâtiments industriels.

1. TRÄGERVERBUND, DYNAMISCHE FESTIGKEIT

1.1. Allgemeines

Verbundträger und Verbunddeckenkonstruktionen im Industriebau werden nicht immer nur vorwiegend ruhend belastet. Oft treten nicht vorwiegend ruhende Belastungen auf, z. B. aus Gabelstaplerbetrieb, bei Kranbahnen, bei Hänge- und anderen Fördersystemen. Auch stoßartige Belastungen können auftreten.

An der Universität Kaiserslautern wurden 21 Versuche mit dynamischer Einstufenbelastung durchgeführt. Sie waren vom DASt und der AIF gefördert und finanziell unterstützt worden /7/. Die Untersuchungen wurden im Zeitfestigkeitsbereich bei Lastspielzahlen um 100.000 und mit einer hohen Ausnutzung der Verbundmittel bis zu 82 % der tatsächlichen statischen Festigkeit durchgeführt. Dies trägt der hohen Dübelbeanspruchung im Gebrauchszustand bei plastischer Bemessung im Hoch- und Industriebau Rechnung. Im einzelnen handelt es sich um
- 6 Trägerversuche und
- 15 Scherversuche.

1.2 Scherversuche

Für die Scherversuche wurden Versuchskörper nach Bild 1 verwendet.

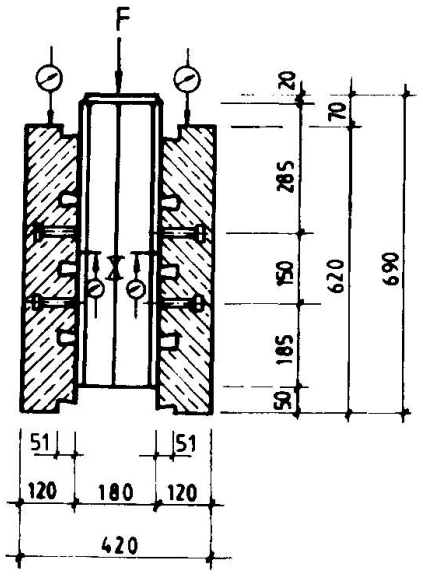

Bild 1: Scherversuchskörper

Die Darstellung in Bild 2 zeigt die auch für die anderen Scherversuche typische Zunahme der Relativverschiebungen zwischen Betongurt und Stahlprofil mit der Lastspielzahl N beim Versuch S 2/5.

Zu Beginn der Versuche betrug der Anfangsschlupf 1.1 mm, dann erfolgte der Bereich stabilen Schlupfwachstums, in dem der Beton vor dem Dübelfuß wegen der konzentrierten Belastung langsam zerstört wurde. Von etwa 10^6 Lastspielen an nahmen die Relativverschiebungen überproportional zu, bis der Bruch der Bolzen oberhalb des Schweißwulstes eintrat.

Um die Wöhlerlinie, die bei doppeltlogarithmischer Auftragung näherungsweise eine Gerade darstellt, zu erhalten,werden die Spannungsdifferenzen und Lastspielzahlen bis zum Bruch aufgetragen und statistisch ausgewertet. Die Neigung der

Wöhlerlinie wird durch den aus den Versuchen berechneten Exponenten k = 8,26 bestimmt und beträgt 1/k.

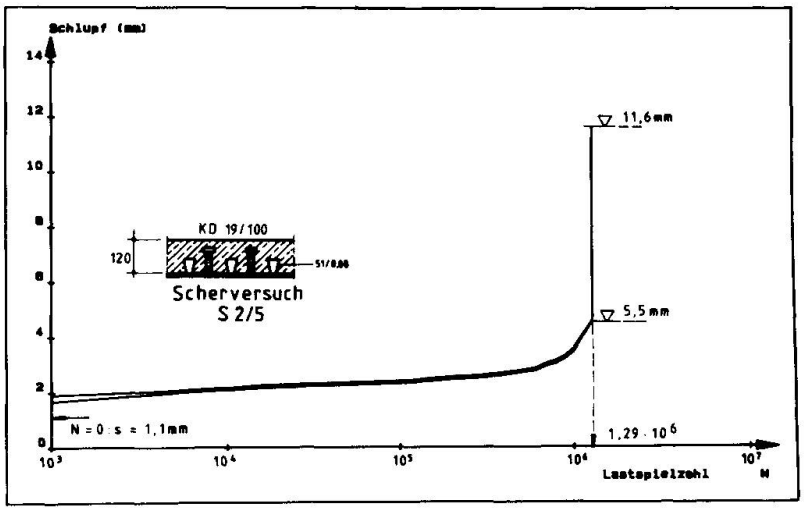

Bild 2: Schlupf im Versuch S 2/5

Im Dübel und in seiner Umgebung stellt sich ein komplexes Kräftespiel ein, was nur global durch ΔD_S oder durch eine Schubspannungsdoppelamplitude $\Delta\tau$ im Bolzenschaft als Maß für die Höhe der Beanspruchung erfaßt werden soll.

Im Vergleich zu den Bochumer Versuchen von Roik /3, 5/ mit massiven Vollplatten liegen die hier mit Profilblechen ermittelten Zeitfestigkeiten niedriger, und zwar um etwa 18 %. Diese Reduktion muß man aber im Zusammenhang mit der statischen Dübeltragfähigkeit sehen, die bei Holoribblechen um ca. 3O % niedriger liegt als bei massiven Vollplatten. Die Kopfbolzendübel verhalten sich - trotz der sehr hohen Ausnutzung der Dübel - in Verbindung mit Profilblechen unter dynamischer Belastung vergleichweise günstiger als bei statischer Beanspruchung.

1.3 Trägerversuche

Trägerversuche haben den Vorteil, daß Betongurt, Dübelzone, Dübel, Schweißung und Stahlträger wie bei einem tatsächlichen Träger wirklichkeitsnah beansprucht werden können. Das gilt in besonderem Maße für die gleichzeitige Beanspruchung von Dübelfuß und Stahlflansch durch Dübelkräfte und Gurtspannungen.

Neben dem Probelm, mit wenigen Trägerversuchen zu statistisch aussagekräftigen Ergebnissen zu gelangen, besteht die Schwierigkeit vor allem in der Ermittlung der tatsächlich auftretenden Dübelkräfte, da diese sich nicht direkt messen lassen. Sie werden deshalb zunächst auf der Grundlage des elastischen Schubflusses mit Hilfe der Q·S/I-Formel berechnet. Zusätzlich wird jedoch eine Versuchssimulation mit einem leistungsfähigen Computerprogramm durchgeführt, welches die nichtlineare Trägeranalyse einschließlich der Nachgiebigkeit der Verdübelung berücksichtigt. Damit kann insbesondere gezeigt werden, daß die Rückrechnung von Dübelkräften über starren Trägerverbund im allgemeinen fehlerhaft ist.

Weiterhin zeigt sich, daß sich durch diese Korrektur der Dübelkräfte, wie sie mit Hilfe der Q·S/I-Formel ermittelt worden sind, die Ergebnisse von Scher- und Trägerversuchen deutlich angleichen lassen.

Bild 3 enthält den Versuchsträger T2/2 der Serie 2 mit Betongurt in der Zugzone. Die drei Träger der Serie T1 waren gleich ausgebildet, aber so angeordnet und belastet, daß der Betongurt in der Druckzone lag. Das Bild enthält auch die Lage der Meßstellen (DMS und Wegaufnehmer).

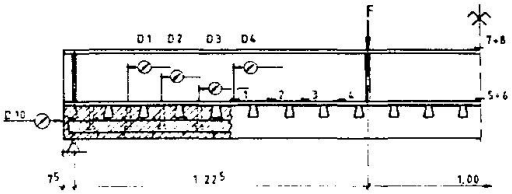

Bild 3: Versuchsträger T2/2

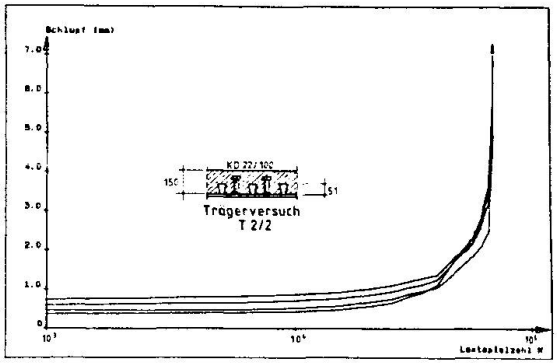

Bild 4: Trägerversuch T2/2; Schlupf bei Oberlast

In Bild 4 wird die Vergrößerung der Relativverschiebung bis zum Bruch gezeigt, während Bild 5 die entsprechenden Dehnungsverläufe wiedergibt.

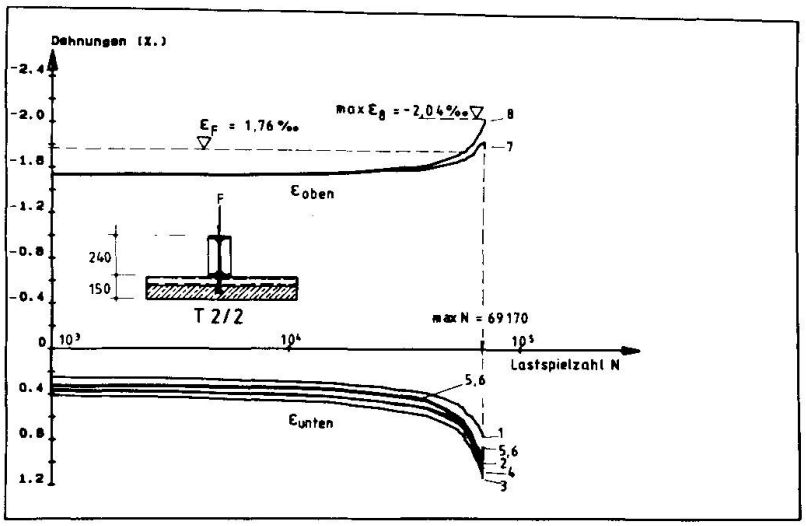

Bild 5: Trägerversuch T2/2; Dehnungen bei Oberlast

Aus diesen Last-Schlupf-Verläufen sieht man, daß die Verdübelung mit der Lastspielzahl N weicher wird. Auch die hier dargestellten Stahlträger-Randdehnungen lassen das erkennen. Infolge der abnehmenden Dübelsteifigkeit wird das Zusammenwirken unvollständiger. Insbesondere nimmt die Biegebeanspruchung im Stahlträger zu, und die vormals elastischen Dehnungen überschreiten die elastische Streckgrenze. Das bedeutet gleichzeitig, daß die wirklichen Dübelkräfte mit der Zeit kleiner werden. Tatsächlich liegt damit nun keine reine Einstufenbelastung der Dübel mehr vor.

Mit dem o. g. Rechenprogramm /6/ wurden dann die rein statischen Vergleichsberechnungen durchgeführt, deren Ergebnisse in den Bildern 6 und 7 dargestellt sind.

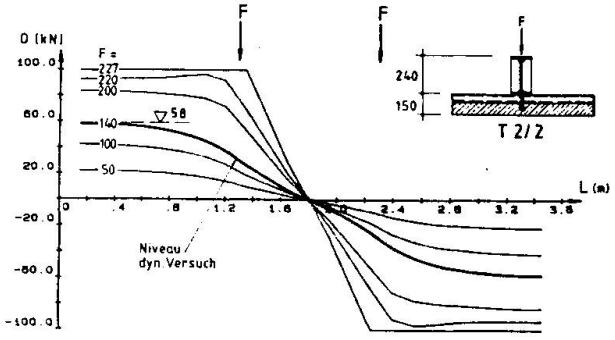

Bild 6: Verlauf der Dübelkräfte

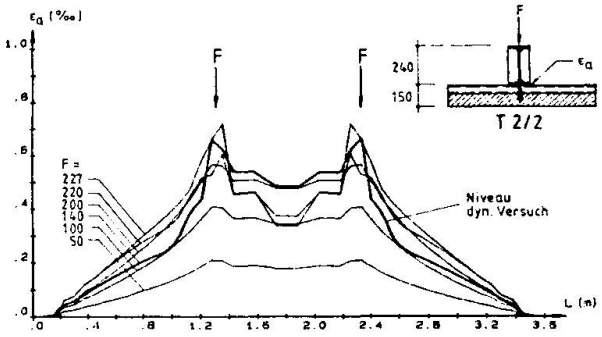

Bild 7: Verlauf der Stahldehnungen

In Bild 6 sind die berechneten Dübelkraftverläufe unter statischer Last bis zur rechnerischen Traglast dargestellt. Auch im mittleren Trägerbereich, in dem die Gesamtquerkraft gleich null ist, treten Dübelkräfte auf.

Die Q·S/I-Formel für starren Verbund bei linear elastischem Verhalten sowie Beton im Zustand I würde den Maximalwert 73 kN ergeben. Infolge des unvollständigen Zusammenwirkens sind die Dübelkräfte mit D_S = 58 kN deutlich kleiner als die mit starrem Verbund berechneten:

Zustand I: Reduktion von 73 auf 58 kN (79 %)
Zustand II: Reduktion von 67,5 auf 58 kN (86 %)

Tatsächlich nehmen die Dübelkräfte außerdem mit der Lastspielzahl ab. Deshalb sind hier über die MINER-Regel schädigungsgleiche Dübelkräfte berechnet. Dadurch ergibt sich eine weitere Reduktion der vergleichbaren Dübelbeanspruchung, und zwar im Fall des Trägers T2/2 von 58 auf 54 kN.

Die Ergebnisse der Trägerversuche sind im Bild 8 in das Diagramm der Scherversuche eingetragen.

Ohne Berücksichtigung der Nachgiebigkeit der Verdübelung liegen die Werte deutlich über dem Streuband der Scherversuche: Trägerversuche scheinen günstigere Ergebnisse zu liefern! Wir haben jedoch gerade zeigen können, wie wir bei der Auswertung des Trägerversuches T2/2 die Nachgiebigkeit rechnerisch berücksichtigt haben.

Bei Versuch T2/2 führt die dadurch verursachte Reduktion um insgesamt 26 % auf eine Lage im Streuband, dasselbe gilt für T1/3 und vermutlich auch für alle anderen Trägerversuche: richtig ausgewertet, werden die Ergebnisse von Scher- und Trägerversuchen wieder miteinander vergleichbar.

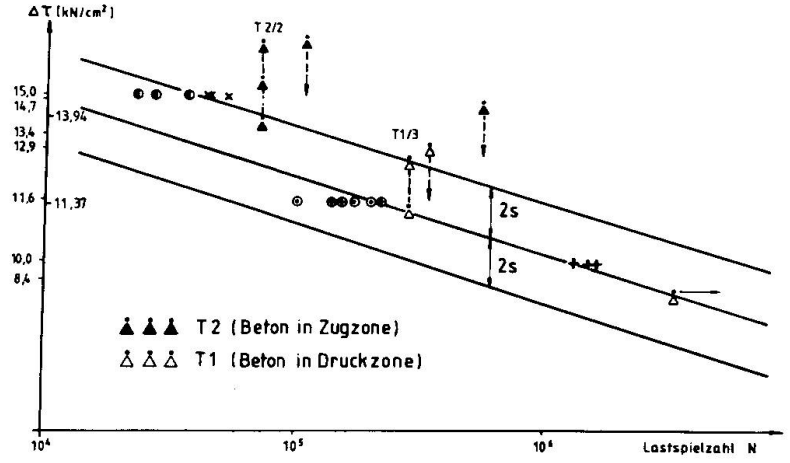

Bild 8: Zeitfestigkeiten der Scher- und Trägerversuche

1.4 Literaturhinweise

/1/ Richtlinien für die Bemessung von Stahlverbundträgern

/2/ H. Bode, R. Künzel: Zur Verwendung von Profilblechen beim Trägerverbund Festschrift Baehre, Karlsruhe 1988

/3/ K. Roik, H.-J. Holtkamp: Untersuchungen zur Dauer- und Betriebsfestigkeit der Verdübelung von Verbundträgern mit Hilfe von Kopfbolzendübeln. Studiengesellschaft für Anwendungstechnik von Eisen und Stahl, P 1O1, Düsseldorf 1986

/4/ R. P. Johnson, R. J. Buckby: Composite structures of steel and concrete. Vol. 2, London 1979

/5/ K. Roik, G. Hanswille: Zur Dauerfestigkeit von Kopfbolzen dübeln bei Verbundträgern Bauingenieur 62/1987

/6/ J. Schanzenbach: NG-Verbund-Programm zur physikalisch nichtlinearen Berechnung von Verbunddurchlaufträgern mit nachgiebiger Verdübelung. Universität Kaiserslautern, 1988

/7/ H. Bode, J. Kretz: Trägerverbund im Industriebau unter nicht ruhender Belastung bei Verwendung von Profilblechen. DASt/AIF-Forschungsbericht (unveröffentlicht), Kaiserslautern 1988

Strength of Freeze-Thaw Deteriorated Concrete

Résistance du béton détérioré par des cycles gel-dégel

Festigkeit von durch Frost und Auftauen beanspruchtem Beton

Jesper KRUS
Civil Eng.
Royal Inst. of Technology
Stockholm, Sweden

Jesper Krus, born 1961, graduated as a Master of Sicence in Civil Engineering at the Royal Institute of Technology in Stockholm in 1987, since then he has been studying for a doctorate at the Dep. of Structural Engineering.

SUMMARY

Tests have been performed in which drilled-out concrete cores were first subjected to an environmental load in the form of freezing-thawing and then to a functional load in the form of a fatigue or static failure load. The aim was to study the combined influence of the deterioration factors on the strength of concrete. Measured results show that a concrete without entrained air which freezes in pure water shows no appreciable loss of strength. In contrast, if salt is present in freezing medium, strength degradation of up to 50 per cent can occur very quickly.

RÉSUMÉ

Des carottes de béton prélevées par forage ont été soumises à des contraintes dues au gel et dégel, puis à des contraintes physiques, sous forme d'essais de fatigue ou statiques, l'objet étant d'étudier l'influence combinée de ces facteurs de décomposition sur la résistance du matériau. Ces essais on montré qu'un béton sans adjonction d'air, qui gèle dans de l'eau pure, ne perd que très peu de sa résistance. Par contre, si le liquide contient du sel, on note une dégradation rapide de la résistance.

ZUSAMMENFASSUNG

Es wurden Versuche an Betonbohrkernen durchgeführt, welche nach einer umweltmässigen Beanspruchung in Form von Einfrieren/Auftauen einer funktionsbedingten Beanpruchung (Ermüdungs- oder Bruchbeanspruchung) ausgesetzt wurden. Ziel war, die kombinierte Einwirkung dieser Zerstörungsfaktoren auf die Festigkeit des Betons zu untersuchen. Die Ergebnisse zeigen, dass die Festigkeit von in sauberem Wasser eingefrorenem Beton ohne Luftzusatz kaum nennenswert nachlässt. In einem Medium mit Salz hingegen kann sich die Festigkeit sehr schnell um bis zu 50% verschlechtern.

1. BACKGROUND

In the survey by Ingvarsson & Westerberg [1], it emerged that the interaction between environmentally and functionally caused deterioration was a subject on which research was considered a matter of importance. In the first instance, this concerned the problem area of fatiguing of salt- and frost-damaged concrete and fatiguing of concrete with embedded, corroded reinforcement steel. As a continuation, tests on the strength and fatigue properties of freeze-thaw deteriorated concrete have been carried out on behalf of the Swedish National Road Administration and the Swedish Transport Research Board. These tests are reported below.

2. TESTS

2.1 Test specimens

The purpose of the tests was to reflect the combined effect of environmentally caused and functionally caused degradation factors and how this effect varies with different concrete mixes. To this end, tests were carried out according to Fig. 1 in three subseries. These were:

I W/C = 0.60, without air entrainment
II W/C = 0.50, without air entrainment
III W/C = 0.50, with approx. 8 % entrained air

In all cases, use was made of pure standard Portland cement and an aggregate with a maximum size of 16 mm. The weight ratio cement:gravel:stone was 1:3.5:1.4 in series I, 1:2.3:1.7 in series II and 1:2.1:1.6 in series III.

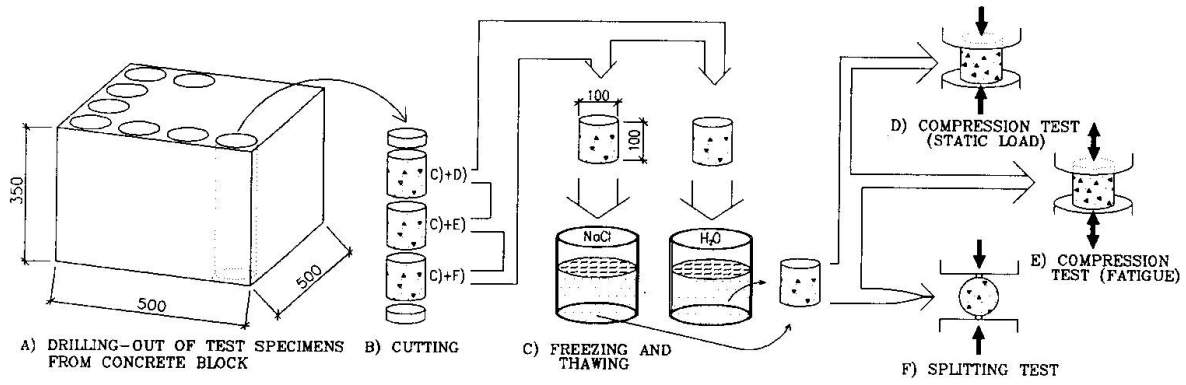

Fig. 1: Test procedure

Cores with a diameter of 100 mm were drilled out of specially cast concrete blocks. The cores were cut into three cylinders with lengths of 100 mm, see Fig. 1:A and 1:B. Each subseries comprised 54 concrete cylinders.

2.2 Environmental load

Half the number of cylinders were frozen in water and half the number in a 3 per cent sodium chloride (NaCl) solution. The 54 cylinders were divided into 9 groups exposed to 0, 7, 14, 28 or 56 freeze-thaw cycles, with or without NaCl in the freezing medium, see Fig. 1:C. After

being cast the cylinders were kept continuously moist, until freeze-loading.

2.3 Functional load

After being subjected to freezing and thawing, the strengths and fatigue properties of the concrete cylinders were tested by means of a static load test until failure in compression (Fig. 1:D), a fatigue test (Fig. 1:E) and a splitting test (Fig. 1:F).

3. TEST RESULTS

3.1 Static load tests

3.1.1 Compressive strength

The static load tests to compression failure were conducted with a constant velocity of 5 μm/sec. The results from these tests formed the basis for the load levels used in the fatigue tests, see Section 3.2 below. The ultimate stresses measured in the static load tests are shown in Fig. 2.

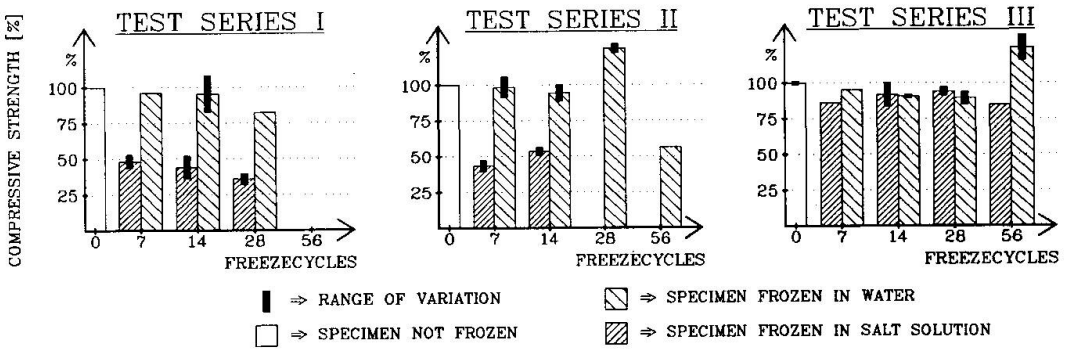

Fig. 2: Results of static compressive strength tests

The measured ultimate compressive strengths of the cylinders are shown in Fig. 2 for the different subseries I, II and III. The results are presented as mean values for each group. The columns are grouped two by two according to the number of freeze cycles. The left-hand columns show the values for the NaCl-frozen cylinders and the right-hand columns those of the water-frozen cylinders. The thick line at the top shows the range of variation for the compressive strength of all cylinders in the group. In some freeze groups one or both columns are missing, the reason being that the specimens did not withstand the freeze-thaw cycles. Cylinders which had passed the fatigue test without rupturing and then were loaded statically to failure are not included in the results shown in Fig. 2.

It is evident from the results that the ultimate compressive strength rapidly decreases on freezing in NaCl solution, if the concrete does not contain an air-entraining admixture. From series I and II it can be concluded that the ultimate strength has fallen to approx. 50 per cent of the original value. On the other hand, the ultimate strength is very good in series III where entrained air was added to the concrete. Measured strengths and deformations also indicated that the moduli of elasticity decreased upon freezing in both water and salt solution. This was valid for all subseries I, II and III.

An interesting observation that can be made is that those strength values which have decreased

at only seven freeze cycles tend to become stabilized at this level, or occasionally even to increase slightly again. See Fig. 2.

3.1.2 Splitting strength

It is evident from the results of splitting tests, as presented in Fig. 3, that the tensile strength of the concrete, as well as its compressive strength, is considerable decreased when the concrete freezes in the presence of NaCl. This applies, according to Fig. 3, in the first instance to subseries I and II where the concrete did not contain entrained air. The results from subseries III instead indicates an increasing splitting strength, probably due to deviations in the concrete itself. Also in series III the strengths of the NaCl-frozen cylinders are slightly inferior.

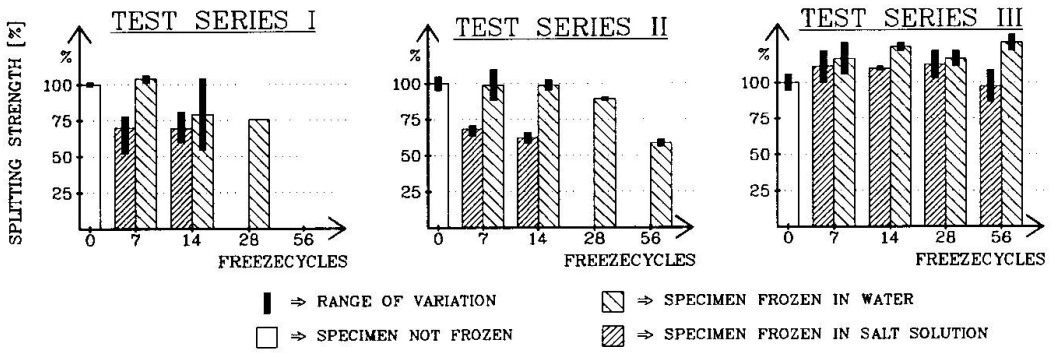

Fig. 3: Results of splitting tests. Designation as per Fig. 2

3.2 Fatigue test

The fatigue tests were performed with a compressive load frequency of 7 Hz at night and 15 Hz during the day. The fatigue test results observed are presented in Fig. 4.

In Fig. 4, σ is used for the maximum stress to which the cylinder was exposed in each load cycle, while f_u designate the ultimate compressive stress measured at the static load tests, see section 3.1.1 above. In each load cycle, the load was varied between 0 and σ. In the diagrams of Fig. 4, the Wöhler curve according to Bennet & Muir [2] is shown in order to make a comparison possible. From this it can be concluded that the fatigue properties of the concrete are affected by freezing and thawing irrespective of whether the freezing medium was provided with NaCl or not. This conclusion is valid for concrete without air entrainment only. With respect to fatigue, concrete cylinders with air entrainment, series III, were not affected at all. These results are somewhat confusing, as they do not correspond to those obtained by Antrim & Mc Laughlin [3]. In this reference concrete cylinders both with and without entrained air are subjected to fatigue. No significant differences in fatigue resistance were detected.

For the cylinders which had not ruptured at $2 \cdot 10^6$ load cycles, the tests were discontinued. Insted these cylinders, which are not included in Fig. 4, were loaded to either static compressive or splitting failure. These cylinders normally showed a higher compressive and lower splitting strength than those not fatigue tested. This tendency however, was not discernible throughout. An explanation may be that these cylinders did not rupture by fatigue due to their high compressive strength. On the contrary, internal cracking due to the fatigue load caused a decrease in splitting strength, i.e. tensile strength.

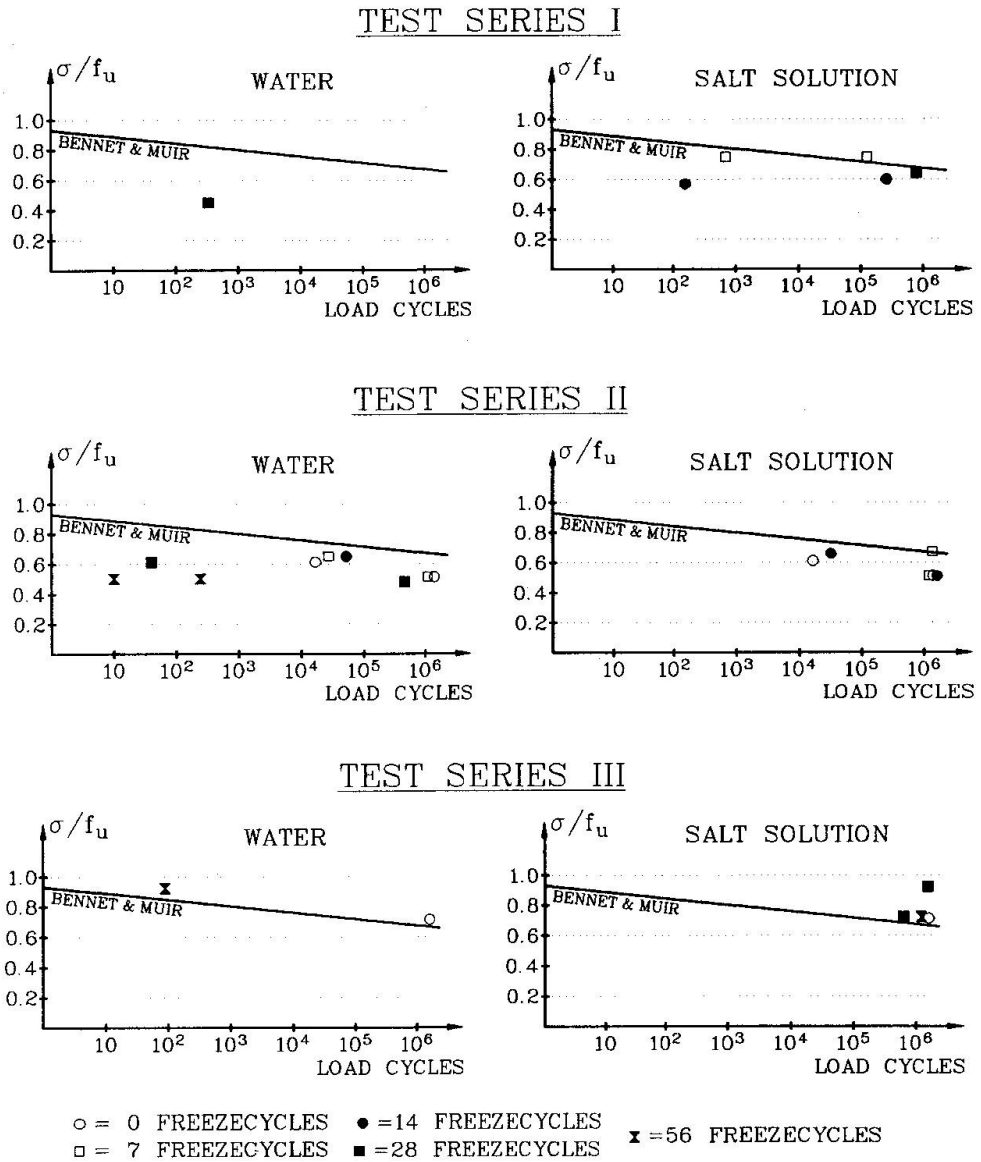

Fig. 4: Results of fatigue tests, series I, II and III

4. CONCLUSIONS

The conclusions from the tests can be summarized as follows:

1. Concrete which freezes in pure water retains its strength properties well.
2. Concrete which freezes in the presence of NaCl very quickly loses its strength properties, unless air is entrained. The strength properties which decrease directly upon freezing in salt solution tend to become stabilized after a small number of freeze cycles.
3. Concrete which freezes in pure water or in salt solution loses some of its fatigue resistance. However, if air is entrained the resistance retains.

Older concrete structures which have regularly been exposed to de-icing salts or seawater may now have deteriorated, resulting in a considerably inferior concrete strength and decreased fatigue resistance. In determining the load-carrying capacity of older structures it is therefore essential to drill cores and to examine the strength and fatigue properties of these. It is thus a doubtful procedure to recalculate older structures in accordance with new codes on the basis of the strength which the concrete had when the structure was built, taking for granted that this strength is retained.

5. FUTURE WORK

In addition to the test series described above, the interaction between functionally and environmentally caused load impacts will be studied. The planned work will embrace both mild (non-tensioned) reinforced concrete beams and prestressed concrete beams. The beams will be exposed either to freeze-thaw cycles or to corrosion of the reinforcement. This will be accomplished by giving the reinforcement a positive electric potential in relation to the concrete. By this means, chlorides will be led in towards the reinforcement and the reinforcement will corrode. When the beams have been exposed to this environmental load, they will be subjected to a functional load in the form of a static load test to failure or a fatigue test.

6. REFERENCES

1. INGVARSSON H., WESTERBERG B., 1986, Operation and maintenance of bridges and other bearing structures, Publ. No. 42 from the Swedish Transport Research Board, Stockholm, Sweden, ISSN 0282-8022.
2. BENNET E. W., MUIR S. E. St J., 1967, Some fatigue tests of high-strength concrete in axial compression, Magazine of concrete research, Vol. 19, No 59, pp 113-117.
3. ANTRIM, J. C. and Mc LAUGHLIN, J. F., 1959, Fatigue study of air-entrained concrete. ACI Journal, May, pp 1173-1182.

Crack Widths and Deformation Behavior of Reinforced Concrete Structures

Largeur de fissures et comportement en déformation de structures en béton armé

Rissbreiten und Verformungsverhalten von Stahlbetontragwerken

Gerd GÜNTHER
Gesamthochschule Kassel
Fachgebiet Massivbau
Kassel, Fed. Rep. of Germany

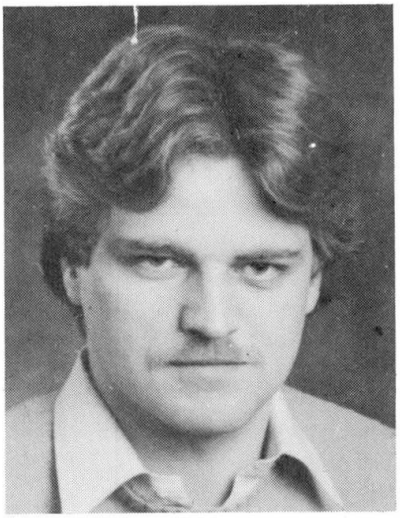

Gerd Günther, born in 1957, 1985 Dipl.-Ing., University of Kassel since 1985 Assistant in the Division of Reinforced Concrete of the University of Kassel.

Gerhard MEHLHORN
Gesamthochschule Kassel
Fachgebiet Massivbau
Kassel, Fed. Rep. of Germany

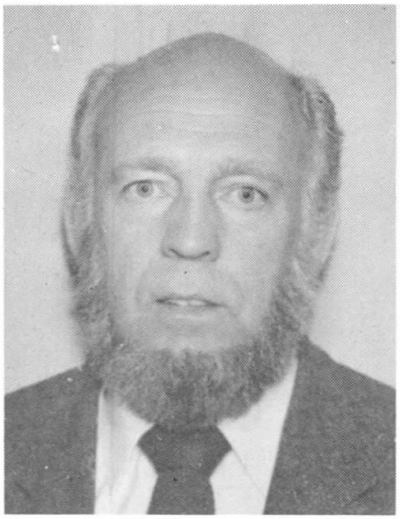

Gerhard Mehlhorn, born in 1932, apprenticeship as steel construction worker, 1959 Dipl.-Ing., TH Dresden, 1959-1965 Design Engineer, 1965-1983 TH Darmstadt, Dr.-Ing. 1970, since 1972 Professor of Civil Engineering, 1982 Visiting Professor University of Toronto, since 1983 Professor of Civil Engineering at University of Kassel, since 1984 also Consulting Engineer at Kassel (until 1984 at Darmstadt).

SUMMARY

In this contribution the results of tests are shown. With the tests the increase of crack widths and deformations in dependence on load duration and number of load cycles was investigated. Especially considered are the consequences of the initial stress state caused by shrinkage on the crack width development. Besides simple tension and bending tests biaxial compression-tension tests were also carried out on reinforced concrete panels.

RÉSUMÉ

Gracê à des essais, l'augmentation des largeurs de fissures et des déformations dépendant de la durée et de la valeur de la charge devait être clarifiée. Les conséquences de l'état d'auto-contraintes créé par le retrait sur l'évolution des largeurs de fissures sont prises en considération. Outre les essais de traction et de flexion, des essais biaxiaux compression-traction on été réalisés.

ZUSAMMENFASSUNG

Mit Versuchen sollte geklärt werden, wie gross die Verformungs- und Rissbreitenzunahmen in Abhängigkeit von der Belastungsdauer und der Anzahl der Lastwiederholungen sind. Die Auswirkungen des durch Schwinden verursachten Eigenspannungszustandes auf die Rissbreitenentwicklung wurden besonders berücksichtigt. Neben den reinen Zug- und Biegeversuchen wurden auch biaxiale Druck-Zugversuche an Stahlbetonscheiben durchgeführt.

1. INTRODUCTION

The durability of reinforced concrete structures mainly depends on crack widths and deformations. The protection against corrosion of the reinforcement is lost when crack widths are large and the stability is endangered. With too large deformation increases owing to long-term loads considerable usage restrictions of the building may result. In this contribution the results of about 120 tests on crack spacing, crack widths, and deformation behavior of reinforced concrete structures under monotonically increasing, cyclic, and long-term loads are presented.

2. CRACK SPACINGS

The average and maximum crack spacings of the reinforced concrete panels [1, 2], the centrically and eccentrically reinforced tension specimens [3, 4, 5], and the reinforced concrete beams [6] are presented in table 1. A dependence of the crack spacing on the concrete compressive strength and on the related rib area was not observed.

Owing to repeated loads and permanent loads no new cracks occured (not considering a few exceptions) with constant top load. As a result of unintentional eccentricities with the regularly and centrically reinforced tension specimens the cracks separated the concrete only partially at initial loading. Thus, the cracks still developed with repeated and permanent loads.

The crack development which occured with the eccentrically reinforced tension specimens (see Fig. 3) and the reinforced concrete beams are to be traced back to the decrease of concrete tensile strength owing to repeated loads.

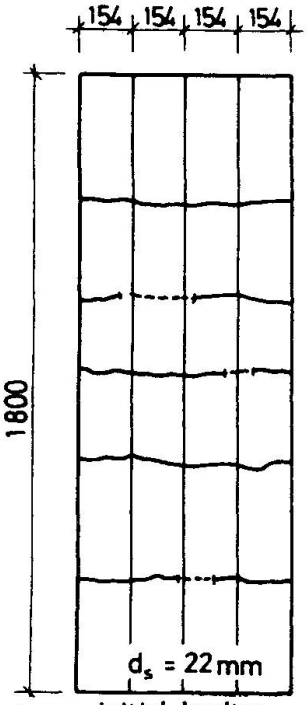

——— initial loading
----- as a result of repeated loads

Fig. 1 Crack pattern of intended centrically reinforced specimen S 22

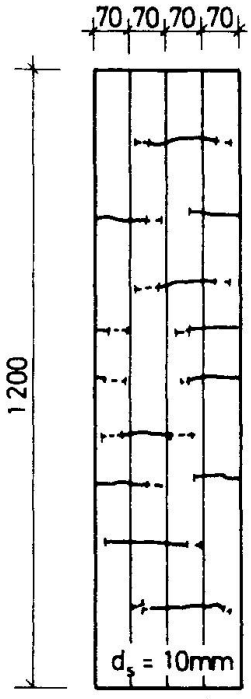

——— initial loading
----- after permanent load of 144 days

Fig. 2 Crack pattern of intended centrically reinforced specimen DAUER 4

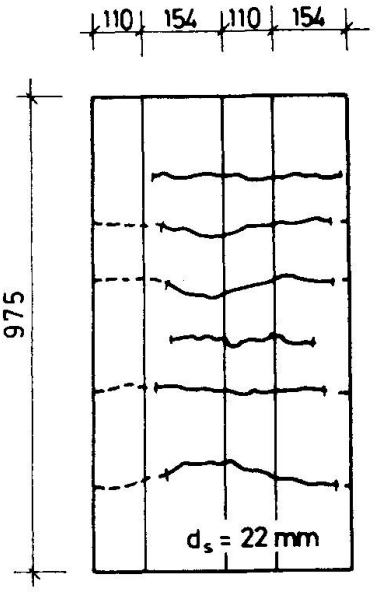

——— initial loading
----- as a result of repeated loads

Fig. 3 Crack pattern of eccentrically reinforced specimen E 11

In the crack patterns of the reinforced concrete panels [2] without transverse compression (see Fig. 4) and with 0,6 β_c transverse compression (see Fig. 5) no dependence of the amount of cracks on transverse compression can be seen.

Specimen		d_s [mm]	ü [mm]	s [mm]	reinforcement	number of specimens	crack spacing [mm] a_m	crack spacing [mm] a_{max}	calculated average crack spacing [mm] $a_m = 2\,(ü + 0{,}1 \cdot s) + 0{,}1\,\frac{d_s}{\mu}$	calculated average crack spacing [mm] $1{,}7 \cdot a_m$
reinforced concrete panels	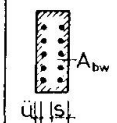	10x8,S	10	50	ribbed bars with transverse reinforcement	2	134	185	105	178
					ribbed bars	5	136	200		
					ribbed mats	2	107	150		
		10x5,5	11	50	ribbed bars with transverse reinforcement	2	126	200	147	249
					ribbed bars	2	103	200		
					ribbed mats	1	102	125		
	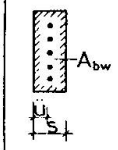	5x16,0	42	100	ribbed bars	2	140	250	183	311
centrically reinforced tension specimens	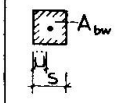	1x10,0	30	70	ribbed bars	10	128	210	135	230
		1x10,0	40	90		2	127	220	200	340
		1x16,0	32	80		3	115	160	131	223
		1x16,0	48	112		2	183	240	219	372
		1x16,0	64	144		2	333	390	322	547
		1x22,0	44	110		20	174	310	180	306
		1x22,0	66	154		27	290	450	300	511
		1x22,0	88	198		16	359	630	442	752
		1x28,0	56	140		2	200	300	229	390
		1x28,0	84	196		2	333	450	382	650
		1x28,0	112	252		2	417	530	563	957
excentrically reinforced tension specimens	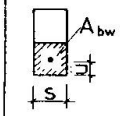	1x22,0	44	110	ribbed bars	8	156	280	180	306
		1x22,0	66	154		4	285	425	300	511
reinforced concrete beams	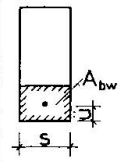	1x22,0	44	150	ribbed bars	3	244	300	214	363
	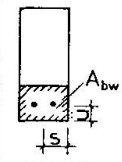	2x22,0	44	75	ribbed bars	2	162	250	151	256
	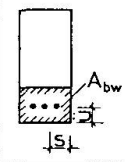	3x22,0	44	54	ribbed bars	2	113	185	131	223

Tab. 1 Crack Spacings

In accordance with the approach in the CEB/FIP requirements [7] for the calculation of the average crack spacing a_m the following equation resulted for ribbed bars and mats:

$$a_m = 2\,(ü + k \cdot s) + 0{,}1\,\frac{d_s}{\mu}\,; \qquad k = 0{,}1 \text{ for ribbed bars}$$

This yields a satisfactory agreement with the experimentally determined crack spacings (see table 1) for design of buildings. The effective zone of the reinforcement was established as in Fig. 6 according to Gergely and Lutz [8] as with the eccentrically reinforced tension specimens no dependence of the crack spacing on the height of the specimen was stated.

Furthermore a differentiation between tensile and flexural load could be neglected with respect to the CEB/FIP requirements so that it can generally be calculated with k = 0,1 for ribbed bars. The average crack spacings multiplied by 1.7 are in approximate accordance with the largest crack spacings of the experiment (see table 1).

With smooth mats the bond strength is generally transferred by the transverse reinforcement only. Cracks always form at the transverse reinforcement because of the smaller concrete cross section in this area. Forces can be transferred into the concrete until only two transverse reinforcement bars are left between two cracks. Thus the maximum crack spacing corresponds to the double spacing of transverse reinforcement. With this spacing only one transverse reinforcement bar is left between two cracks and no more forces can be introduced into the concrete.

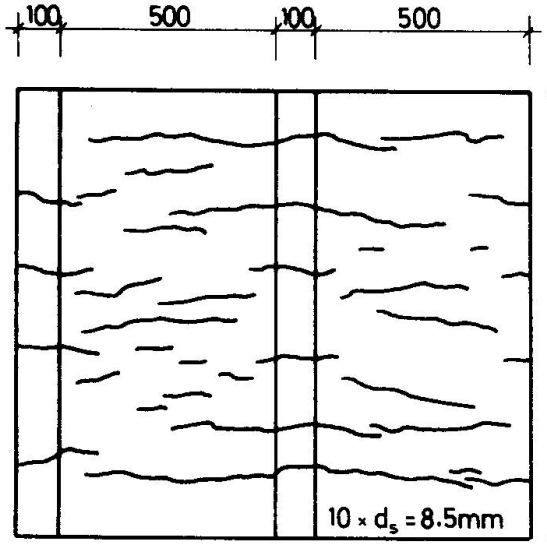

Fig. 4 Crack pattern of reinforced concrete panel B 19 (Q = 0)

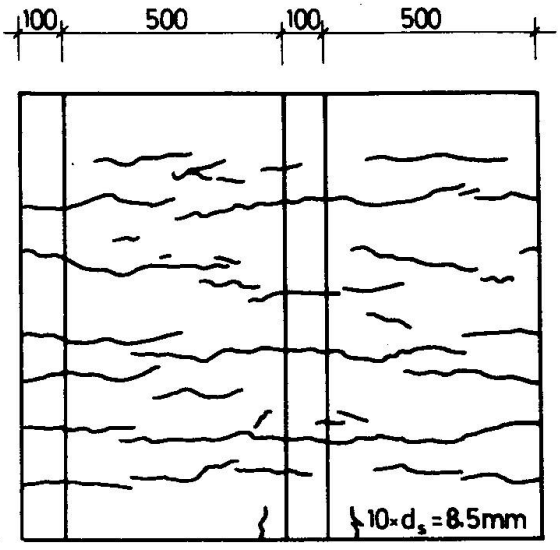

Fig. 5 Crack pattern of reinforced concrete panel B 11 (Q = 0,6 β_c)

3. CRACK SPACINGS

It was shown in [4] that the deformations of a reinforced concrete specimen mainly occur in the cracks and that the average crack w_m widths can be calculated with the equation stated in [7]:

$$w_m = \varepsilon_m \cdot a_m. \tag{2}$$

The maximum crack width results in approximately:

$$w_{max} = 1{,}7 \cdot w_m. \tag{3}$$

4. DEFORMATION BEHAVIOR OF CENTRICALLY AND ECCENTRICALLY REINFORCED TENSION SPECIMENS

The principal correlations between average strain over the cracks and external load related to the steel cross sectional area resulting from monotonically increasing and cyclic loading are shown in Fig. 7.

In order to describe the stress-strain behavior of centrically reinforced concrete specimens loaded in tension neglecting shrinkage of concrete the following idealization for initial loading.

$$\varepsilon_m = \frac{\sigma_s}{E_s} \sqrt{1 - \left(\frac{\sigma_s^1}{\sigma_s}\right)^2} \tag{4}$$

yielded a good agreement. This idealization is also valid for reinforced concrete panels under transverse load and for eccentrically reinforced tension specimens, if the effective concrete cross section according to Fig. 6 and the centrical concrete tensile strength are taken as a basis for the determination of the steel stress σ^1_s. The largest average strain at top load which stabilizes after a certain number of repeated lods can be approximately recorded with:

$$\varepsilon^o_{m,max} = \frac{\sigma^o_s}{E_s}\sqrt{1 - \left(\frac{\sigma^1_s}{\sigma^o_s}\right)^S} \quad (5)$$

At complete unloading a residual strain of about

$$\varepsilon_r = 0{,}2 \cdot 10^{-3} \quad (6)$$

remains in the specimen. This is independent of the number of load cycles.

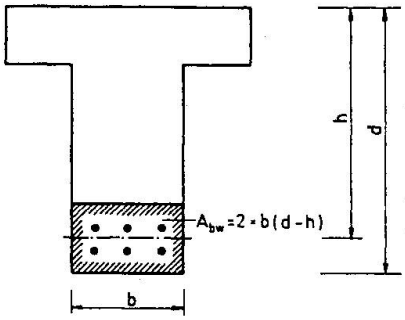

Fig. 6 Effective zone of reinforcement (acc. to [8])

It was stated with all tests that after approximately 5000 load cycles or after a 6-months permanent load no considerable deformation increases occured.

The initial stress state caused by shrinkage results, related to the load beginning, in larger average strains compared with the specimens without shrinkage. The stress-strain behavior of specimen S07 shown in Fig. 8 makes clear that the average strains can exceed those of the pure steel.

In case the shrinkage influence is considered for the determination of the steel stress in the cracked cross section directly after the first crack, the average strain related to the initial load can also be calculated according to Eq. (4) using $\sigma^1_{s,schw}$

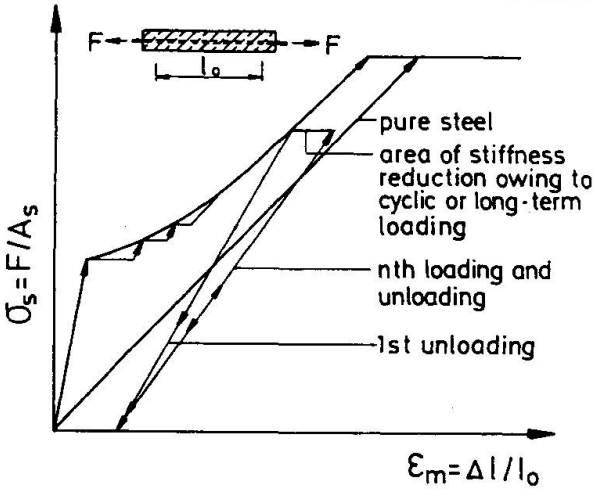

Fig. 7 Stress-strain relationships for axially loaded reinforced concrete

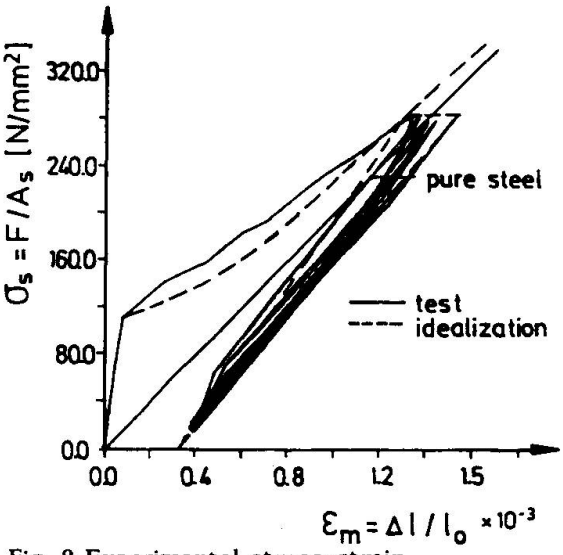

Fig. 8 Experimental stress-strain relationships of specimen S07 under shrinkage and idealization

$$\varepsilon_m = \frac{\sigma_s}{E_s}\sqrt{1 - \left(\frac{\sigma^1_{s,schw}}{\sigma_s}\right)^2} \quad (7)$$

The largest average strain increase at top load which stabilizes after a certain number of load cycles results to approximately

$$\Delta\varepsilon^o_{m,schw} = \frac{\sigma^o_s}{E_s}\left[\sqrt{1 - \left(\frac{\sigma^1_s}{\sigma^o_s}\right)^S} - \sqrt{1 - \left(\frac{\sigma^1_s}{\sigma^o_s}\right)^2}\right] \quad (8)$$

as with specimens without shrinkage.

At complete unloading of the specimens a residual strain of

$$\varepsilon_r = 0{,}2 \cdot 10^{-3} + \varepsilon_m^o + \Delta\varepsilon_{m,schw}^o - \varepsilon_s^o \quad (9)$$

is left.

5. NOTATIONS

b	= width
d	= total height
h	= height from center of gravity of tension reinforcement to compression edge
d_s	= diameter of reinforcement bar
$\ddot{u}$	= smallest concrete cover of reinforcement at pure tension = distance between bottom side of reinforcement bar and tension edge at eccentric tension and flexion
s	= distance of reinforcement bar (see table 1)
A_s	= steel cross sectional area
A_{bw}	= effective concrete cross section (see Fig. 6)
$A_{b,n}$	= area of concrete (net)
μ	$= \frac{A_s}{A_{bw}}$
F	= force
E_s	= modulus of elasticity of steel
β_c	= cylinder crushing strength
σ_s	= steel stress
Q	= lateral pressure
σ_s^1	= steel stress in concrete cross sectional area directly after first crack
σ_s^o	= maximum steel stress at cyclic or long-term loading
$\sigma_{s,schw}^1$	= steel stress in crack cross sectional area directly after the first crack considering shrinkage influence
ε_s^o	= steel strains at top load
ε_m	= average strain
ε_m^o	= average strain at top load
$\varepsilon_{m,max}^o$	= largest average strain owing to cyclic or long-term loading
ε_r	= residual strain in specimen after unloading
$\Delta\varepsilon_{m,schw}^o$	= strain increase owing to repeated loads at top load considering shrinkage influence
a	= average crack spacing
a_{max}	= maximum crack spacing
w_m	= average crack width
w_{max}	= maximum crack width

References

[1] KOLLEGGER, JOHANN; GÜNTHER, GERD; MEHLHORN, GERHARD: Zug- und Zug-Druckversuche an Stahlbetonscheiben. Forschungsbericht Nr. 1 aus dem Fachgebiet Massivbau, Gesamthochschule Kassel, 1986. *

[2] GÜNTHER, GERD; MEHLHORN, GERHARD: Versuche an Beton- und Stahlbetonscheiben unter ein- und zweiaxialer Beanspruchung. Forschungsbericht Nr. 9 aus dem Fachgebiet Massivbau, Gesamthochschule Kassel, erscheint 1989.*

[3] GÜNTHER, GERD; MEHLHORN, GERHARD: Untersuchungen zur Mitwirkung des Betons zwischen den Rissen für monoton steigende und schwellende Belastung. Forschungsbericht Nr. 3 aus dem Fachgebiet Massivbau, Gesamthochschule Kassel, 1987. *

[4] GÜNTHER, GERD; MEHLHORN, GERHARD: Beeinflussung des Spannungs-Dehnungs-Verhaltens von Stahlbetonzugkörpern durch die Art der Rißöffnung und den durch Schwinden verursachten Eigenspannungszustand. Forschungsbericht Nr. 8 aus dem Fachgebiet Massivbau, Gesamthochschule Kassel, 1989. *

[5] GÜNTHER, GERD; MEHLHORN, GERHARD: Langzeitverformungsverhalten von Stahlbetonkörpern. Forschungsbericht Nr. 8 aus dem Fachgebiet Massivbau, Gesamthochschule Kassel, 1989. *

[6] GÜNTHER, GERD; MEHLHORN, GERHARD: Verformungsverhalten von Stahlbetonbalken unter wiederholter Belastung. Forschungsbericht Nr. 5 aus dem Fachgebiet Massivbau, Gesamthochschule Kassel, 1988. *

[7] CEB/FIP-Mustervorschrift für Tragwerke aus Stahlbeton und Spannbeton. Deutscher Ausschuß für Stahlbeton, 1978.

[8] GERGELY, PETER; LUTZ, L.A.: Maximum Crack Width in Reinforced Concrete Flexural Members. In: Causes, Mechanics and Control of Cracking in Concrete, SP-20, American Concrete Institute, Detroit, 1968, S. 87-117.

* Summary, notations, and legends to pictures both in German and in English.

A 12 Year Case Study of a Reinforced Concrete Building

Une étude de cas d'une durée de 12 ans concernant un bâtiment en béton armé

Eine 12 Jahre umfassende Fallstudie eines Stahlbetongebäudes

Leslie PARROTT
Research Engineer
British Cement Assoc.
Slough, UK

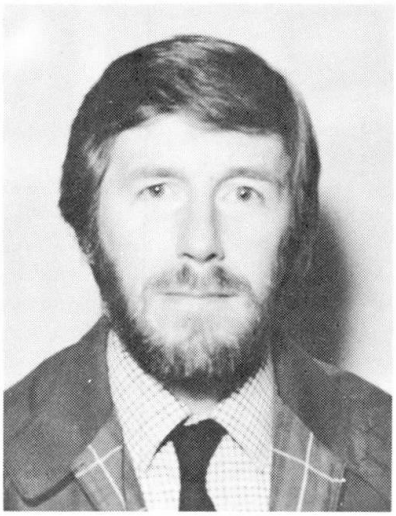

Leslie Parrott received his Bachelor and Doctor degrees in civil engineering from London University. His research on various aspects of concrete performance, including internal moisture, deformation properties, carbonation, durability and high strength, has resulted in about 80 published papers.

SUMMARY

Shrinkage and stress-induced strains in a two-storey office building were measured using vibrating wire gauges embedded in the roof and intermediate floor. The floor dried more quickly than the roof. This contributed to tensile stresses in the floor, differential movements and associated cracking of glazed panels and internal block wall. The bituminous membrane on the flat roof deteriorated after 7 years and water leaked through the carbonated concrete roof slab. This case study shows that service behaviour is greatly affected by concrete moisture conditions.

RÉSUMÉ

Le retrait et les déformations dues aux contraintes dans un bâtiment à deux étages ont été mesurés à l'aide de jauges à fils vibrants noyées dans le toit et le plancher intermédiaire. Le plancher a séché plus rapidement que le toit. Cela a entrainé des efforts de traction dans le plancher, des déplacements différentiels et une fissuration du vitrage et du mur interne en parpaing. La membrane bitumineuse du toit plat a été détériorée après 7 ans et l'eau s'est infiltrée à travers les dalles de toiture en béton carbonaté. Cette étude de cas montre que l'entretien ets largement affecté par les conditions d'humidité du béton.

ZUSAMMENFASSUNG

Mit Hilfe vibrierender, im Dach und in der Gebäudedecke eingebetteter Messstreifen wurden Schwinden und durch Beanspruchung verursachte Verformung in einem zweistöckigen Bürogebäude gemessen. Die Decke trocknete schneller als das Dach. Dies trug zu Zugspannungen in der Decke, Differentialbewegungen und damit verbundenem Platzen von Glasfassadenplatten und innerer Blockwand bei. Die bituminöse Schicht auf dem Flachdach war nach 7 Jahren schadhaft und Wasser drang durch die karbonisierte Betondachplatte. Diese Fallstudie zeigt, dass die Haltbarkeit in starkem Masse von den Feuchtigkeitsbedingungen des Betons beeinflusst wird.

1. INTRODUCTION

Investigations of in-situ movements in concrete structures were initiated by the British Cement Association in the mid-1970's as part of a programme on the prediction of concrete deformation properties. The reported investigation of a two-storey office building has been continued because it is providing valuable information relating to long-term moisture conditions, carbonation and durability in reinforced concrete.

2. DESCRIPTION OF BUILDING

A diagram of the two-storey office building is shown in Figure 1. There are twelve bays each 5.4m long with a stairway at the ninth bay providing some longitudinal restraint. The 4.4m wide offices are accessed by 1.3m wide corridors on the ground and first floors. The longer portion of the building between the stairway and an old stone tower can move longitudinally by virtue of a movement joint at the interface of the tower and office corridors. At this interface and for one bay the width of the structure is reduced to that of the corridor and the walls are fully glazed. The continuous floor and roof slabs were cast in-situ on precast concrete cross beams that were supported by a frame of precast columns and longitudinal beams.

The in-situ and precast concretes were made with lightweight coarse aggregate and a natural sand. 100mm cube strengths at 7, 28 and 182 days were 35.9, 42.4 and 55.0 MPa respectively. The mix constituents per cubic metre were 170kg free water, 350kg Portland cement, 730kg zone 2 sea dredged sand and 600 kg of lightweight aggregate plus about 100kg of absorbed water.

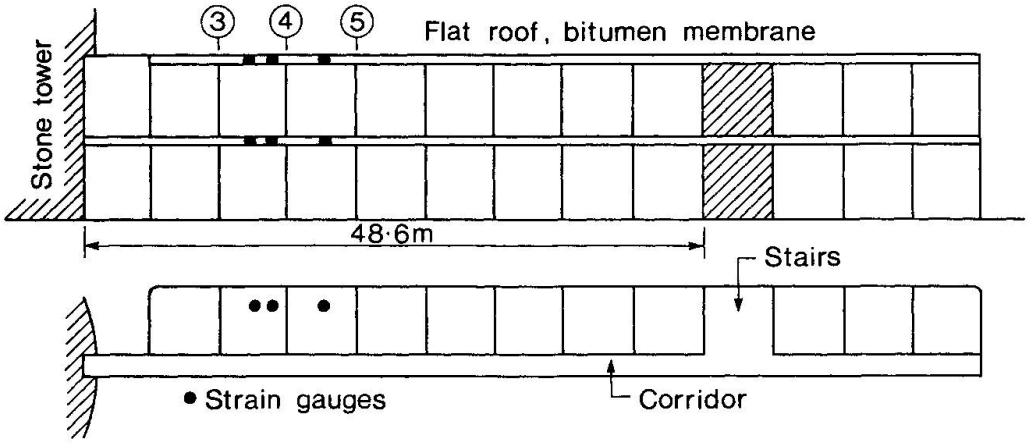

Fig. 1 Elevation and plan of two-storey office structure

3. MEASUREMENT METHODS

The 165mm deep floor and roof slabs in bays 3-4 and 4-5 were instrumented at mid-span with embedded vibrating wire strain gauges set at three depths above the neutral axis. Bays 3-4 of the floor and roof were also instrumented near the neutral axis at quarter-span (i.e. where stresses were expected to be small). The strain gauges were installed horizontally in orthogonal pairs with the longitudinal gauge parallel to the length of the building. This

arrangement of gauges permits separate calculation of shrinkage and stress-induced strains [1].

A small correction was made (2.5 microstrain/^{o}C) to allow for the difference in thermal expansion of the concrete and the steel wire in the strain gauge and was based upon in-situ temperature measurements. The shrinkage and stress-induced strains (Esh and Est) were calculated from the longitudinal and transverse strains (El and Et) using the relations Est = (El - Et)/1.18 and Esh = El - Est. The factor 1.18 derives from the assumption that Poisson's Ratio is 0.18 for short and long-term loading [1]. Contraction and extension are regarded as positive and negative strains, respectively.

Prisms measuring 100 x 100 x 290mm were cast from the in-situ concrete for various site and laboratory tests.

4. RESULTS AND DISCUSSION

4.1 Concrete prisms and measured strains

Six prisms were stored beneath the roof for long-term measurements of shrinkage and weight loss. The shrinkage results in Figure 2 suggest that approximate moisture equilibrium was reached after about 3 years and this was consistent with the weight loss measurements: thereafter the small increase in shrinkage was accompanied by a slight gain of weight that was indicative of carbonation [2].

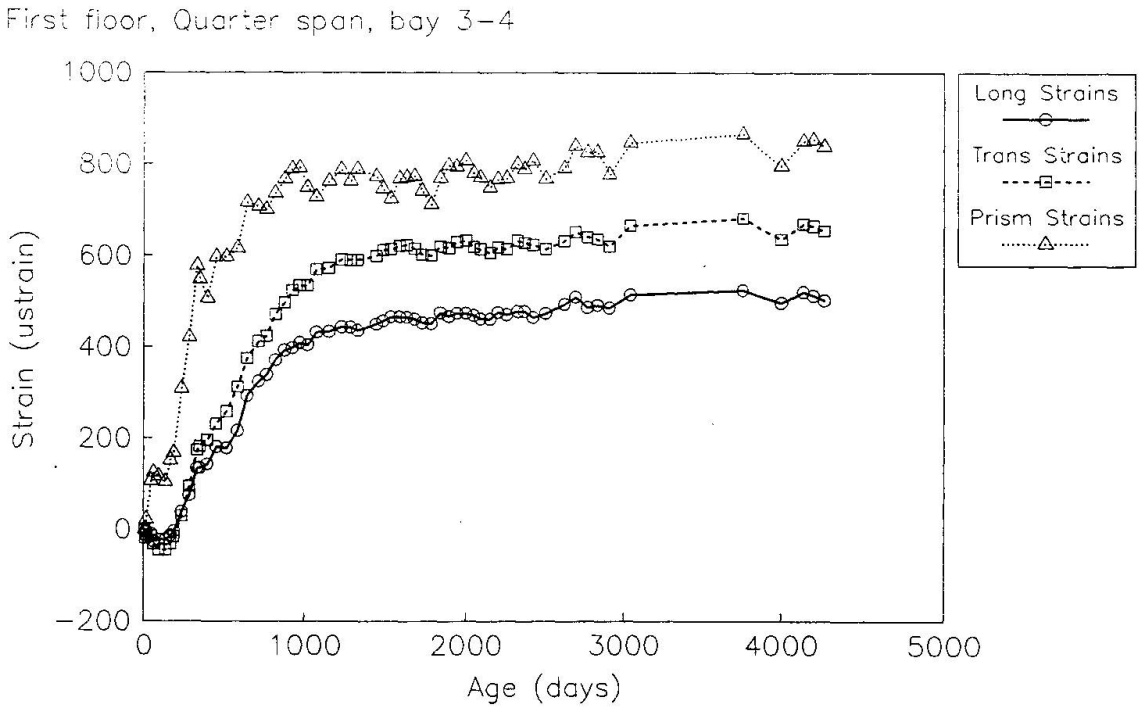

Fig. 2 Strains in prisms; longitudinal and transverse strains at quarter span, bay 3-4 in floor.

Figure 2 shows that initially longitudinal strains are slightly larger than transverse strains at quarter-span in the floor. This is consistent with the expected, small flexural stresses. After about 250 days the transverse strains exceed the longitudinal strains and this indicates that axial tensile stresses develop at later ages. Similar patterns of transverse and longitudinal strain were observed at mid-span in bays 3-4 and 4-5 of the floor.

4.2 Shrinkage and stress-induced strains

The calculated strains for bay 4-5 of the floor slab are shown in Figure 3. There were only small differences in shrinkage between the three instrumented sections. The shrinkage of the floor slab developed more slowly than the prism shrinkage (Fig 2) and appears to be stabilizing at a smaller, final strain. These effects are attributable to differences in drying path length [3]. The stress-induced strains exhibit the expected pattern for flexural loading but they are superposed by the development of tensile strains.

The calculated strains for the roof slab in Figure 3 show that shrinkage developed more slowly than that in the floor. Although the roof slab was similar in thickness to the floor slab drying was retarded by the waterproof layer on its upper surface. The stress-induced strains exhibit the expected pattern for flexural loading but they are superposed by the slow development of small tensile strains. The tensile strains in the roof develop more slowly than those in the floor.

The strain patterns in Figure 3 suggest that longitudinal drying shrinkages of the floor and, to a lesser extent, the roof are restrained and thus cause the development of longitudinal tensile stresses. This is consistent with the similarity in shape and period of occurrence of the shrinkage versus age and stress-induced strain versus age curves. Restraint may have derived from the columns, longitudinal beams, internal block walls and the foundation.

4.3 Movement and cracking

Qualitative corroboration of the more rapid drying shrinkage of the floor compared with the roof and foundation was provided by visible movement between the building and the adjacent stone tower. Furthermore, several glazed panels in the corridor next to the tower cracked at an age of about 5 years due to the shearing action of the floor movement. Cracking of internal block walls provided additional evidence of the relative movement of the floor. The replacement glazing has not shown any sign of distress. A mastic-filled joint was provided between the block wall and the structural components of the building: this has prevented any further cracking of the walls.

4.4 Roof leakage and carbonation

Solar radiation caused local expansion and deterioration of the bituminous roof membrane after 7 years, in spite of a surface layer of white, reflective stone chippings. Consequently the central drainage gully did not function properly and after rainfall it acted as a reservoir for water leaking through the roof slab. Continued deterioration of the roof membrane and leakage of water over a period of five years caused damage to internal finishes and raised the question of reinforcement corrosion. Measurements on a prism stored beneath the roof suggested that the roof slab may be carbonated to a

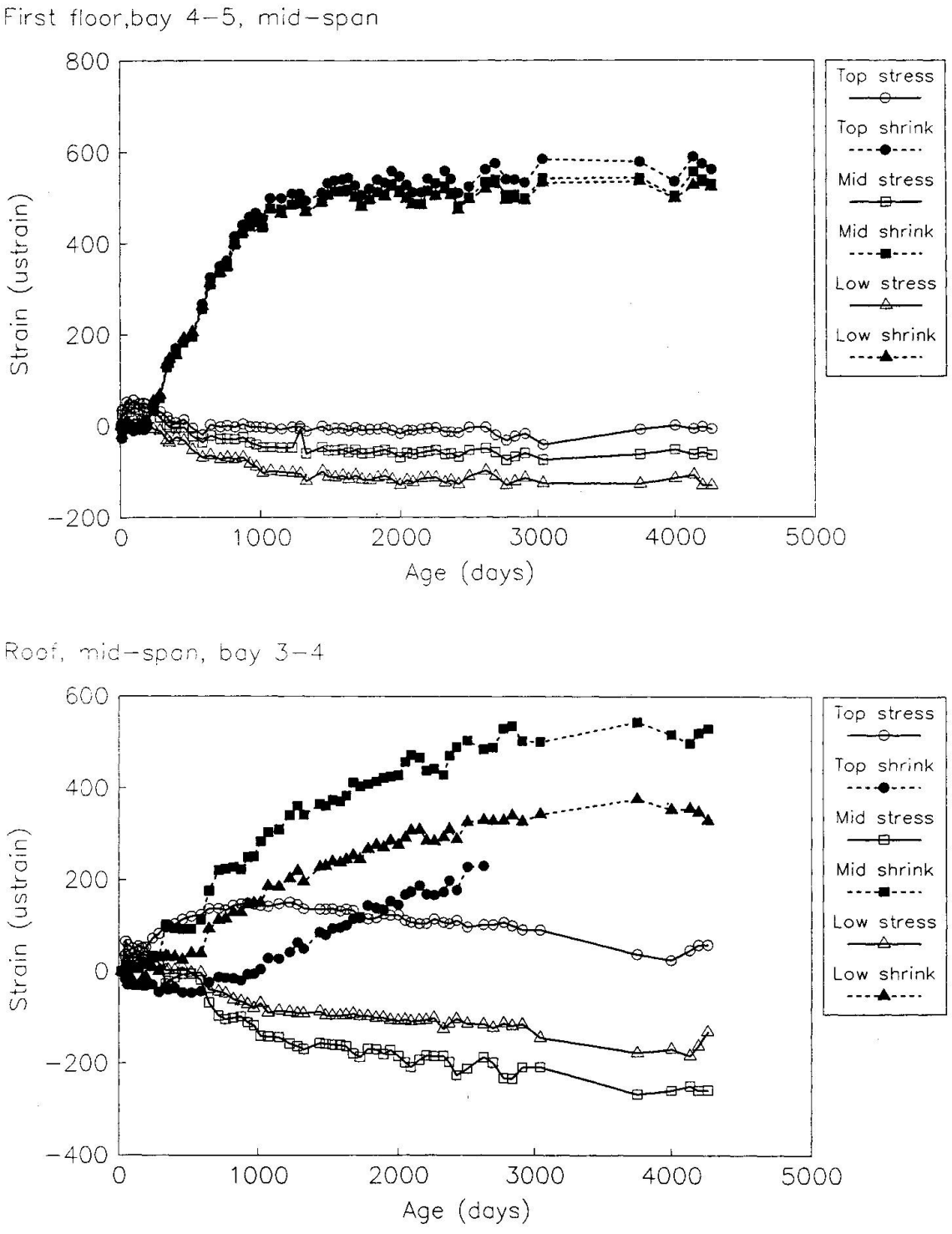

Fig. 3 Shrinkage and stress-induced strains in floor(upper) and roof(lower).

depth of 12mm (standard deviation = 3mm). The specified depth of cover was 20mm and with the standard deviation typically in the range 5 to 15mm [4] there is a risk that some of the reinforcement may be corroding[2]. Further inspection for signs of corrosion is planned.

5. CONCLUSIONS

The reported long-term case study of a two-storey office building showed that moisture conditions can have an important effect upon the service performance of a concrete structure; they can affect building movements, component stresses and durability.

Restraint of drying shrinkage caused the development of an axial, tensile component of stress in the floor and, to a lesser extent, in the roof.

It seems advisable to use carbonation-resistant concrete for flat roof construction to minimise the risk of reinforcement corrosion in the event of leakage.

ACKNOWLEDGEMENT

The long-term support of this project by the British cement industry is gratefully acknowledged.

REFERENCES

1. PARROTT L., A study of some long-term strains measured in two concrete structures. Proc. RILEM Internat.Symp. on Testing in-situ of concrete structures. Budapest 1977 Vol.2, 123-139.

2. PARROTT L., A review of carbonation in reinforced concrete. Cement and Concrete Association Report C/1-0987, July 1987, 126 pages.

3. CEB-FIP., International recommendations for the design and construction of concrete structures. June 1970, 80 pages.

4. Clear C., Review of cover achieved on site. To be published.

Durability of Foundation Concrete in an Aggressive Environment

Durabilité du béton de fondation dans un environnement agressif

Dauerhaftigkeit von Betonfundationen unter aggressiven Bedingungen

D. V. MALLICK
Technical Advisor
National Consulting Bureau
Tripoli, Libya

M. M. TAWIL
Prof. of Civil Eng.
University of El Fateh
Tripoli, Libya

A. A. SHIBANI
Chairman
Nat. Consult. Bureau (NCB)
Tripoli, Libya

Prof. Mallick, born 1936, received his doctorate at Bristol University, U.K. Professor and Consultant for 13 years. Prof. Mallick, now in a consulting firm, is a technical advisor. Fellow ICE (India) and ASCE.

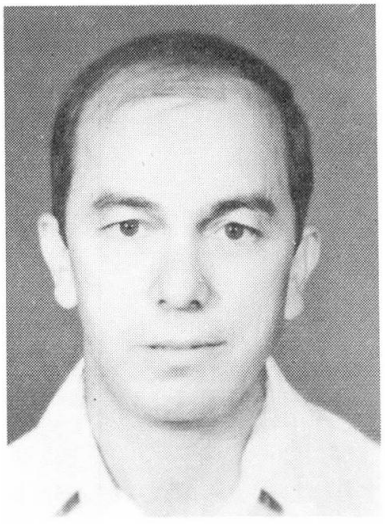

Prof. Tawil, born 1945, received his doctorate at University of Colorado, USA. Prof. Tawil is a University staff member for 13 years. He has also been a part-time technical advisor to the National Consulting Bureau, Tripoli, for the last 11 years.

Dr. Shibani, born 1944, received his doctorate at North Carolina State University, USA. Dr. Shibani, besides his duties at NCB, has been a part-time staff member in the Mechanical Eng. Dep., University of El Fateh, Tripoli for the last 13 years.

SUMMARY

A case study assessing the durability of foundation concrete in the vicinity of the sea where a number of aggressive conditions exist is presented. The use of OPC compared to SRC is preferred when sulphates and chlorides coexist due to its high resistance to chloride diffusion. Durability of foundation concrete can be enhanced by a sacrificial layer all around and applying a waterproof coating.

RÉSUMÉ

L'étude évalue la durabilité d'un béton de fondation dans des conditions extrêmes d'agressivité dues à la proximité de la mer. L'utilisation de l'OPC est préférée à celle du SRC due à sa haute résistance à la diffusion chlorique lorsque des sulphates et chlorides co-existent. La durabilité du béton de fondation peut être augmentée par une "couche de sacrifice", ainsi que par un agent imperméable appliqué sur la fondation.

ZUSAMMENFASSUNG

Vorgestellt wird eine Fallstudie zur Dauerhaftigkeit von Betonfundationen in einer Region mit aggressiven Bedingungen in Meeresnähe. Die Verwendung von OPC ist dem SRC vorzuziehen, wenn Sulfate und Chloride gleichzeitig vorkommen, da Ersterer zu einem dichteren und weniger durchlässigen Beton führt. Die Dauerhaftigkeit der Fundamente kann durch eine "Opferschicht" von mindestens 50 mm Beton und durch einen wasserdichten Anstrich verbessert werden.

1. INTRODUCTION

This study is devoted to the assessment of durability of concrete foundations of overhead transmission line towers constructed in a number of aggressive conditions commonly met in Sebkha region. Environmental aggression to foundation concrete occurs due to: (a) Aggressive compounds in the sub-soil or ground water surrounding the concrete, and (b) Effect of wetting and drying.

For foundation concrete, the effects of aggressive compounds in sub-soil and ground water are more predominant. It is well known that chemicals in the dry state will not attack concrete; this applies particularly to sulphates as these are often found in the form of lenses in soil strata. The tolerable level of sulphate concentration in relatively dry, well drained soils is about four times the acceptable limit when the sulphates are in the form of a solution in ground water. In most soils, it is the concentration of aggressive chemicals in the ground water which decides the type of cement and the quality of concrete to be used.

All portland cement concrete is prone to acid attack. Some of the chemical compounds which may be encountered in ground water of Sebkha region and which are aggressive to ordinary portland cement are described below. Further, their effects on the durability of the concrete are also presented.

2. AGGRESSIVE CHEMICAL COMPOUNDS IN SEBKHA

2.1 Sebkha

The soil in Sebkha in the vicinity of sea is generally aggressive and is very little compacted. The ground water level is very near the surface and contains aggressive chemical compounds like sulphates and chloride in solution, and acids in various proportions. In winter the lowest parts of Sebkha form shallow lakes and in summer the ground dries out and hardens. Aggressive compounds in the subsoil and ground water surrounding the foundation concrete attack it by reacting with hardened cement paste. Attack on cement can thus take place, sulphates reacting with Ca(OH)2 and with calcium aluminate hydrate. The products of the chemicals reactions gypsum and calcium sulpho aluminate, have considerable large volume than the compounds they replace, so that the reaction with the sulphate leads to expansion causing tensile stresses which finally leads to cracking of concrete.

2.2 Sulphates in Solution in Ground Water

The most commonly found sulphates in Sebkha ground water are those of calcium, magnesium and sodium. Calcium sulphate is less soluble at normal temperatures than the other sulphates mentioned above; and the solution is saturated at about 2000 mg/litre of SO3.

Sodium and Magnesium sulphates are very soluble in water and therefore their concentration can be much higher than calcium sulphate. Magnesium sulphate is more aggressive to portland cement concrete than the sulphates of sodium, calcium and pottassium, when in equal concentration. Magnesium sulphate attacks calcium silicate hydrate as well as Ca(OH)2 and calcium aluminate hydrate and, decomposes the hydrated calcium silicates.

The rate of sulphate attack increases with an increase in the strength of the solution, but beyond a concentration of about 0.5% of Mg SO4 the rate of increase in the intensity of the attack slows down. If the w/c ratio is low, the deteriorating effect of sulphate takes much longer time.

The concentration of the sulphates is expressed as the number of parts by weight of SO3 per million (ppm). Conversion of SO4 to SO3 can be made as follows:

$$SO3 = 0.83\ SO4$$

A concentration of 1000 ppm of SO3 is considered moderately severe and 2000 ppm are severe especially if Mg SO4 is the predominant constituent.

In addition to the concentration of sulphate, the speed with which the concrete is attacked depends also on the rate at which the sulphate removed by the reaction with cement can be replenished. Thus in assessing the danger of the sulphate attack the movement of ground water has to be known. Alternating saturation and drying in Sebkha leads to rapid deterioration of concrete.

2.3 Chlorides in Solution in Ground Water

Chloride is generally present in ground water as a solution of sodium chloride (common salt). The chloride solution of high concentration can attack the cement paste. Chlorides in solution react with the calcium aluminate phase in the cement to form calcium chloro aluminate, and although there is a debate as to the precise mechanism involved, it is well known that in certain circumstances where there are high concentrations of chloride expansive disruption of the concrete can occur. However, the chloride salts are highly soluble and can be leacked from the concrete preventing their concentration.

2.4 Sulphates and Chlorides in Ground Water

It is however known that in the case of sulphates co-existing with chlorides in ground water, the latter inhibits the expansion of concrete [1, 2] and the question of sulphate attack is then considered less critical and the chloride attack becomes more alarming. Chlorides in ground water of Sebkha near the sea have a tendency to combine with a part of the C3A forming a "more or less insoluble chloro aluminate" [3].

It has been a common practice and is even today to use cement with low C3A content to overcome sulphate attack in concrete exposed to sulphates either soluble in ground water or present in marine environment. Among these cements are the sulphate resisting cement (SRC) where the C3A content is limited to a maximum of 3.5% by B.S. 4627 and the ASTM Cement V in which C3A is limited to a maximum of 5%. Recent research, however, indicates that concrete made with SRC has less resistance to chloride ingress (or migration).

2.5 Acids in Ground Water

When the pH of subsoil and/or ground water is below the neutral point of 7.0 the water is then acidic and is liable to attack concrete made with any type of portland cement. The severity of the attack depends upon a number of factors. The pH value is a measure of the intensity of the acidity, and by itself does not give any indication of the type or the amount of acid present.

3. DETERIORATION OF FOUNDATION CONCRETE IN SEBKHA

Solid salts do not attack concrete, but when present in a solution they react with hardened cement paste. Disruption of concrete mass may occur by the expansive reaction of voluminous crystalline salt formations, normally caused by the ingression of chloride and sulphate solutions. Erosion of materials by dissolution of the cement mainly due to the action of acids, if present, can take place. Chemical reactions can lead to the type of damage generally known as 'Concrete Corrosion'.

Foundation concrete below or near the ground water table are affected by chemical effects accompanied with alternative cycles of drying and wetting. When the water table is high the concrete becomes saturated and when it goes down, part of the water evaporates from concrete causing salts to crystallize. A subsequent rise in water level causes the concrete to saturate again with water containing higher concentration of salts. The recurrence of such a process in course of time causes crystal growth within the pores, if the concrete is permeable, resulting in swelling action leading to cracking of concrete. There is a limit to the size of cracks allowable for various types of exposure; these limits range from 0.1 mm for very severe environment to 0.4 mm for mild environment.

Maximum precautions must be taken to ensure crack free concrete in order to stop ingression of chlorides. Steel reinforcement is protected from corrosion by the surrounding concrete provided this concrete is dense and of adequate thickness. The corrosion potential of steel due to the presence of soluble chlorides in the ground water is increased in porous concrete which in turn can result from inadequate compaction, high w/c ratio and low cement content. In case of reinforced concrete, the migration of chloride ions from the ground water establishes anodic and cathodic areas, the resulting electrolytic action leads to an accumulation of the corrosion products on the steel which causes its expansion with a consequent rupture of concrete.

As mentioned earlier, the chloride solution of high concentration can attack the cement paste and expansive disruption of the concrete can occur. Fortunately, the chloride salts are highly soluble and can be leacked from cement preventing their concentration.

When sulphates co-exist with chlorides in ground water of Sebkha, the latter inhibits the expansion of concrete and the question of sulphate attack is then considered less critical and the chloride attack then becomes more predominant. The rate of diffusion of chlorides in SRC is more than in OPC. In the circumstances where chlorides coexist with sulphates and are in higher quality, the effect of chloride attack and subsequent corrosion of reinforcement is relatively increased by the use of SRC.

4. MEASURES TO ENHANCE DURABILITY OF FOUNDATION CONCRETE IN SEBKHA

In the light of chemical expansive reactions which are responsible for the deterioration of concrete in Sebkha containing aggressive water soluble salts in ground water as mentioned above, it is necessary to take some special precautions to protect the foundation concrete from cracking and corroding.

Protection against subsoil chemical action has to be preventive in nature because the affected areas of concrete in contact with the soil and the ground water are practically impossible to inspect after construction. The protective

measures should obviate the need for maintenance and repairs and should serve as water proofing. Some of the preventive measures recommended are as follows:

- Use of cement low in C3A. In practice, it has been found that a C3A content of 7% provides an approximate border line between cements of good and poor performance.

- Where chloride and sulphates co-exist with a large quantity of chlorides, use of OPC should be preferred over SRC.

- Use of a dense, impervious and high strength concrete.

5. CASE HISTORY

A doubt regarding the durability of concrete consisting of OPC of overhead transmission towers foundation in Sebkha area necessitated an investigation into chemical aggressiveness of Sebkha. Results of the chemical analysis of a water samples conducted by Raymond International of Deleware Inc. (Tripoli branch) in April 1978 are presented below:

Sample No. 1/W/3.0; Site: Misurata Sebkha.

Chemical Analysis

pH	=	7.3
Chlorides	=	80250 mg/l
Hardness as CaCO3	=	23600 mg/l
Calcium	=	900 mg/l
Magnesium	=	5200 mg/l
Sulphates	=	9200 mg/l

A proper chemical analysis demonstrated that first $CaSO_4$ will be formed consuming 1500 mg/l of sulphates necessary for a saturated solution of calcium sulphate. The remaining sulphate (9200 - 1500 = 7700 mg/l) will react with (7700 x 0.253) 1948.1 mg/l of magnesium forming maximum possible amount of $MgSO_4$. The balance magnesium will either react with the chloride or will remain in the ground water in the form of hardness. Hence, all magnesium available will not react to form $MgSO_4$ which is more aggressive to portland cement concrete than the sulphates of sodium, calcium and pottassium when in equal concentration.

It is well known that in addition to the concentration of sulphates, the speed at which foundation concrete is attacked depends upon the rate at which sulphates removed by reaction with cement can be replenished. Thus the movement of ground water plays a key role since alternating saturation and drying leads to rapid deterioration of concrete. Most of the tower foundations were either in the submerged state or in a dry state, hence the effect of ground water movement with less variation was considered less serious.

Normally, SRC should be used when sulphates in higher concentration are present. But this recommendation is not obligatory when sulphates and chlorides co-exist

in the ground water since the later inhibit the expansion of concrete and the question of sulphate attack is then less critical. Recent research [4] has indicated that SRC has poor resistance to chloride ingression as compared to OPC. Therefore the use of OPC in the present circumstances was considered more acceptable than SRC provided other precautions for concrete in Sebkha are also taken into design consideration.

6. CONCLUSIONS AND RECOMMENDATIONS

- Durability of concrete foundations in Sebkha can be ensured with the following precautions:

  a) Adequate concrete cover to the reinforcement. 50 to 75 mm concrete cover is recommended.

  b) Provision of a sacrificial concrete layer (minimum thickness 50 mm) all around the foundation concrete.

  c) Use of a dense, impermeable and high strength concrete is made.

- Although SRC is generally recommended for use in foundation concrete in Sebkha; but when sulphates and chlorides co-exist, in ground water, the use of OPC can be preferred over SRC due to its higher resistance to chloride ingression.

- A coating of a water proofing material around the foundation concrete will enhance the durability.

REFERENCES

1. NEVILLE, A.M., Properties of Concrete, Pitman, 3rd edition, 1981.

2. MURDOCK, L.J. and BROOK, K.M., Concrete Materials and Practice, Edward Arnold, 5th edition, 1979.

3. CIRIA, the CIRIA Guide to Concrete Construction in the Gulf Region, Construction Industry Research and Information Association, Special Publication 31, London 1984.

4. STUVO, Concrete in Hot Countries, Netherland, 1985.

Porosity and Permeability as Indicators of Concrete Performance

Porosité et perméabilité comme indicateur de comportement du béton

Porosität und Durchlässigkeit als Indikatoren des Betonverhaltens

J. G. CABRERA
Senior Lecturer
University of Leeds
Leeds, England

A. R. CUSENS
Prof. of Civil Eng.
University of Leeds
Leeds, England

C. J. LYNSDALE
Research Fellow
University of Leeds
Leeds, England

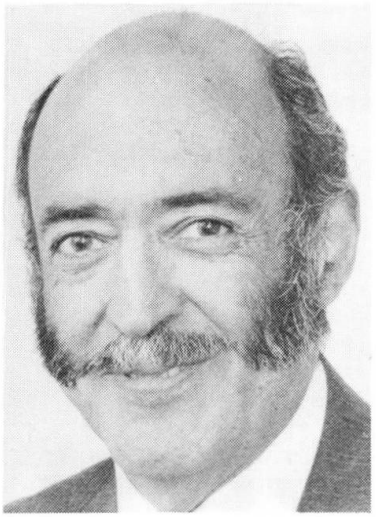

Joe Cabrera has lectured in Leeds since 1967. His main research is performance and durability of engineering materials.

Tony Cusens was appointed to his current position in Leeds in 1979. His main research fields concrete structures, especially bridges. He is Vice-Chairman of the British Group of IABSE.

Cyril Lynsdale has been engaged in concrete research since 1983. His main interests are the study of durability and the use of admixtures in concrete.

SUMMARY

Based on the results of an extensive laboratory study, this paper proposes statistical models which link numerically oxygen permeability to pore structure characteristics, total porosity and compressive strength, water/cement ratio, air content and age. The models are used to predict adequate levels of performance for concrete in bridge structures.

RÉSUMÉ

Fondé sur les résultats d'un essai étendu de laboratoire, cet article offre des modèles statistiques qui lient numériquement la perméabilité à l'oxygène aux caractéristiques de la structure des pores, à la porosité totale, à la résistance à la compression, au rapport eau-ciment, à la teneur en air et à l'âge. Ces modèles sont employés pour prédire des niveaux de comportement suffisants pour le béton dans la construction des ponts.

ZUSAMMENFASSUNG

Basierend auf den Resultaten von umfangreichen Laboruntersuchungen werden statistische Modelle vorgeschlagen, welche die Sauerstoffdurchlässigkeit mit der Charakteristik der Porenstruktur, der Gesamtporosität, der Druckfestigkeit, dem Wasser/Zement-Verhältnis, Luftgehalt und Betonalter verknüpfen. Die Modelle werden zur Prognose des Verhaltens von Betonbrücken verwendet.

1. INTRODUCTION

It is now accepted that the performance of concrete under a particular environment cannot be solely related to its strength but that it is a function of its pore structure and permeability [1, 2]. The new British code of practice for the structural use of concrete [3], for example, specifies strength, cement content and water/cement ratio as criteria for design. This, although not satisfactory, is an attempt to control performance by indirectly controlling porosity. The new draft for the Eurocode [4] in concrete has, however, proposed the measurement of permeability as a sole criterion for durability. Notwithstanding the fact that in recent years a large amount of work has been devoted to this problem [5, 6, 7], there is no accepted method for measuring permeability.

This study presents empirical statistical models which relate the oxygen permeability of concrete to other intrinsic and compositional properties of the material. The models are used as an aid to understanding which properties of concrete have a relevant effect on its permeability and also to predict long-term permeability from measurements made at early ages. The paper proposes the use of these models to set criteria for the design of durable concrete mixes.

2. MIX DESIGN AND MATERIALS

The mix design used in this investigation is based on the criterion of "minimum porosity" [8] which involves the selection of the components of concrete to achieve maximum packing.

The composition of the mix designed by the method indicated gave a mix of the following proportions: 1 part of cement, 2.33 parts of sand and 3.5 parts of gravel. The ordinary Portland cement (opc) content of the mix was 325 kg/m^3. This composition was used to prepare three "control" concretes by varying the water/cement ratio (see Table 1).

Table 1: Mixes investigated and their fresh properties

Mix	w/c ratio	Superplasticiser		PFA	Slump	Flow Table	Air Content
		Type	Dosage*(%)	(%)	(mm)	(mm)	(%)
A	0.65	None	None	None	215	580	0.6
B	0.55	None	None	None	55	390	1.65
C	0.40	None	None	None	0	-	2.8
BN2	0.55	SNFC1	0.2	None	172	550	1.2
BN3	0.55	SNFC1	0.4	None	240	690	0.9
CN2	0.40	SNFC1	1.2	None	50	350	2.6
BM2	0.55	SMFC	0.2	None	155	500	1.3
BM3	0.55	SMFC	0.4	None	225	650	0.9
CM2	0.40	SMFC	1.4	None	50	305	1.60
BP2	0.55	Co-Po	0.08	None	200	545	3.25
BP3	0.55	Co-Po	0.16	None	230	600	5.70
CP1	0.40	Co-Po	0.19	None	50	320	3.9
BSF2	0.55	SNFC2	0.3	None	210	555	3.4
BSF3	0.55	SNFC2	0.45	None	220	600	2.7
CSF1	0.40	SNFC2	0.70	None	50	310	5.4
BLS2	0.55	MLS	0.2	None	200	560	3.5
BLS3	0.55	MLS	0.4	None	215	615	4.3
CLS2	0.40	MLS	0.45	None	65	345	8.4
PFA1	0.50	None	None	30	60	360	1.3
PFA2	0.55	None	None	30	160	485	1.2
PFN	0.40	SNFC1	1.0	30	45	310	2.2
PFM	0.40	SMFC	1.2	30	45	300	1.9
PFL	0.40	MLS	0.45	30	45	320	6.3
PFS	0.40	SNFC2	0.6	30	50	320	4.3
PFH	0.40	Co-Po	0.15	30	50	310	7.0

*Dosage is based on solid/solid weight/weight of cement

Five superplasticisers (see Table 2) were added to the control mixes at different dosages to obtain concretes with a wide range of workabilities up to flowing concrete (see Table 1).

Code	Superplasticiser Description
MLS	Modified lignosulphonate
SNFC1	Sulphonated naphthalene formaldehyde condensate (Powder)
SNFC2	Sulphonated naphthalene formaldehyde condensate (Liquid)
SMFC	Sulphonated melamine formaldehyde condensate
CP	Co-polymer based on acrylic acid and hydroxy-propyl-methacrylate

Table 2: Superplasticisers used in the investigation

Some mixes were also prepared by substituting 30% of the opc with pulverised fuel ash (pfa).

3. PROPERTIES AND METHODS

Air content, slump, flow table (see Table 1) and cube compressive strength were measured according to the relevant parts of BS 1881 [9]. The porosity was obtained by helium pycnometry using a Micromeritics Autopycnometer. Oxygen permeability was measured using the Leeds cell [7].

Although some of the hardened concrete properties were monitored for ages of up to one year, the results used in this paper correspond to ages of 1, 3, 7, 28 and 90 days. The samples were cured in a fog room kept at 20°C and 100% relative humidity. Prior to testing for porosity and oxygen permeability the samples were dried in an oven at 105°C. This method of drying was found not to affect the order of ranking of oxygen permeability values [10, 11].

4. RESULTS AND DISCUSSION

The abundance of data from the 25 mixes studied required the use of statistical techniques for interpretation and evaluation of the effects of the various parameters measured. The data was therefore analysed using a standard statistical package (Statistical Analysis System, SAS). The models presented have a confidence limit of 95%.

4.1 Parameters affecting permeability

Pore structure characteristics directly affect the permeability of concrete, therefore any parameters influencing these characteristics should have an effect on the resistance of concrete to penetration of gases, liquids and ions.

The statistical analysis allowed the evaluation of a large number of properties of concrete with regard to their effects on permeability. From this analysis the most important properties and the extent to which they affected oxygen permeability (K, m^2) were: water/cement ratio (w/c), age (t, days), air content (a, %) and porosity of the fraction of cement paste of concrete (Pp, %). The statistical model (coefficient of correlation $R^2 = 0.80$) which relates these parameters to permeability is:

$$\text{Log } K = -16.853 + 0.077(a)\ (w/c) - 0.012(t)^{0.66} + 0.037(Pp)(w/c)$$

In this model, the air content and the water/cement ratio are considered interactively since (a) is inversely related to (w/c) and its effect on permeability depends on the value of (w/c), i.e. the lower the value of (w/c) the smaller the effect of (a) on the oxygen permeability (10, 12).

4.2 Relation between permeability, strength and porosity.

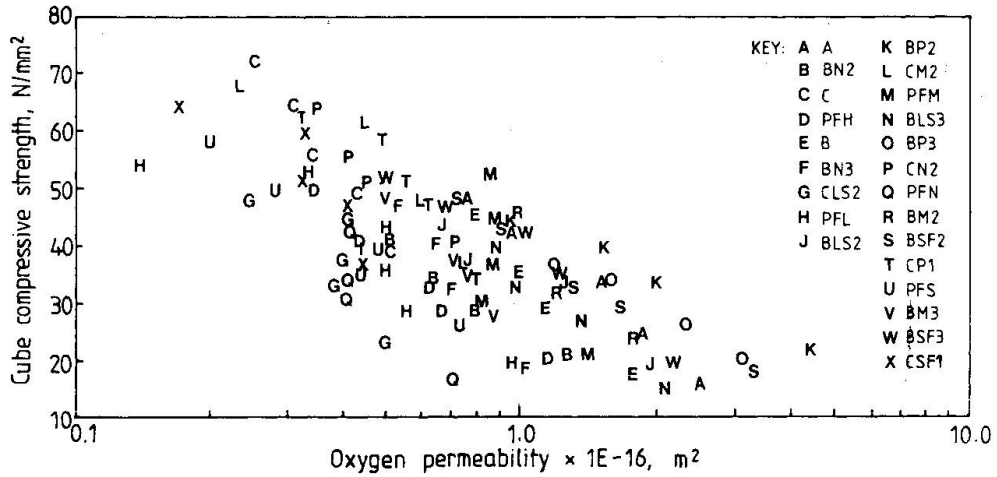

Figure 1: Cloud diagram relating compressive strength to permeability

The compressive strength of concrete is, in most specifications, the dominant parameter used to "control" the quality of concrete. Although there is a good relation between permeability and strength for a particular concrete, the relation cannot be generalised for concretes where the composition is varied either by changing the aggregate-cement ratio or by changing the type of cement or using chemical additives. The results of this investigation confirm the fact that permeability is related to compressive strength for any one mix but when a relationship is attempted for all mixes the result is a cloud diagram as shown in Figure 1. Results reported by Lawrence [13] for concrete mixes made with opc, opc/pfa and opc/slag cured in water at 20°C show similar trends to those shown in Figure 1, i.e. a series of permeability-strength curves within a wide band. Lawrence, [13] however, concludes that there is a single relationship between oxygen permeability and cube strength, despite the fact that his results indicate that at a particular permeability concrete strength varies between 30 and 60 N/mm² depending on the mix.

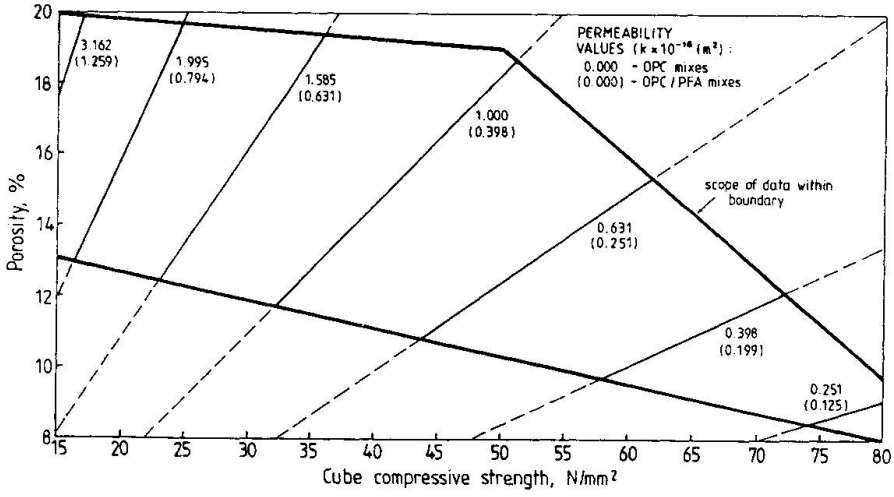

Figure 2: The porosity-strength-permeability model

Statistical analysis of the data gathered in this investigation indicates that oxygen permeability (K) is directly related to porosity (P, %) and inversely related to strength (fcu, N/mm²). The analysis also revealed that the

statistical validity improved by separating the data into two groups; one for opc mixes and one for mixes made with opc/pfa. The models are shown below:

(a) opc concretes:

$$\log K = -15.54 + 1.114 \log \left(\frac{P}{fcu}\right), \quad R^2 = 0.71$$

(b) opc/pfa concretes:

$$\log K = -15.95 + 1.01 \log \left(\frac{P}{fcu}\right), \quad R^2 = 0.85$$

These models are presented in Figure 2, where the cartesian co-ordinates correspond to porosity and compressive strength and parametric space is divided by contour lines of equal permeability.

4.4 Prediction of long-term permeability from early age values

The use of a permeability test as a quality control test would require measurements at early ages during the mix design stage; therefore relations to predict the long-term permeability of concrete from values at early ages would be very useful. From the data collected in this work, a statistical model to predict the permeability of concrete samples up to the age of 90 days from its one-day value (K_1, m^2) has been obtained. The model is:

$$\log K = -3.688 + 0.789 \log K_1 + \frac{0.356}{t} \; ; \; R^2 = 0.89$$

This model can be used to establish tentative one-day permeability values as a criterion for designing for durability at the stage of trial mixes for a particular job, from the knowledge of the permeability of 'good' and 'bad' in-service concrete. In this investigation, oxygen permeability values of in-service 30 year old concretes, both 'good' concrete and 'bad' concrete showing signs of distress and cracking have been obtained; these were 5×10^{-17} (m^2) and 190×10^{-17} (m^2) respectively. If these values are used in the models as the target permeabilities (i.e. K) then the one-day values will be:

For 'good' concrete $K_1 = 1.02 \times 10^{-16}$ m^2

For 'bad' concrete $K_1 = 1.02 \times 10^{-14}$ m^2

These values can be used as a guide to design for durable concrete. It has, however, to be mentioned that for this model to be of general use, the data base has to be expanded to cover a wider range of concrete mixes.

Similar analysis was carried out on chloride permeability and statistical models have also been developed for its prediction [10]. This will be published elsewhere.

5. CONCLUSIONS

(a) The parameters affecting the oxygen permeability of concrete are: air content, water/cement ratio, porosity and age.
(b) Oxygen permeability is related to the porosity/strength ratio. This relationship is influenced by the presence of pfa in the concrete.
(c) Oxygen permeability, porosity and strength influence the performance of concrete in a particular environment, and at least two of these three parameters are required to predict the performance of concrete.
(d) It is suggested that the target value for oxygen permeability, at one day, for design should be 1×10^{-16} m^2.

6. REFERENCES

1. J G Cabrera, "The use of pulverised fuel ash to produce durable concrete", Improvements in Concrete Durability, Thomas Telford, London, 1985, pp 19-35.
2. A R Cusens and J G Cabrera, "Development in Concrete and Related Materials", Institute of Physics, Conference No 89, Session 7, Paper presented on New Materials and their Applications, Warwick, September 1987, IOP Publishing Ltd, 1988, pp 237-249.
3. British Standards Institution, BS 8110:Part 1:1985, Structural Use of Concrete, Code of Practice for design and construction, London, BSI, 1985.
4. European Committee for Standardisation Draft of ENV 206 Concrete - Performance, Production, Placing and Compliance Criteria, CEN, 1988.
5. The Concrete Society, "Permeability testing of site concrete - a review of methods and experience", Report of a Concrete Society Working Party. Permeability of Concrete and its Control, Papers for a one-day conference, London, 12 December 1985, The Concrete Society, 1985, pp 1-68.
6. P B Bamforth, "The relationship between permeability coefficients for concrete obtained using liquid and gas", Magazine of Concrete Research, Vol 39, No 138, 1987, pp 3-11.
7. J G Cabrera and C J Lynsdale, "A new gas permeameter for measuring the permeability of mortar and concrete", Magazine of Concrete Research, Vol 40, No 144, 1988, pp 177-182.
8. J G Cabrera, "Concrete mix design using minimum porosity (in preparation).
9. British Standards Institution BS 1881:1983, Parts 102, 105, 106, 116, London, BSI, 1983.
10. C J Lynsdale, "The influence of superplasticisers on the engineering properties and performance of concrete", PhD Thesis, Dept of Civil Engineering, University of Leeds, in preparation.
11. C Bohring and W Riedel, "Gas permeability of concrete and its influence on the corrosion resistance in salt solution", Proceedings of RILEM/IUPAC on Pore Structure and Properties of Materials, Prague, 1973, pp F95-F118.
12. M F Al-Khoory, "The effect of air entrainment on the permeability of concrete", MSc Dissertation, Department of Civil Engineering, University of Leeds, 1988.
13. C D Lawrence, "Measurements of permeability", Proceedings of the 8th International Congress on the Chemistry of Cement, Rio de Janeiro, 1986, FINEP, Vol V, 1986, pp 29-34.

Retrait de Carbonatation
Karbonatisierungsschwinden
Carbonation Shrinkage

Yves F. HOUST
Chimiste
École Polytechnique Fédérale
Lausanne, Suisse

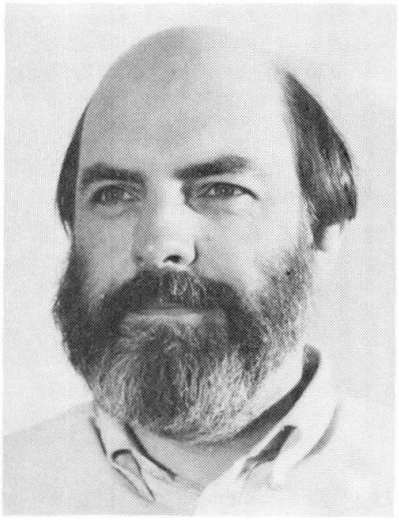

Yves F. Houst, né en 1946, est diplômé de chimie de l'Université de Lausanne. Il travaille dans le domaine des matériaux de construction depuis 16 ans. Il est actuellement chef de la section chimie au Laboratoire des Matériaux de Construction de l'École Polytechnique Fédérale de Lausanne.

Folker H. WITTMANN
Professeur
École Polytechnique Fédérale
Zürich, Suisse

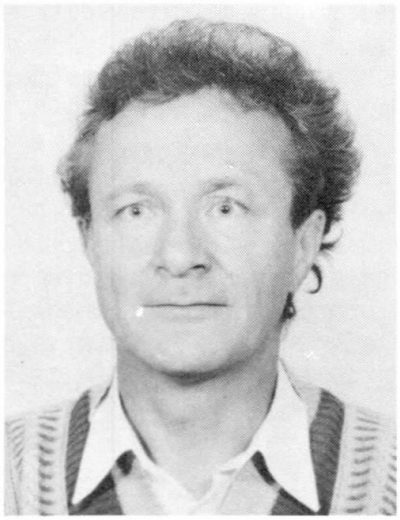

Folker H. Wittmann, né en 1936, est gradué en physique. Il fut 4 ans professeur de matériaux de construction à l'Université technique de Delft (Pays-Bas) et 8 ans à l'École Polytechnique Fédérale de Lausanne. Il est actuellement Professeur ordinaire de matériaux de construction à l'École Polytechnique Fédérale de Zürich.

RÉSUMÉ

Des mesures du retrait de carbonatation ont été effectuées sur des éprouvettes de béton cellulaire de différentes résistances et de la pâte de ciment durcie. L'influence de la teneur en eau et du rapport eau/ciment a été étudiée. Deux mécanismes possibles sont indiqués. La signification du retrait de carbonatation pour la pratique est également discutée.

ZUSAMMENFASSUNG

Das Karbonatisierungsschwinden wurde an Gasbetonproben mit unterschiedlicher Qualität und an Zementsteinproben gemessen. Der Einfluss des Feuchtigkeitsgehaltes und des Wasser/Zement- Wertes wurde untersucht. Zwei mögliche Mechanismen werden vorgeschlagen. Die Bedeutung des Karbonatisierungsschwindens in der Praxis wird diskutiert.

SUMMARY

Carbonation shrinkage of autoclaved aerated concrete with different strengths and hardened cement paste have been measured. The influence of moisture content and of water/cement ratio have been studied. Two possible mechanisms are proposed. The significance of carbonation shrinkage in building practice is also discussed.

1. INTRODUCTION

La carbonatation des bétons et mortiers est un phénomène qui n'altère pas ces matériaux, bien au contraire: la résistance mécanique, le module d'élasticité et la dureté augmentent, la perméabilité aux gaz et aux liquides diminue, les hydroxydes solubles sont transformés en carbonates. Cependant, si le béton est armé, la carbonatation du matériau qui enrobe l'acier d'armature supprime l'immunité dont bénéficie ce dernier. Les aciers peuvent alors se corroder et ainsi limiter la capacité portante des éléments en béton armé. Lorsque les armatures sont proches de la surface du béton, la formation de rouille peut provoquer la fissuration ou l'éclatement du béton superficiel. Ces types de dégâts sont actuellement assez bien connus, parce que malheureusement trop répandus. Il est toutefois un autre inconvénient dont les conséquences négatives sont heureusement plus rares et en général moins graves : c'est le retrait de carbonatation. Lorsque le ciment réagit avec le gaz carbonique, il y a neutralisation des composés basiques et diminution de volume. Cette diminution de volume se traduit par un retrait différentiel entre la surface et le coeur du béton qui est à l'origine de craquelures et de fissures superficielles.

Dans cette communication, on donne les résultats de mesures du retrait de carbonatation du béton cellulaire en fonction de l'humidité relative de l'environnement. Sur des éprouvettes en pâte de ciment durcie on a étudié l'influence du rapport eau/ciment sur le retrait de carbonatation. Les résultats sont comparés avec les données disponibles de la littérature et discutés sur la base des théories proposées.

2. LA CARBONATATION

2.1. La réaction chimique

L'hydratation des deux silicates de calcium du ciment portland conduit à la formation de silicates hydratés et d'hydroxyde de calcium, $Ca(OH)_2$. Les silicates hydratés n'ont pas une composition chimique bien définie et on les symbolise par la formule C-S-H (où C = CaO, S = SiO_2 et H = H_2O). La composition du C-S-H varie et dépend de nombreux facteurs tels que la composition chimique du ciment, la quantité d'eau de gâchage, l'âge, etc... Pour un ciment donné, la quantité de C-S-H et de $Ca(OH)_2$ formés dépend essentiellement du rapport eau/ciment et du temps de réaction. Un calcul simple montre que par exemple dans un m^3 de béton dosé à 300 kg/m^3 d'un ciment portland, plus de 50 kg de $Ca(OH)_2$ sont libérées si l'on admet un degré d'hydratation du ciment de 60%. La teneur en $Ca(OH)_2$ dans le béton peut être réduite de façon importante par l'emploi de matériaux à propriétés pouzzolaniques, comme les pouzzolanes naturelles ou artificielles, les cendres volantes et la fumée de silice condensée (condensed silica fume).

La carbonatation du béton est un phénomène naturel que subit tout matériau à base de ciment. On appelle carbonatation la réaction du gaz carbonique (CO_2) qui est normalement présent dans l'air à raison de 0,03% en volume avec les produits d'hydratation du ciment. Dans les locaux fermés non ventilés, cette teneur peut atteindre 0,1% et même 0,3% dans certaines atmosphères urbaines, des tunnels ou des garages. Les réactions chimiques de carbonatation peuvent être décrites de manière simplifiée par les équations suivantes :

$$Ca(OH)_2 + CO_2 \rightarrow CaCO_3 + H_2O$$
$$C\text{-}S\text{-}H + CO_2 \rightarrow CaCO_3 + SiO_2 + H_2O$$

Ces réactions, qui décrivent des réactions de produits solides avec un gaz, sont très lentes. En réalité, c'est essentiellement le gaz carbonique dissous dans l'eau qui réagit avec $Ca(OH)_2$ en solution et le C-S-H solide, ce dernier étant pratiquement insoluble dans l'eau, tandis que la solubilité de l'hydroxyde de calcium est de 2,5 g/litre à 25 °C. Toutefois, l'eau des pores contient d'importantes quantités d'hydroxydes de sodium et potassium qui sont très solubles et, comme la solubilité de l'hydroxyde de calcium dépend fortement de la présence d'ions OH^-, il n'y a en réalité que de petites quantités de $Ca(OH)_2$ dissous dans la solution des pores du béton. Lorsque le dioxyde de carbone diffuse dans le béton, NaOH et KOH se carbonatent, ce qui augmente la solubilité de $Ca(OH)_2$. Ce dernier doit alors passer en solution pour réagir, ce qui peut prendre un certain temps et expliquer que la propagation de la carbonatation se produit par déplacement d'une zone

qui a une épaisseur variable selon la compacité du béton. Les aluminates du ciment réagissent également pour donner un gel d'alumine [1, p.546].

Une pâte de ciment en équilibre avec l'air ambiant qui a une humidité relative supérieure à 0% contient de l'eau libre (qui s'évapore si l'on diminue l'humidité relative de l'air ambiant). Cette eau est adsorbée à des humidités relatives basses et condensés dans les capillaires pour des humidités plus élevées. Si les pores et les capillaires ne sont pas remplis d'eau, le gaz carbonique peut diffuser dans tout le système poreux [2]. Il se dissout alors dans l'eau condensée où il réagit immédiatement avec les bases.

La réaction de carbonatation principale qui se produit dans le béton peut alors être représentée par l'équation suivante :

$$Ca(OH)_2 + 2H^+ + CO_3^{2-} \rightarrow CaCO_3 \downarrow + H_2O$$

où le $Ca(OH)_2$ doit être dissous avant qu'il puisse réagir. Pour carbonater une couche d'une épaisseur de 1 cm d'un béton contenant 50 kg $Ca(OH)_2/m^3$, on a besoin de.45'000m^3 d'air à 0.033 % de CO_2 par m^3. On comprend mieux ainsi que la carbonatation dans des conditions normales soit un processus lent. $CaCO_3$, le carbonate de calcium qui est le résultat de la réaction existe sous trois formes polymorphes, la calcite, la vaterite et l'aragonite. Bien que la calcite soit la forme la plus stable, les produits initiaux de la réaction de carbonatation naturelle peuvent être l'aragonite ou la vaterite; ces derniers se transforment alors en calcite au cours du temps [1, p.544]. Goodbrake et al. [3] ont trouvé que la principale espèce formée par une carbonatation artificielle était l'aragonite, lorsque les produits d'hydratation peuvent sécher. Toutefois, les conditions de réaction de leur étude étaient bien éloignées de la carbonatation naturelle.

2.2. Variation de volume

La réaction de carbonatation de $Ca(OH)_2$ entraîne une augmentation du volume. Si l'on ne tient compte que des produits solides, l'augmentation de volume de $Ca(OH)_2$ est, selon les produits de réaction formés, la suivante :

	→ calcite ($CaCO_3$)	+ 12 %
portlandite ($Ca(OH)_2$)	→ aragonite ($CaCO_3$)	+ 3 %
	→ vaterite ($CaCO_3$)	+ 19 %

La distribution de la taille des pores d'une pâte de ciment durcie est modifiée par la carbonatation [4]. Elle montre une notable réduction du volume des pores après carbonatation, le phénomène étant plus marqué pour une carbonatation accélérée [5].

La réduction de la porosité entraîne une augmentation des résistances mécaniques. La calcite qui s'est formée consolide la structure de la pâte de ciment durcie. Il est bien connu que le carbonate de calcium qui se forme par carbonatation de $Ca(OH)_2$ est un excellent liant. C'est lui qui assure l'essentiel de la résistance mécanique des mortiers à la chaux. La résistance à la compression et à la flexion de bétons au ciment portland conservés dans une atmosphère de CO_2 peut augmenter jusqu'à 30% par rapport aux mêmes bétons conservés en atmosphère exempte de gaz carbonique [1, p.547]. L'augmentation de résistance est d'autant plus marquée que le rapport eau/ciment du béton est bas [6]. La carbonatation accélérée qui permet l'augmentation des résistances mécaniques entraîne également une diminution du fluage [7] ou une augmentation du fluage si la carbonatation se produit lorsque le béton est sous charge [8]. La dureté, l'imperméabilité et la stabilité de volume sont favorablement influencées par la carbonatation [9].

Les matériaux poreux à base de ciment subissent diverses déformations volumiques que l'on nomme retrait (ou gonflement). Les causes de ces déformations sont multiples et peuvent être classées en quatre catégories[10] :

- retrait thermique lié à une variation de température (causée dans le béton par le refroidissement qui suit l'élévation de température provoquée par l'hydratation du ciment);

- retrait capillaire lié à la formation de ménisques d'eau entre les particules par évaporation superficielle de l'eau de gâchage;
- retrait de dessiccation lié à une diminution de la quantité d'eau dans les pores du matériau;
- retrait chimique (ou gonflement) lié aux réactions chimiques entre le ciment et l'eau ou à la carbonatation par exemple.

Ces divers types de retrait peuvent se produire simultanément, c'est ce qui se passe en général dans la pratique, ou consécutivement. Si l'on élimine le retrait thermique et le retrait de carbonatation qui sera traité plus en détail par la suite, on peut séparer les retraits en *retrait de dessiccation* (sans vieillissement, c'est-à-dire que l'hydratation est bloquée) et en *retrait endogène* d'un béton qui vieillit sans échange d'eau à l'extérieur [11]. Lorsqu'un béton vieillit et sèche en même temps, son retrait n'est pas la somme du retrait de dessiccation et du retrait endogène. Dans la pratique, il faut donc tenir compte de l'interaction de ces phénomènes.

3. PARTIE EXPERIMENTALE

3.1. Béton cellulaire

Des prismes de béton cellulaire 20/20/150 mm ont été prélevés par sciage dans des parpaings de trois qualités courantes du commerce. Ces bétons cellulaires se distinguent essentiellement par leur résistance à la compression et leur masse volumique apparente après séchage à 105 °C, qui est respectivement de 307, 386 et 501 kg/m^3 pour les types L, N et H. Ces prismes ont été placés immédiatement après sciage à différentes humidités relatives dans une enceinte climatique à 25 °C. Les variations de longueurs ont été mesurées au moyen d'un capteur inductif placé sur le prisme posé verticalement. Dès l'obtention de l'équilibre (plus de variation notable de longueur), les prismes ont été mis en contact avec de l'air contenant 2 % de CO_2, ceci toujours à la même humidité relative. Les variations de longueurs ont été mesurées au moyen de capteurs déjà décrits jusqu'à stabilisation.

3.2. Pâte de ciment

3.2.1. Echantillons cylindriques

Les échantillons cylindriques de diamètre 3 mm et de longueur 80 mm ont été obtenus en coulant de la pâte de ciment dans un moule constitué de deux plaques fixées ensemble et percées dans le plan de leurs surfaces communes. Le diamètre et la longueur des trous définissent les dimensions de l'échantillon. Les pâtes de ciment sont injectées au moyen d'une seringue. Les échantillons ont été conservés 28 jours dans l'eau.

A cause de leur fragilité, les échantillons ont été montés sur des bâtis. Ils ont été placés verticalement au sommet d'un triangle équilatéral et collés sur une plaque métallique. Une autre plaque a été collée sur les échantillons. Un appareil simple permet de les positionner correctement et de les tenir en place et parfaitement verticaux pendant le collage. Le dispositif permet de mesurer une moyenne des variations dimensionnelles au moyen d'un seul capteur inductif placé sur la plaque supérieure. Les bâtis ont ensuite été placés dans une chambre climatisée à 25 °C et 55 % h.r. Après obtention de l'équilibre hydrique, on a introduit dans l'enceinte du CO_2 pur.

3.2.2. Echantillons prismatiques

Nous avons utilisé des prismes de pâte de ciment de dimension 3/3/9 mm, prélevés par sciage dans des cylindres de 160 mm de diamètre. La méthode de fabrication de ces cylindres, dont le rapport eau/ciment varie entre 0.3 et 0.8, est décrite dans une autre communication à ce symposium [12]. Ces échantillons ont été montés sur les mêmes bâtis que ceux déjà décrits pour les échantillons cylindriques, mais après au moins une année de conservation dans l'eau. Ensuite, les bâtis ont été placés dans une chambre climatique à 30 °C jusqu'à obtention de l'équilibre. On a alors introduit dans l'enceinte de l'air contenant 2 % de CO2. Le retrait de carbonatation a été mesuré au moyen des capteurs déjà décrits.

4. RESULTATS ET DISCUSSION

Le retrait de carbonatation, mesuré sur les échantillons de béton cellulaire en fonction de l'h.r., est montré à la figure 1. On constate que le retrait a un maximum autour de 80 % h.r. et il diminue brusquement à des humidités plus basses que 70 % h.r. Le béton cellulaire ne contient que très peu de $Ca(OH)_2$. Le retrait est donc à attribuer à la réaction des silicates calciques hydratés avec le CO_2. Vu la grande porosité du béton cellulaire, l'eau libérée pendant la carbonatation ne change pas autant l'h.r. du matériau que dans une pâte de ciment durcie. Il est à remarquer que la densité (type de béton cellulaire) n'a qu'une très faible influence sur le retrait.

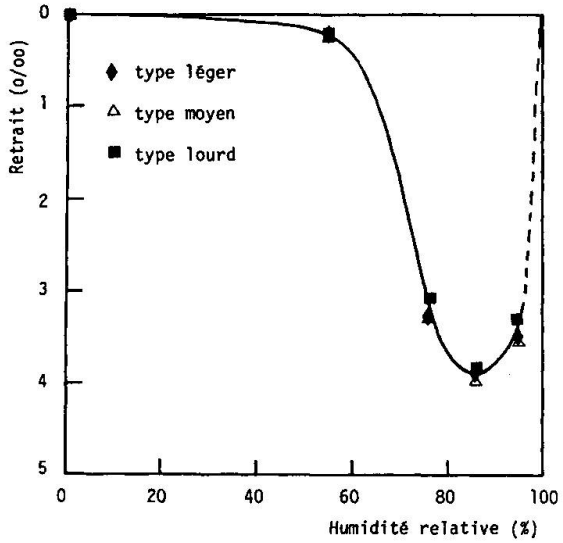

Fig. 1 Retrait de carbonatation de trois types de béton cellulaire autoclavé préalablement équilibré à différentes h.r.

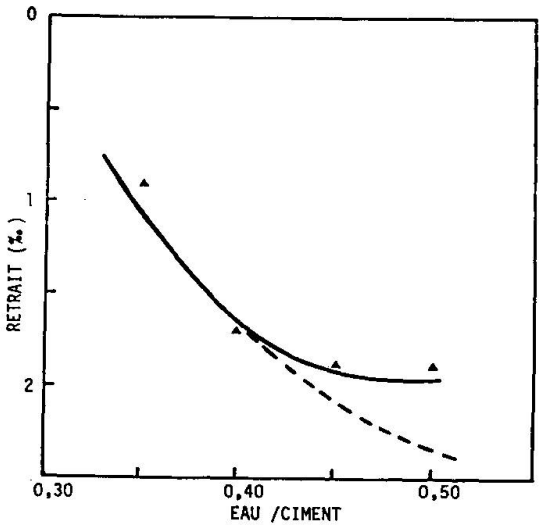

Fig. 2 Retrait de carbonatation de pâtes de pâtes de ciment en fonction de e/c à 55% h.r.

A la figure 2, le retrait de carbonatation mesuré sur des éprouvettes de pâte de ciment durcie équilibrées à 55 % h.r. est montré en fonction du rapport eau/ciment. On constate que le retrait augmente avec le rapport e/c. Il est bien connu que le degré d'hydratation et donc la quantité de produit d'hydratation y inclus le $Ca(OH)_2$ sont plus élevés dans les pâtes avec un rapport e/c plus grand. Pendant la fabrication des échantillons cylindriques avec un rapport e/c plus élevé que 0.4, on n'a pas pu éviter une certaine décantation. Ceci signifie que les valeurs de e/c réelles sont plus basses qu'indiquées à la figure 2 (voir courbe traitillée). Afin d'éviter ce problème, nous avons préparé les échantillons prismatiques décrits ci-dessus. Actuellement, le retrait de carbonatation n'a pas pu être mesuré à cause de la longue période d'équilibrage. Toutefois, les résultats seront présentés au symposium.

A première vue, il est étonnant qu'une réaction chimique qui est associée à une augmentation de volume puisse provoquer du retrait. Il y a plusieurs hypothèses de ce phénomène décrites dans la litérature [13-16]. On sait qu'une partie du $Ca(OH)_2$ est bien cristallisée; on l'observe facilement à l'aide des rayons X. Cependant, environ 20 % du $Ca(OH)_2$ se trouve sous forme colloïdale.

Les cristaux ne subissent pas de retrait de dessiccation, tandis que le gel de C-S-H qui les entoure et la partie du $Ca(OH)_2$ amorphe se rétrécissent. Les cristaux sont donc sous contrainte dans la pâte de ciment durcie partiellement séchée et ils empêchent le retrait. La carbonatation nécessite la dissolution des cristaux et les contraintes peuvent être ainsi libérées. Ce phénomène permet un retrait supplémentaire de la pâte qui entoure les cristaux.

D'autre part, en mesurant l'isotherme d'adsorption, on a constaté qu'à une h.r. donnée la pâte de ciment durcie carbonatée ne contient qu'une fraction de l'eau d'équilibre d'une même pâte non carbonatée. Cette perte d'eau s'explique par le fait que la microstructure des produits d'hydratation devient plus grossière [4]. Ce deuxième mécanisme accroît le retrait de carbonatation.

5. CONCLUSION

Nous avons élaboré une méthode de mesure du retrait de carbonatation. Il est indispensable d'équilibrer les échantillons avant la carbonatation avec des h.r. différentes, si on veut comprendre les mécanismes du phénomène. Etant donné que le retrait de carbonatation est de l'ordre de 1 %, il faut s'attendre que la couche carbonatée soit fissurée. Le risque pour la pratique n'est pas dramatique pour autant qu'il s'agisse d'un béton de bonne qualité. Les techniques modernes de traitement des surfaces du béton permettent de freiner considérablement la carbonatation et les conséquences néfastes.

BIBLIOGRAPHIE

1. LEA F.M., The Chemistry of Cement and Concrete (2nd Ed.), Edward Arnold, London (1970).
2. HOUST Y.F., WITTMANN F.H., The diffusion of carbon dioxide and oxygen in aerated concrete, in (F.H. Wittmann Ed.), Materials Science and Restoration, Technische Akademie Esslingen, Ostfildern (1986) 629-634.
3. GOODBRAKE C.J., YOUNG J.F. and BERGER R.L., Reaction of hydraulic calcium silicates with carbon dioxyde and water, J. Amer. Ceram. Soc., 62 (1979) 488-491.
4. PIHLAJAVAARA S.E., Some results of the effect of carbonation on the porosity and pore size distribution of cement paste, Mat. Constr., 1 (1968) 521 -526.
5. BIER Th.A., KROPP J. and HILSDORF H.K., Carbonation and realcalinisation of concrete and hydrated cement paste in Durability of Construction Materials (J.C. Maso Ed.), Chapman and Hall, London-New York (1987) Vol. 3, pp. 927-934.
6. FREY R. und GOERKE, H.-J., Derzeitiger Stand der Kenntnis des Einflusses der Carbonatisierung auf die Festigkeitseigenschaften von Betonen, TIZ-Fachberichte, 106 (1982) 184-187.
7. ALEXANDRE J., Influence de la carbonatation sur le fluage en compression du béton, Rev. mat. Constr., No 684 (1973) 22-30.
8. PARROTT L.J., Increase in creep of hardened cement paste due to carbonation under load, Mag. Concr. Res., 27 (1975) 179-181.
9. KAMIMURA K., SEREDA P.J. AND SWENSON E.G., Changes in Weight and Dimensions in the Drying and Carbonation of Portland Cement Mortars, Mag. Concr. Res, 17 (1965) 5-14.
10. FERRARIS C.F. et WITTMANN F.H., Retrait de la pâte de ciment durcie, Chantiers/Suisse, 18 (1987) 289-292.
11. BARON J., Les retraits de la pâte de ciment in Le béton hydraulique, Presses de l'ENPC, Paris (1982), chap. 27.
12. HOUST Y.F., WITTMANN F.H., Diffusion de gaz et durabilité du béton armé, Communication à ce symposium.
13. POWERS T.C., A Hypothesis on Carbonation Shrinkage, J. PCA R. & D. Lab., May 1962, pp. 40-50.
14. HUNT C.M. and TOMES L.A., Reaction of blended Portland Cement Paste with Carbon-Dioxide, J. Res. Nat. Bur. Stand., 66A (1962) 473-481.
15. SWENSON E.G. and SEREDA P.J., Mechanism of the Carbonation Shrinkage of Lime and Hydrated Cement, J. Appl. Chem., 18 (1968) 111-117.
16. VERBECK G., Carbonation of Hydrated Portland Cement, ASTM Spec. Techn. Publ. No 205 (1958) 17-36.

Effect of Aggregates on Concrete Properties

Effet des granulats sur les propriétés du béton

Wirkung von Zuschlagstoffen auf die Eigenschaften von Beton

Yoshiaki HIRONAKA
Civil Engineer
Sato Kogyo Co., Ltd
Tokyo, Japan

Y. Hironaka graduated in 1975 as a Civil Engineer from Tokai Univ. He is researching into Acoustic Emission characteristics of concrete structures.

Keizo SAKOTA
Lecturer
Tokai Univ.
Shizuoka, Japan

K. Sakota graduated from Keio University. He is researching into materials of concrete, especially aggregates.

Sadao KIMURA
Civil Engineer
Sato Kogyo Co., Ltd
Tokyo, Japan

S. Kimura gratuated in 1984 from Toyo Univ. and received his M. E. degree in Civil Eng. He is researching into Acoustic Emission characteristics of concrete structures.

Tetsu ISHIBASHI
Civil Engineer
Sato Kogyo Co., Ltd
Tokyo, Japan

T. Ishibashi graduated in 1985 as a Civil Engineer from Kyushu Univ. He is researching into Acoustic Emission characteristics of concrete structures.

SUMMARY

This paper presents a study on the characteristics of concrete with aggregates of inferior quality (low gravity and high absorption). Acoustic emission measurements were performed during uniaxial compressive testing of concrete specimens. According to the results, the quality of aggregates appear more clearly in the static Young's modulus than the compressive strength of concrete. These are simply phenomena caused by the quality of aggregates, but the difference of the fracture process of concrete due to the quality of aggregates is directly indicated by acoustic emission measurements.

RÉSUMÉ

Ce document présente les résultats d'une étude sur les caractéristiques du béton à granulats de qualité inférieure (faible gravité et haute absorption). Les mesures d'émission acoustique ont été exécutées durant l'essai compressif uniaxial d'échantillons de béton. Les résultats on révélé que la qualité des granulats se manifeste plus clairement dans le module de Young statique que dans la résistance du béton à la compression. Ces phénomènes sont causés par la qualité des granulats, mais la différence dans le processus de fissuration du béton due à la qualité des granulats est directement indiquée par les mesures d'émission acoustique.

ZUSAMMENFASSUNG

Diese Arbeit untersucht die Eigenschaften von Beton mit Zuschlagstoffen minderwertiger Qualität (niedriges Gewicht und hohe Absorption). An Betonproben wurden im Verlauf einachsiger Druckprüfungen Schallemissionsmessungen durchgeführt. Die Ergebnisse zeigten, dass sich die Qualität von Betonzuschlagstoffen am deutlichsten im Elastizitätsmodul und nicht in der Druckfestigkeit von Beton zeigt. Anhand der Schallemissionsmessungen war es jedoch möglich, das unterschiedliche Bruchverhalten von Beton in Abhängigkeit von der Qualität der Zuschlagstoffe direkt zu bestimmen.

1. INTRODUCTION

Deterioration of aggregates caused by exhaustion of sound aggregates has become a widespread problem. It is generally known that physical quality of aggregate effects the strength, Young's modulus and durability of concrete. The factor of these effects is considered to be the lower strength of aggregate compared to the strength of mortar or cement paste matrix. So, it is assumed that because of excessive load or repeated load, destruction occurs inside or on the surface of aggregates before it occurs inside mortar or cement paste matrix.Therefore, reduction of water cement ratio of concrete in order to make compensation for the low strength of aggregate is a generalized method. However, the fracture process of concrete with inferior aggregates not yet elucidated must be clarified in order to use such aggregates for concrete. In this paper, the fracture process of concrete with water cement ratio varying from 30 to 70% and with several kinds of aggregates contained is studied by AE measurement and observation with a microscope.

2. PROPERTIES OF AGGREGATES AND MIX PROPORTIONS OF CONCRETE

Table-1 shows the properties of aggragates used for the experiments. Sound aggregates are River Sandstone and River Sand. Inferior coarse aggregate is Crushed Andesite. And inferior fine aggregate is Scoria. Mix proportions of concrete are shown in Table-2. Water cement ratios are 30,50, and 70%. The volume of each material is fixed in order to make clear comparison of effect of aggregates. Table-3 shows the combination of coarse and fine aggregates.

3. PROCEDURE OF EXPERIMENTS

Fig-1 shows the AE measurement system employed during the uniaxial compressive testing of the specimens. The diameter of the specimen is 10cm and the height is 20cm. AE measurement system includes the one-dimensional location system using two transducers installed on the side of the specimen in the axial direction. Determination of AE source location was performed only at the center portion (10cm) of the specimen in the axial direction in order to eliminate the effects of noise generated by the friction between the specimen and the loading plates. Table-4 shows the conditions of AE signal detection. Compressive loading test was carried out using a teflon sheet laid between the loading plate and the specimen to minimize the generation of noise. Loading rate was set at 500N/sec. Three specimens for each combination were used for the observation of cracks either inside or on the surface of aggregates.At first, 30% of the breaking load was applied and removed. The specimen was cut and polished after loading, then inspected with a microscope. In this way, 50% and 100% of the breaking load was applied and observation was performed respectively.

4. RESULTS AND CONSIDERATION OF THE EXPERIMENTS

4.1 Compressive strength and Young's modulus

Figs-2,3 show the compressive strength and the Young's modulus of concrete containing several kinds of coarse aggregates. The compressive strength of the concrete with inferior coarse aggregate was lower than that of the concrete with sound aggregate. However, according to the result of the experiment, the compressive strength showed a variation of 10%. Therefore, there will be some cases where the quality of aggregate cannot be accurately evaluated by the compressive strength of the concrete. According to Fig-3, the difference of Young's modulus caused by the quality of aggregate was more conspicuous than

TABLE-1 PROPERTY OF AGGREGATES

	Specific gravity	Absorption (%)	Kind of stone
Sound Coarse Aggregate	2.62	0.81	Sandstone
Inferior Coarse Aggregate	2.26	4.66	Crashed Andesite
Sound Fine Aggregate	2.59	1.02	Sandstone
Inferior Fine Aggregate	1.94	15.11	Scoria

TABLE-2 MIX PPOPORTION OF CONCRETE

W/C (%)	s/a (%)	W (kg/m³)	C (kg/m³)	S (ℓ/m³)	G (ℓ/m³)
30	40.8	189	630	249	361
50	44.9	189	378	310	381
70	48.8	189	270	354	371

TABLE-3 COMBINATION OF AGGREGATES

Fine Aggregate	Coarse Aggregate	W/C (%)		
		30	50	70
Sound	Sound	SS3C	SS5C	SS7C
Sound	Inferior	SI3C	SI5C	SI7C
Inferior	Sound	IS3C	IS5C	IS7C

TABLE-4 CONDITIONS OF AE DETECTION

Wave Speed	3500-4500	(m/sec)
Attenuation	35	(dB/m)
Pre-gain	40	(dB)
Main-gain	40	(dB)
Threshold Level	1.0	(V)

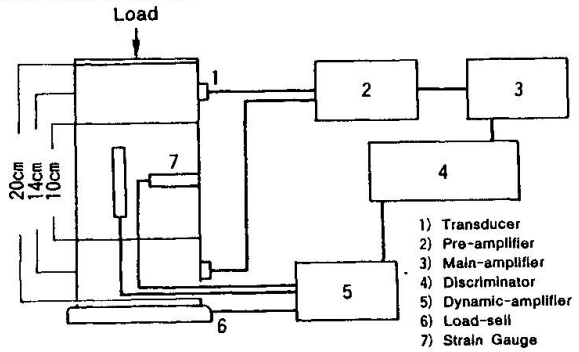

FIG-1 AE MEASUREMENT SYSTEM

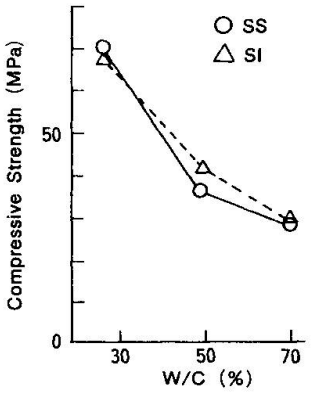

FIG-2 COMPRESSIVE STRENGTH OF SI SERIES

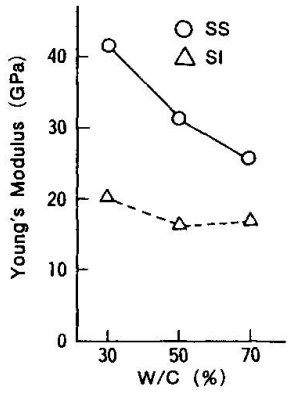

FIG-3 YOUNG'S MODULUS OF SI SERIES

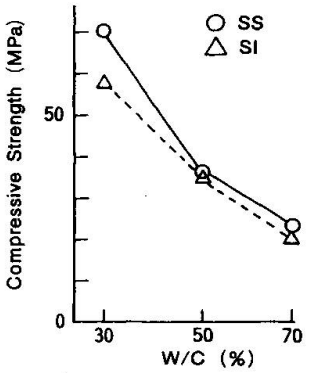

FIG-4 COMPRESSIVE STRENGTH OF IS SERIES

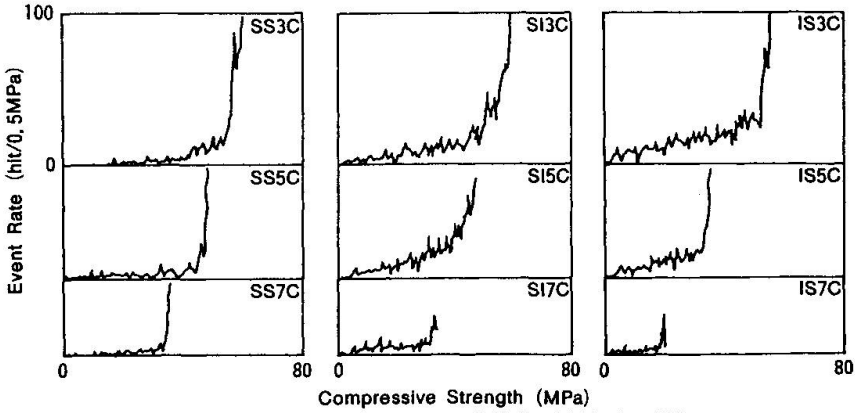

FIG-5 RELATION BETWEEN COMPRESSIVE STRESS AND EVENT RATE OF AE

that of compressive strength. Fig-4 shows the results of compressive test of concretes which contained several kinds of fine aggregates. These results also show that the compressive strength of concrete with inferior sand was lower than that of concrete with sound sand.

4.2 Compressive stress and AE events

Fig-5 shows the relationship between compressive stress and event rate of AE detected from the concrete with sound aggregate (SS series), sound fine aggregate and inferior coarse aggregate (SI series) and inferior fine aggregate and sound coarse aggregate (IS series). The event rate means the number of AE per loading stress of 0.5MPa. These results show that, in the case of the SS series, most AE signals occured at the stress near the breaking point without reference to the water cement ratio. On the other hand, in both cases of the SI and IS series, a large amount of AE signals occured from the low stress level stage, and this phenomenon was obvious in the concrete with a low water cement ratio of less than 50%. The difference of AE characteristic is assumed to be caused by the quality of aggregate. It is considered that the sound aggregate can accumulate the strain energy,so that the generation of micro cracks inside or on the surface of aggregate are restrained at a low stress level. In addition, at the stress near the breaking point, a precipitious destruction occur. This tendency is considered to be remarkable in the concrete with low water cement ratio because the effect of breeding or vacant spaces around the aggregate become negligible in such concrete. But the effect of water cement ratio was not confirmed in the experiments on the SS series. On the contrary, in the case of concrete with inferior coarse aggregate, the stiffness of coarse aggregate is the same or lower than that of mortar. Accordingly, it is assumed that many micro cracks inside or on the surface of aggregate are generated at a low stress level because of the small capacity of strain energy accumulated in aggregate and the stress concentration on them. In the concrete with inferior fine aggregate, the stiffness of mortar is much lower than that of coarse aggregate, therefore, the inside or on the surface of fine aggregate is considered to be easily destructed because of the stress concentration on the mortar.

4.3 Peak amplitude distribution of AE

Fig-6 shows the relationship between the peak amplitude and event counts of AE signals. Specimens are the SS series, the SI series and the IS series concrete with water cement ratio of 30%. In the figure, the stress level i.e. the percentage of compressive stress to the compressive strength, is divided into 2 ranges (0-50%, 0-100%), and the amplitude distribution curve for each range is shown respectively. The solid line is the approximation of the amplitude distribution curve. At the stress level of 0-50%, in the case of SS3C, the event counts of AE were generally small, regardless of amplitude. However, in the case of SI3C or IS3C, many AE signals with small amplitude of 0.1-1.0mv were detected. Then at the stress level of 0-100%, the event counts of AE detected from every specimen increased, but the amplitude distribution showed a tendency to vary with the quality of aggregate. In the case of SS3C, a considerable number of AE with large amplitude, apx. 10mv, were detected. On the contrary, in the case of SI3C or IS3C, most AE signals showed small amplitude of 0.1-1.0mv. This phenomenon is considered to be caused by the quality of aggregate, that is, the difference of the capacity of strain energy accumulated in the aggregate as mentioned in 4.2. Therefore, the fracture process of the concrete with inferior aggregate is different from that of the concrete with sound aggregate.

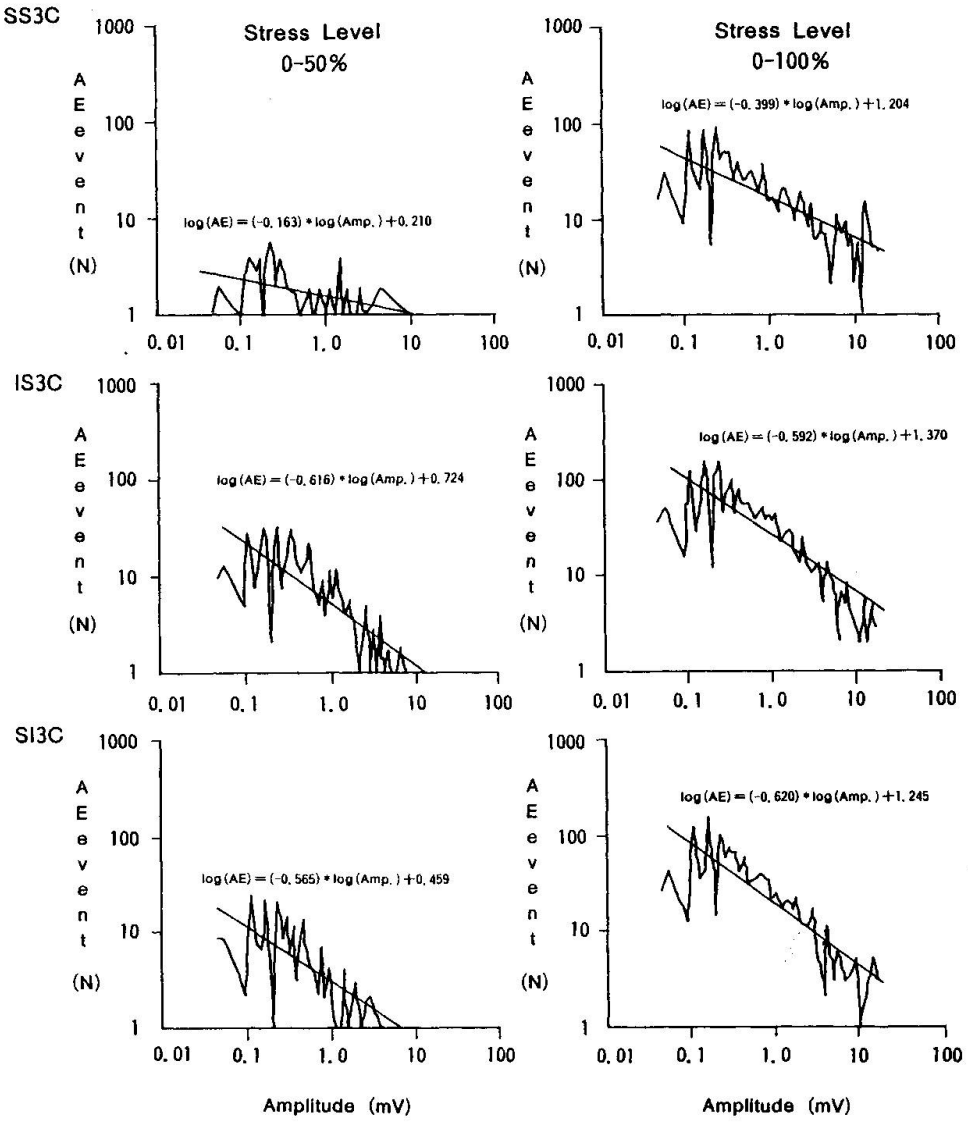

FIG-6 RELATION BETWEEN THE MAXIMUM AMPLITUDE AND EVENT COUNT OF AE

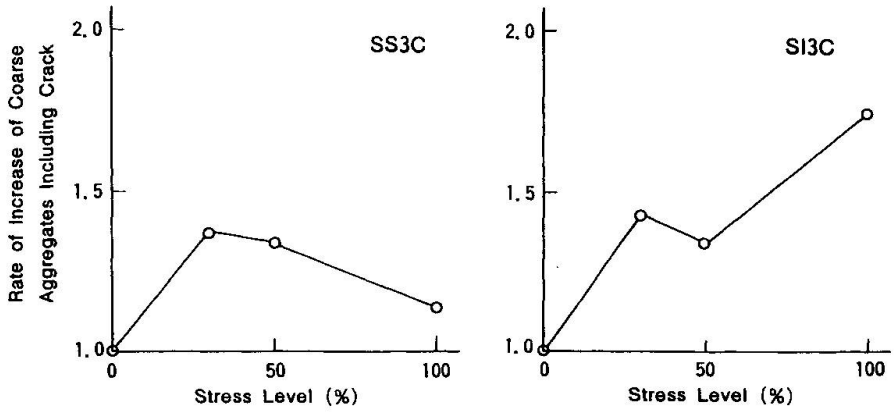

FIG-7 RELATION BETWEEN THE STRESS LEVEL AND THE RATE OF THE INCREASE OF COARSE AGGREGATES WITH CRACK INSIDE THEM

4.4 Micro cracks inside aggregates

Fig-7 shows the relationship between the stress level and the rate of increase of coarse aggregate with crack inside them. The rate of increase of coarse aggregate with crack was obtained by the following process.

1) To obtain the rate of destruction of coarse aggregate in the section of the specimen by observation with a microscope.

$$R = Gc/Go$$

where, R : the rate of destruction of coarse aggregate
Gc : the number of coarse aggregate with crack inside of them
Go : total number of coarse aggregate in the section of the specimen

2) To obtain the rate of increase of coarse aggregate with crack using the following equation.

$$C = Ra/Ro$$

where, C : the rate of increase of coarse aggregate with crack
Ra : the rate of destruction of coarse aggregate at the stress level of a %
Ro : the rate of destruction of coarse aggregate before loading

The results show that the number of inferior coarse aggregate with crack increased in proportion to the stress level while the number of sound aggregate with crack didn't indicate such a tendency. But, the fracture process of scoria which includes many voids in it, could not be confirmed clearly.

5. CONCLUSION

We conclude from the experiment as follows.

(1) Both compressive strength and static Young's modulus of the concrete containing inferior aggregates with low gravity and high absorption are lower than those of the concrete with sound aggregates. But because of the variation of compressive strength, there will be some cases where the quality of aggregate cannot be evaluated accurately by the compressive strength of concrete.
(2) During the uniaxial compressive testing of the concrete with sound aggregates, most of AE signals occur at the stress level near the breaking point. However, in the concrete with inferior aggregates, a large amount of AE are generated from the low stress level stage because of destruction inside or on the surface of aggregates.
(3) During the uniaxial compressive testing, many AE signals with relatively large amplitude are generated from the concrete with sound aggregates. On the contrary, amplitude of AE signals generated from the concrete containing inferior aggregates are generally small. This phenomenon is considered to be caused by the quality of aggregate including capacity of strain energy accumulated in them.

Accordingly, the quality of aggregate appears more clearly in the static Young's modulus than the compressive strength of the concrete containing them. These are simply the phenomena caused by the quality of aggregate and can by no means indicate the difference of the fracture process of the concrete. However, the difference of the fracture process of concrete due to the quality of aggregate is obviously indicated by the resuls of AE measurement during uniaxial compressive testing.

Durabilité du béton à haute résistance

Dauerhaftigkeit von Beton mit hoher Festigkeit

Durability of High Strength Concrete

Guy TACHÉ
Ing. CNAM
CEBTP
Paris, France

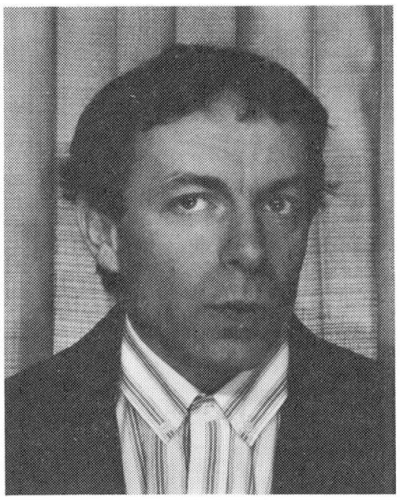

Jacques TRINH
Dr. Ing.
CEBTP
Paris, France

RÉSUMÉ

Cette communication traite de la durabilité du béton à haute résistance en présentant une étude expérimentale réalisée au CEBTP. Deux solutions de poutre fléchie sont comparées, une en béton de résistance courante, et l'autre en béton à haute résistance permettant une réduction de 25% de matière. Elles ont montré une durabilité comparable après avoir été exposées en atmosphères corrosives pendant deux ans.

ZUSAMMENFASSUNG

Dieser Beitrag behandelt die Dauerhaftigkeit von hochfestem Beton durch die Darstellung der im CEBTP durchgeführten experimentellen Forschungsarbeiten. Zwei Lösungen für Biegebalken, einer aus Normalfestigkeitsbeton, der andere aus Hochfestigkeitsbeton — wodurch eine Werkstoffeinsparung von 25% möglich wird — wurden verglichen. Sie zeigten eine vergleichbare Dauerhaftigkeit, nachdem sie zwei Jahre aggressiven Umweltbedingungen unterworfen worden waren.

SUMMARY

The paper deals with the durability of high strength concrete by presenting an experimental study carried out by the CEBTP. Two solutions for flexural beams are compared, one using concrete of normal strength and the other with a high strength concrete allowing a material saving of 25%. They have shown a comparable durability under corrosive atmospheres over a period of two years.

1. INTRODUCTION

L'accroissement de la résistance du béton ($f_{cm} \simeq 85$ MPa) entraîne une amélioration certaine de la compacité du matériau, par rapport à ce qui existe dans du béton de résistance plus usuelle ($f_{cm} \simeq 50$ MPa). C'est une meilleure garantie de la pérennité, que le béton à haute résistance offre avantageusement. Il reste cependant à la vérifier au niveau structural, du fait que dans le béton armé normal et le béton partiellement précontraint la fissuration peut induire la corrosion des armatures.

Toutefois de nombreuses études expérimentales ont été entreprises dans le monde aux fins d'étudier l'influence des fissures sur le développement de la corrosion des armatures. Citons les suivantes, parmi les plus importantes.

- CARPENTIER et SORETZ [1], en examinant des poutres en béton armé à la fois soumises à un chargement statique ou cyclique, et exposées à diverses aspersions agressives pendant une période de 2 ans, ont conclu que :
. l'effet de pompage ("respiration" des fissures) favorise la corrosion des armatures ;
. les fissures parallèles aux barres d'armature sont plus néfastes que celles qui leur sont transversales ;
. avec un enrobage suffisant en béton de bonne qualité, des fissures d'ouverture 0,3 mm n'induisent que des piqûres de corrosion peu dommageables.
- SCHIESSL [2] a étudié le comportement des poutres en béton armé exposées pendant 10 ans dans diverses atmosphères (urbaines, industrielles et marines). Les ouvertures des fissures étaient entre 0,15 et 0,4 mm. L'auteur a relevé que si dans les premiers temps (1 an) le taux de corrosion est fonction croissante de la largeur des fissures, au bout de 10 ans il n'existe plus de corrélation directe.
- Par l'examen de poutres conservées pendant 2 ans dans une ambiance de brouillard salin, ATIMTAYE et FERGUSON [3] ont indiqué que les facteurs primordiaux du phénomène, sont:le rapport eau/ciment ; l'épaisseur de l'enrobage des armatures; et le diamètre des barres. La fissuration semble n'avoir guère d'influence directe.
- MAKITA, MORI et KATAWAKI [4] ont observé, sur des poutres en béton armé, laissées pendant 3 ans dans la baie de Tokyo, qu'avec du béton gâché à l'eau douce, le taux de corrosion croît avec l'ouverture des fissures. Avec de l'eau de mer, les attaques se produisent indifféremment à proximité ou hors des fissures. Les auteurs ont recommandé de limiter la largeur des fissures du béton en surface de l'armature à 0,1 mm !

Ces quelques exemples et d'autres [par ex. 5, 6], concourent à forger l'opinion selon laquelle la largeur des fissures en surface du béton n'est pas un facteur primordial au développement de la corrosion des armatures. Mais toutes ces recherches sont difficilement comparables entre elles. Par ailleurs, il manque encore des références pour des poutres en béton à haute résistance d'une part, et d'autre part, la précontrainte partielle (b.p.p.) à cause du risque de corrosion de l'armature de précontrainte.

2. ETUDE EXPERIMENTALE ENTREPRISE

Dans le cadre du programme général d'études sur la durabilité des structures en précontrainte partielle [7], deux des corps d'épreuve sont réalisés avec du béton de résistance moyenne en compression d'environ 85 MPa. Ce sont des poutres en Té isostatiques (fig. 1), identiques à des poutres associées confectionnées avec du béton de résistance ($f_{cm} \simeq 50$ MPa) à l'exception que l'épaisseur de l'âme et du hourdis est diminuée de 25 %. Les principales informations sur les bétons sont portées au tableau 1.

Un examen préliminaire sous chargement mécanique a montré que l'on est arrivé à obtenir pour les deux solutions, un comportement tout à fait comparable en

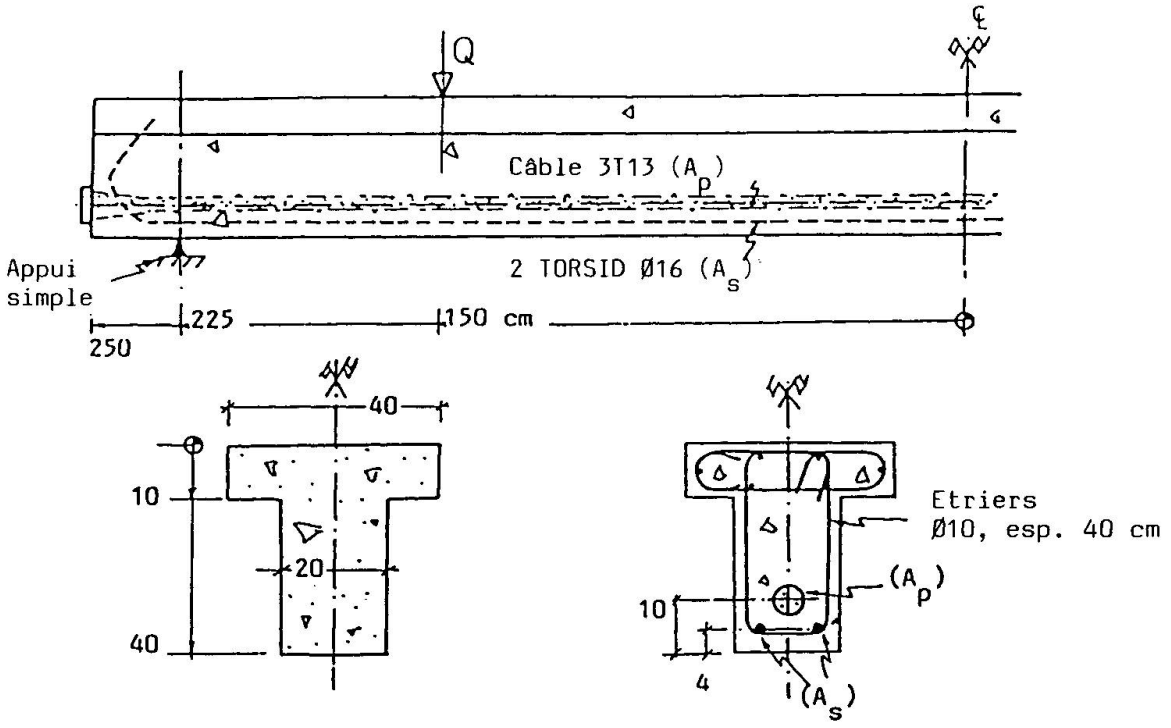

a) Poutres pour béton à résistance 50 MPa

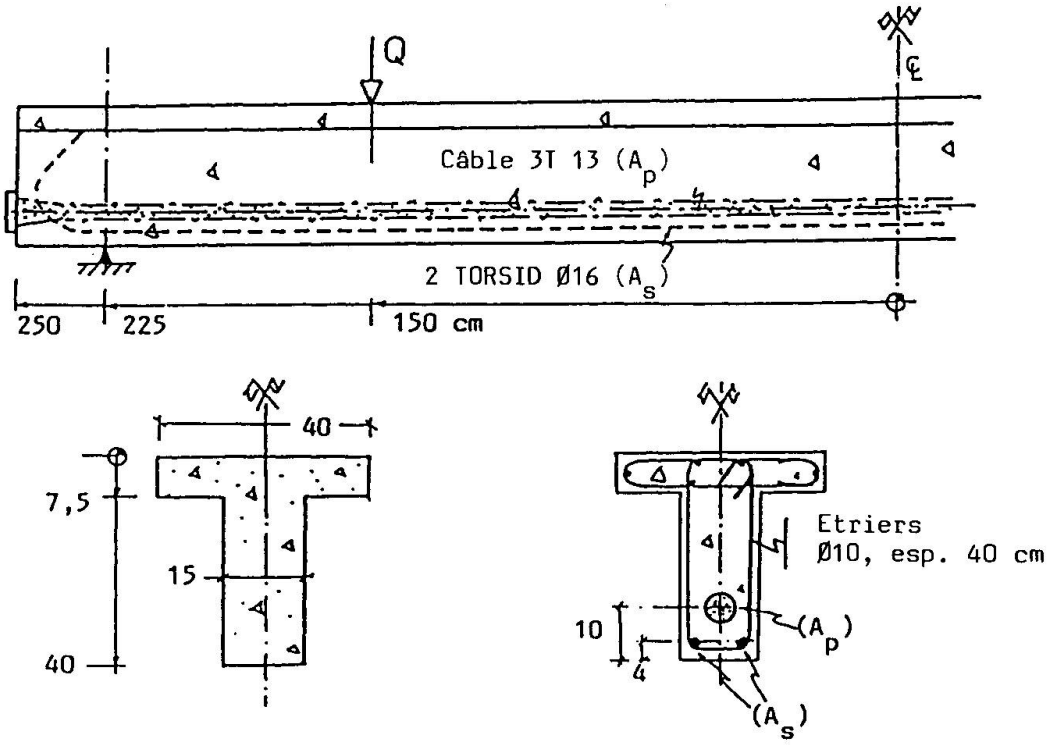

b) Poutres pour béton à résistance 85 MPa

Fig. 1 - Poutres d'essai

		Béton à	
		performance usuelle	haute résistance
(kg/m³)	Granulats (5/20 mm).....	1 080 (1)	1 267(2)
	Sable (0/5 mm).....	720 (1)	326(2) + 326 (1)
	Ciment.....	CPA HP : 350	CPA HP : 425
	Eau.....	190	145
	Plastifiant Sikafluid.....	/	6,37
	Affaissement (mm).....	60	50
	Age à l'essai (jours).....	52	53 et 58
(MPa)	Résistance en compression f_{cj} (3)..	50	85
	Résistance en traction f_{tj}.....	3,7	4,5
	Module de Young E_c	34 000	51 000

(1) Matériaux silico-calcaires de Seine.
(2) Calcaire du boulonnais (concassé).
(3) Essais sur cylindres standards (Ø = 16, h = 32 cm) en compression simple ou en fendage.

TABLEAU 1
Composition des bétons et principales propriétés mécaniques
(recherches NY et OL)

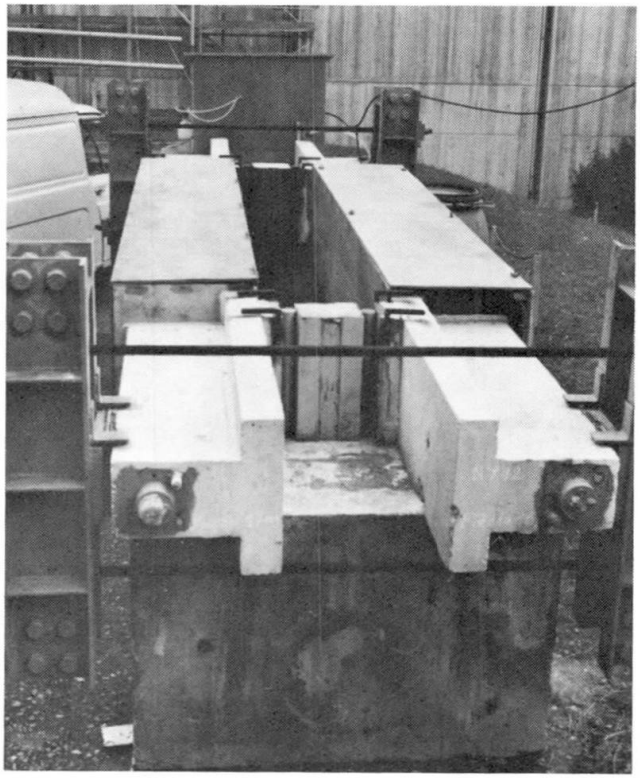

Fig. 2 - Dispositif d'exposition

service selon les règles françaises de calcul BPEL 83 [8].

Chacune des poutres est ensuite conservée durant 2 ans: .dans l'état fléchi atteint à l'application au départ du chargement correspondant à la limite de la précontrainte partielle suivant le BPEL 83. Ainsi les fissures en surface ont une ouverture permanente d'environ 0,15 mm et 0,20 mm, respectivement à la hauteur de l'armature de précontrainte et de l'armature passive ;

. dans une enceinte contenant une atmosphère agressive (fig. 2). Les deux environnements retenus sont, soit une atmosphère constituée d'un mélange gazeux à 50 % d'air et 50 % de CO 2 ; soit une aspersion intermittente (1/4 heure à chaque heure) d'une solution à 35 g de NaCl/litre.

Les conditions thermiques sont celles normales extérieures de Saint Rémy lès Chevreuse (France).

Le suivi pendant l'exposition des poutres est principalement orienté vers :

. la corrosion des armatures, par la mesure du potentiel électrochimique du ferraillage ;
. la pollution du béton, par prélèvement aux fins d'analyses chimiques (détermination des chlorures totaux, et de silice soluble).
Les corps d'épreuve sont aussi examinés périodiquement pour faire la constatation de taches de rouille, d'éclats de béton d'enrobage, des ouvertures de fissures, etc.

Au terme du temps d'exposition, il était prévu de faire un chargement statique des corps d'épreuve pour évaluer la capacité portante résiduelle, et permettre l'examen de l'état des armatures.

3. RESULTATS

3.1 Suivi de la corrosion des armatures

Les diagrammes de la figure 3 montrent l'évolution de la valeur moyenne du potentiel électro-chimique en fonction du temps pour les deux conditions d'exposition retenues.

On y constate qu'en exposition saline, la passivation des aciers survient très vite. De même qu'apparaissent des gradients importants localisés près des fissures où des coulures de rouille sont observées. Avec le temps la dépassivation générale persiste, avec toutefois une tendance à la repassivation à la fin de la 2e année. les gradients tendent également à diminuer mais leur localisation est conservée.

En atmosphère chargée en gaz carbonique, la valeur moyenne n'évolue pratiquement pas, c'est caractéristique de la passivité de l'acier d'armature. Des gradients locaux existent au départ,notamment aux fissures du milieu de la poutre, mais ils s'estompent avec le temps. Ce corps d'épreuve ci a conservé au bout des 2 ans, un aspect parfaitement sain.

3.2 Rupture finale

Seule la poutre conservée en milieu salin ayant montré certaines dégradations (coulures de rouille aux fissures, quelques éclats de l'enrobage) est ensuite soumise à l'essai de chargement jusqu'à rupture. Il n'a pas été constaté toutefois de perte de résistance, ni de ductilité.

L'armature passive présente quelques zones corrodées correspondant à des sections fissurées, de même que les cadres transversaux qui peuvent s'y trouver. Mais aucune corrosion particulière n'est apparue sur la gaine métallique du câble de précontrainte.

Ces résultats sont très analogues à ceux acquis sur des poutres associées confectionnées avec du béton de résistance plus courante.

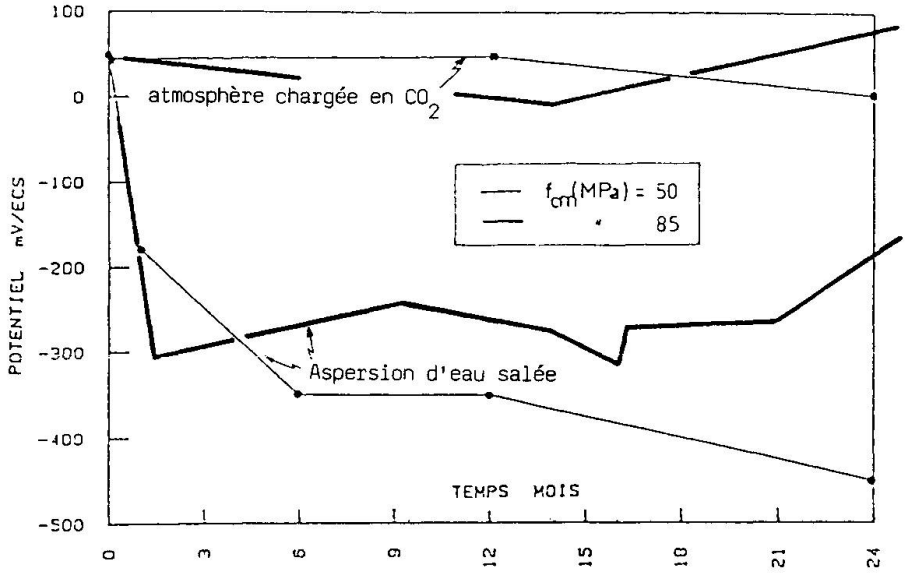

Fig. 3 - Evolution du potentiel électro-chimique.

4. PREMIERE CONCLUSION

Ces essais apportent des références de durabilité de pièces partiellement précontraintes en béton à haute résistance. On peut donc, au vu de ces résultats, escompter une pérennité, comparable au béton de résistance plus usuelle, bien que la solution permet une réduction de béton (≃ 25 %). Toutefois il est encore souhaitable de disposer de résultats d'observations à plus long terme (que 2 ans)

BIBLIOGRAPHIE

1. CARPENTIER L. & SORETZ M.S., Contribution à l'étude de la corrosion des armatures dans le béton armé. Annales de l'ITBTP N° 223-224, Paris, Juillet-Août 1966.
2. SCHIESSL P., Admissible crack-Width in reinforced concrete structures. Colloque inter-Associations "Comportement en service des ouvrages en béton", Liège, Juin 1975.
3. ATIMTAYE & FERGUSON P.M., Early chloride corrosion in reinforced concrete. ACI Journal 55, nov. 1973.
4. MAKITA M, MORI T. & KATAWAKI, Marine corrosion behaviour of reinforced concrete. ACI S.P 65, 16.
5. BEEBY A.W., Corrosion of reinforcing steel in concrete and its relation to cracking. The Structural Engineer, N° 3, Vol. 56 A, Mars 1978.
6. TACHE G. & TRINH J., Fissuration et durabilité du béton partiellement précontraint. Compte rendu du Symposium AIPC, Paris-Versailles 1987.
7. FOURÉ B & TRINH J., Quelques résultats de recherches appliquées au calcul pratique des structures en béton. Annales ITBTP, N° 469, Paris, Nov. 1988.
8. HOANG L.H. & TRINH J., Experimental behaviour in bending of high strength concrete beams. Symposium "Use of High Strength Concrete", Stavanger, mars 1987.

Verbundmittel in spritzbetonverstärkten Stahlbetonbalken

Bond anchors in Shotcrete Reinforced Beams

Goujons d'adhérence dans des poutres renforcées par du béton projeté

Horst G. SCHÄFER
Prof. Dr.-Ing.
Universität Dortmund
Dortmund, BR Deutschland

H. G. Schäfer, geb. 1936, promovierte als Bauingenieur an der TH Darmstadt. Er arbeitete bei der Baufirma Wayss & Freytag und im Ingenieurbüro BGS in Frankfurt. Er lehrte an der TH Darmstadt, war vier Jahre für die GTZ in Dar es Sallam (Tanzania) tätig, bevor er 1985 einem Ruf an die Universität Dortmund folgte.

Gerhard BÄÄTJER
Dr.-Ing.
Universität Dortmund
Dortmund, BR Deutschland

G. Bäätjer, geboren 1941, studierte Bauingenieurwesen an der TU Hannover. Er arbeitete vier Jahre bei der Baufirma Philipp Holzmann im Technischen Büro in Köln. Anschliessend war er an der Ruhr- Universität Bochum tätig, promovierte dort und wechselte 1986 an die Universität Dortmund.

ZUSAMMENFASSUNG

Die Biegetragfähigkeit von Stahlbetonbalken kann vergrössert werden, indem Zulagebewehrung in eine Spritzbetonschicht eingebettet wird. An zwei Versuchsbalken wird der Einfluss von Verbundankern in der Verbundfuge auf das Tragverhalten untersucht. Bis nahe an die Bruchlast verhalten sich spritzbetonverstärkte wie monolithisch hergestellte Balken. Mit Verbundankern versagen die Träger mit Vorankündigung, ohne Verbundanker gehen sie schlagartig zu Bruch.

SUMMARY

The flexural bearing capacity of reinforced concrete beams can be increased by embedding additonal reinforcing bars in a layer of shotcrete. The influence of adhesive anchors crossing the interface between concrete and shotcrete is being studied on two test beams. Up to near failure load the bearing behaviour is the same as for monolithically cast beams. With the application of bond anchors, however, there are evident signs of failure beforehand, whereas the absence of bond anchors leads to an abrupt collapse.

RÉSUMÉ

La résistance à la flexion de poutres en béton armé peut être augmentée par encastrant de l'armature additionelle dans une couche de béton projeté. L'influence de goujons d'adhérence traversant la surface entre le béton original et le béton projeté est étudiée à deux poutres d'essai. Jusqu'au près de la charge de rupture le comportement est le même que pour des poutres en réalisation monolithe. Par l'application de goujons d'adhérence la rupture s'annonce à temps, tandis que l'absence d'un ancrage a pour conséquence une rupture subite.

1. PROBLEMSTELLUNG

Zur nachträglichen Verstärkung von Stahlbetonbalken ist die Spritzbetontechnik besonders geeignet [1, 2]. Nach den deutschen Richtlinien [3] und Normenentwürfen [4] sind zur Übertragung der Schubkräfte in der Verbundfuge "Verbundmittel" anzuordnen. Dieses Bemessungskonzept führt bei nur unterseitig verstärkten Stahlbetonbalken auf Verbundmittelquerschnitte, die häufig nicht untergebracht werden können. Aus diesem Grunde wird an der Universität Dortmund ein Forschungsvorhaben durchgeführt mit dem Ziel, den tatsächlich erforderlichen Bedarf an Verbundmitteln zu ermitteln.

2. VERSUCHSKÖRPER

Um die Grenzen auszuloten, wurden bisher zwei Balken untersucht (Fig. 1). Die beiden Balken waren so ausgelegt, daß die Bügel im Altbeton ausreichende Reserven zur Aufnahme der erhöhten Schubkräfte nach der Verstärkung der Biegezugbewehrung aufwiesen. Über Versuche an Balken mit zugelegter Biegezug- und Schubbewehrung berichtet Eibl [5]. Die beiden Versuchsbalken (VB) unterschieden sich in der Anzahl der Verbundmittel:

- VB1 wurde mit 29 HILTI-Verbundankern M 16 in gleichmäßigen Abständen von 15 cm in versetzter Anordnung vorschriftengemäß ausgelegt;
- in VB2 wurden nur an den Enden der Spritzbetonverstärkung je 2 HILTI-Verbundanker M 10 eingebaut.

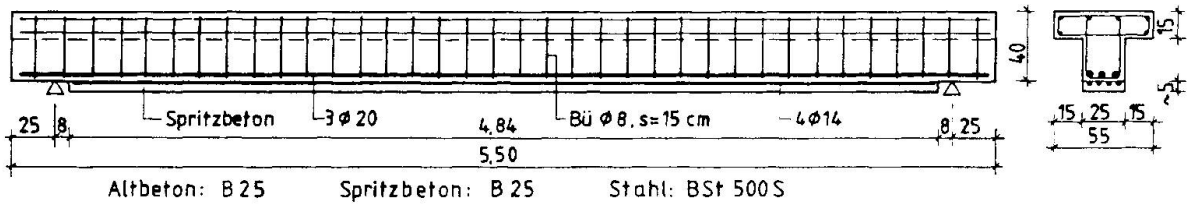

Fig. 1 Abmessungen und Bewehrung der Versuchsbalken (Verbundmittel n. dargest.)

Der Spritzbeton wurde in zwei Lagen im Trockenspritzverfahren aufgetragen; der Altersunterschied zwischen Altbeton und Spritzbeton betrug bei VB1 42 Tage und bei VB2 36 Tage.

3. VERSUCHSDURCHFÜHRUNG

Die Stützweite der Balken wurde im ersten Versuchslauf zu l = 5 m gewählt (Fig. 2). Im zweiten Versuchslauf an der intakten Hälfte wurden die Balken um die Vertikalachse gedreht und so in die Prüfmaschine eingebaut, daß sich die Stützweite auf l = 3 m verkürzte und der Prüfzylinder in der Feldmitte stand.

Erster Versuchslauf (l = 5,00 m):

- Zunächst wurde die Belastung stufenweise etwa bis zur festgelegten Gebrauchslast gesteigert. Die Belastung erfolgte kraftgeregelt mit 126 N/s.
- Nach Erreichen der Gebrauchslaststufe wurden 9000 Lastwechsel aufgebracht (Frequenz 1 Hz; Oberlast/Unterlast = 1,0/0,7-fache Gebrauchslast).
- Anschließend wurden die Balken bis zur Grenztragfähigkeit belastet, wobei die Last weggeregelt mit 1,2 mm/min gesteigert wurde.

Zweiter Versuchslauf (l = 3,00 m):

- Die intakten Restbalken mit 3 m Stützweite wurden zunächst kraftgeregelt mit 126 N/s etwa bis zur Gebrauchslast belastet.
- Nach vollständiger Entlastung wurde die Last weggeregelt mit 1,2 mm/min (VB1) bzw. 0,8 mm/min (VB2) bis zur Grenztragfähigkeit gesteigert.

Bei allen Versuchen wurden Meßdaten für Längsstabdehnungen, Bügeldehnungen, Durchbiegung und Rißbreiten aufgenommen (Fig. 3).

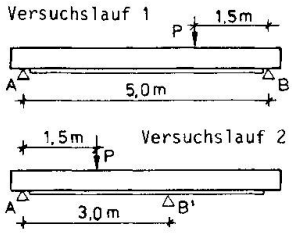

Fig. 2 Systemskizzen

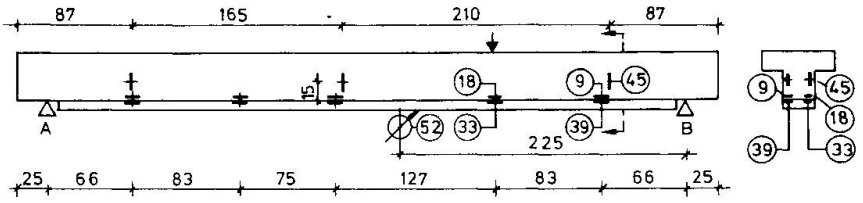

Fig. 3 Lage der Meßstellen

4. VERSUCHSERGEBNISSE

4.1 Tragverhalten

Bei VB1 traten unter höheren Lasten feine horizontale Risse in der Verbundfuge auf. Er zeigte jedoch wie ein monolithisch hergestellter Balken ein ausgeprägtes duktiles Bruchverhalten. Die Tragfähigkeit war erst erschöpft, als sich unterhalb der Einzellast ein Biegeriß weit öffnete und die weggeregelte Last nicht weiter gesteigert werden konnte. Der Versuch wurde abgebrochen als sich in der Betondruckzone unterhalb des Prüfzylinders erste Risse aufgrund der großen Rotation entwickelten. Die Bruchlast betrug 310 kN, was dem $\gamma = 2{,}33$-fachen der rechnerischen Gebrauchslast entspricht.

Bei VB2 traten kurz vor Erreichen der Bruchlast sehr flach geneigte Risse in Höhe der Verbundfuge auf. Das Versagen erfolgte durch schlagartiges Aufreißen der Verbundfuge im gesamten Querkraftbereich zwischen Einzellast und nahem Auflager. Die Zulagebewehrung konnte sich nicht mehr an der Lastabtragung beteiligen. Die weggeregelte Last ging dabei vom Höchstwert $P_u = 303$ kN auf 169 kN zurück und mußte allein vom Altbetonbalken aufgenommen werden. Die Bruchsicherheit bei VB2 betrug gegenüber der rechnerischen Gebrauchslast $\gamma = 2{,}27$. Alle relevanten Daten sind in den Tabellen 1 bis 3 zusammengestellt. Im Versuchslauf 1 ($l = 5$ m) ergaben sich für beide Balken und im Versuchslauf 2 ($l = 3$ m) für Balken VB1 die gleichen Sicherheiten. Im Versuchslauf 2 bei Balken VB2 war sie geringer. Bei VB2 trat das Versagen schlagartig ein, so daß hier nach deutschen Vorschriften eine Sicherheit von 2,1 eingehalten werden müßte. Dieser Wert wurde im Versuchslauf 1 nahezu erreicht, im Versuchslauf 2 dagegen nicht. Beide Balken wiesen bis direkt vor Erreichen der Bruchlast von VB2 nahezu gleiche Durchbiegungen auf (Fig. 4).

Nenndurchmesser [mm]	Istquerschnitt [mm²]	Streckgrenze [MN/m²]	Zugfestigkeit [MN/m²]
6	28,8	490,1	573,1
8	52,3	478,2	539,1
14	159,9	534,1	624,9
20	317,1	532,4	625,7

Tabelle 1 Querschnitts- und Festigkeitswerte der Betonstähle

Balken	Betonalter [Tage]	Druckfestigkeit β_{ws} [MN/m²]
VB1	28	34,6
	104 1)	40,5
	110 2)	36,9
VB2	28	28,7
	96 1)	33,6
	98 2)	30,4

1) Versuchslauf 1 2) Versuchslauf 2

Tabelle 2 Betonfestigkeiten

Versuchs-lauf	Balken	Gebrauchslast [kN]			Bruchlast	Bruchsicherheit	
		unverstärkt	verstärkt				
		nom P_o	nom P_1	ef P_1	P_u [kN]	P_u/nom P_1	P_u/ef P_1
1	VB1	76	133	148	310	2,33	2,09
	VB2	76	133	145	303	2,27	2,09
2	VB1	120	200	222	464	2,32	2,09
	VB2	120	200	218	374	1,87	1,72

Tabelle 3 Gebrauchslasten, Bruchlasten und Bruchsicherheiten

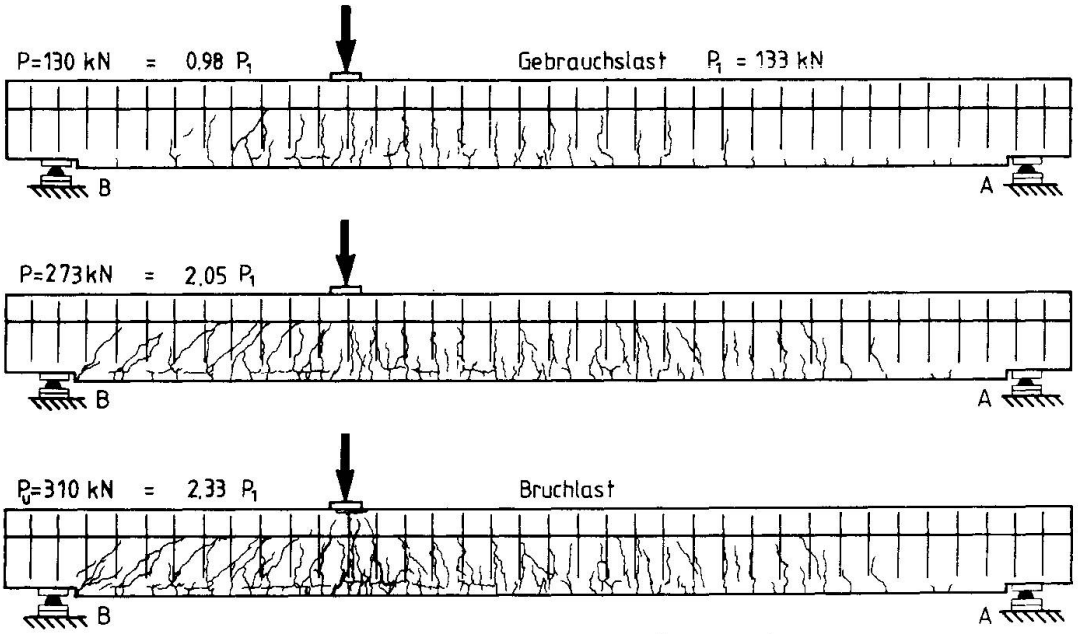

Fig. 5 Rißbilder Balken VB1, Versuchslauf 1 (l = 5 m)

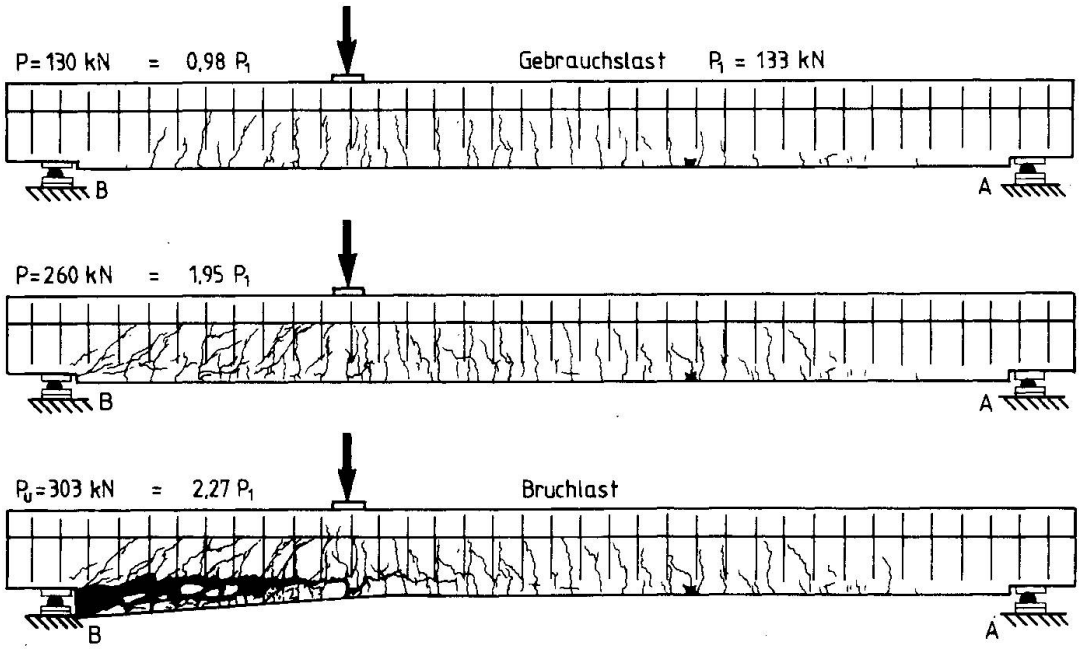

Fig. 6 Rißbilder Balken VB2, Versuchslauf 1 (l = 5 m)

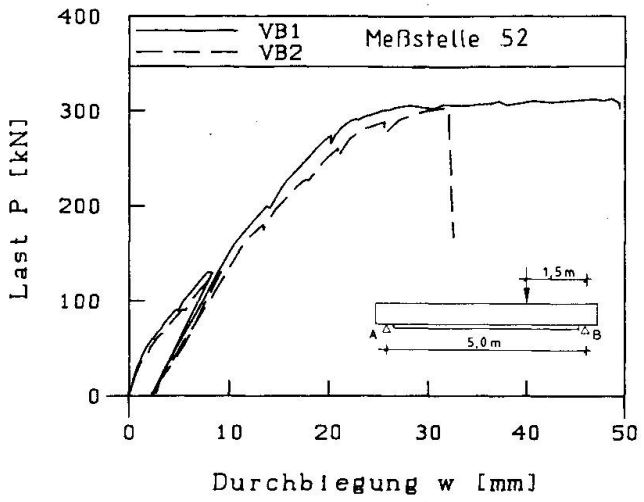

Fig. 4 Last-Verformungs-Diagramme

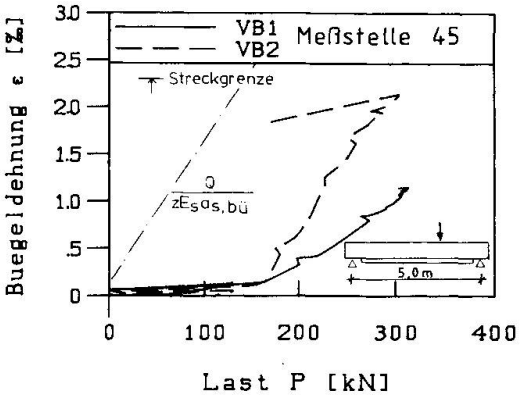

Fig. 7 Bügeldehnungen (VB1 und VB2, Meßstelle 45)

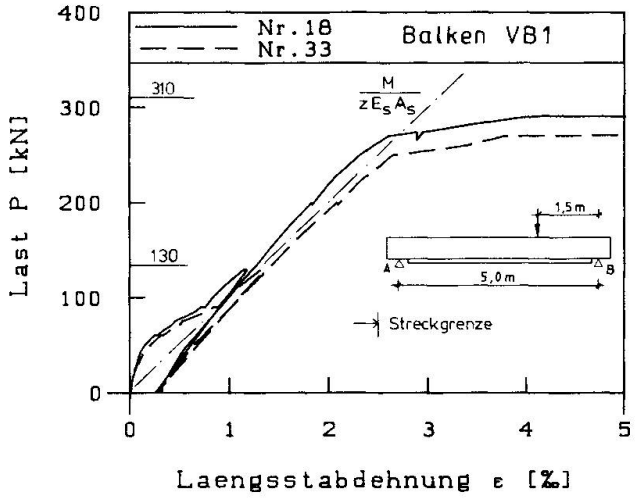

Fig. 8 Längsstabdehnungen (VB1, Meßstellen 18 und 33)

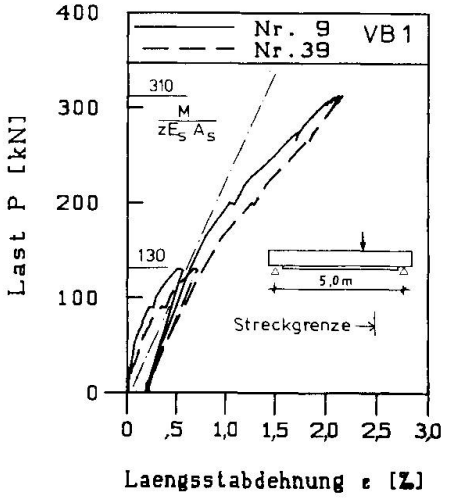

Fig. 9 Längsstabdehnungen (VB1, Meßstellen 9 und 39)

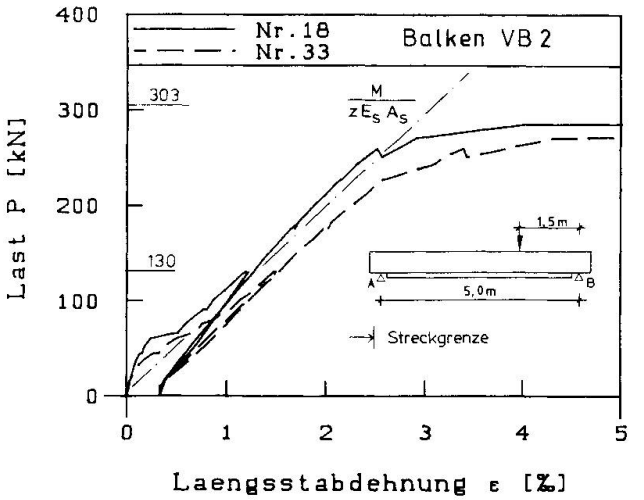

Fig. 10 Längsstabdehnungen (VB2, Meßstellen 18 und 33)

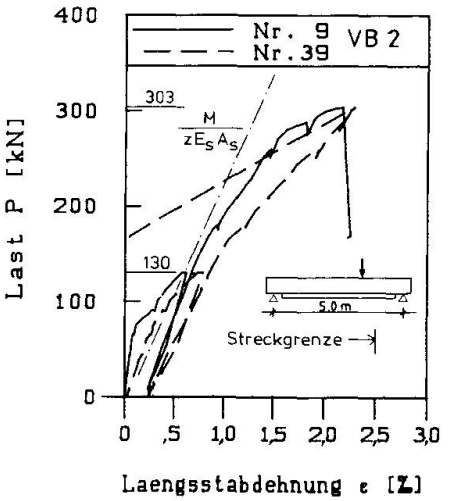

Fig. 11 Längsstabdehnungen (VB2, Meßstellen 9 und 39)

4.2 Rißbild

Die Rißbilder sind in Fig. 5 und Fig. 6 für den jeweils ersten Versuchslauf dargestellt. Beide Balken wiesen im Gebrauchslastbereich ein völlig "normales" Rißbild auf. Die gemessenen Rißbreiten lagen durchweg unter 0,1 mm. Die 9000 Lastwechsel umfassende Schwellbeanspruchung führte nur zu unbedeutenden Veränderungen. Schubrisse bildeten sich erst weit oberhalb der Gebrauchslast.

4.3 Beanspruchung der Bügel

Für VB1 und VB2 mit l = 5 m sind in Fig. 7 die gemessenen Dehnungen eines Bügelschenkels aufgetragen. Es stellte sich bei beiden Balken der typische Dehnungsverlauf ein: erst mit Beginn der Schubrißbildung, im vorliegenden Fall oberhalb der Gebrauchslast, stellte sich das die Bügelbeanspruchung bestimmende Fachwerktragverhalten ein. Die Streckgrenze wurde unter Bruchlast nicht erreicht.

4.4 Beanspruchung der Längsstäbe

Der Verlauf der Längsstabdehnungen ist für VB1 in Fig. 8 und 9 und für VB2 in Fig. 10 und 11 dargestellt. Das Dehnungsverhalten beider Balken ist bis kurz vor Erreichen der Bruchlast das gleiche. Für die Zulagestäbe wurden deutlich größere Dehnungen gemessen als für die Stäbe im Altbetonbalken. Unter der Einzellast überschritt der Stahl die Streckgrenze und erreichte Dehnungen von mehr als 10 ‰. Während bei VB1 die Zulagebewehrung auch unter der Höchstlast noch voll mittrug, fiel bei VB2 als Folge des Verbundfugenversagens die Dehnung auf Null ab. Gleichzeitig stieg die Dehnung der Biegezugbewehrung im Altbeton - obwohl die Last zurückging - etwas an, da die noch vorhandene Last nunmehr allein vom ursprünglichen Stahlbetonquerschnitt übertragen werden mußte. Die Übereinstimmung der rechnerischen mit den gemessenen Werten ist gut, wenn man beachtet, daß sich die berechneten Werte in Fig. 9 und 11 bei Berücksichtigung des Fachwerktragverhaltens entsprechend dem Versatz der Zugkraftlinie gegenüber der M/z-Linie in Richtung der gemessenen Werte verschieben.

5. AUSBLICK

In weiteren Versuchen, die vom Deutschen Beton-Verein unterstützt werden, soll systematisch erkundet werden, welche Mindestmenge an Verbundmitteln erforderlich ist, ohne daß das gutartige duktile Tragverhalten darunter leidet. Es ist zu erwarten, daß künftig die Verbundmittelquerschnitte gegenüber [4] erheblich reduziert werden können.

LITERATURVERZEICHNIS

1. HOLZ K., Anschlüsse, Verstärkungen und Konstruktionsänderungen - flexibel bauen auch mit Stahlbeton. Beton- und Stahlbetonbau 79 (1984), S. 293-298 und S. 322-327.
2. RUFFERT G., Ausbessern und Verstärken von Betonbauteilen. 2. Auflage, Beton-Verlag, Düsseldorf, 1982.
3. Richtlinien für die Ausbesserung und Verstärkung von Betonbauteilen mit Spritzbeton. Fassung Oktober 1983. Deutscher Ausschuß für Stahlbeton.
4. DIN 18551; Spritzbeton. Entwurf 1989.
5. EIBL J., BACHMANN H., FATH F., Abschlußbericht zum Forschungsvorhaben: Nachträgliche Verstärkung von Stahlbetonbauteilen mit Spritzbeton. Universität Karlsruhe, Institut für Massivbau und Baustofftechnologie, 1988.

Frost Resistance of Fibre Reinforced Concrete Containing Microsilica

Résistance au gel de béton renforcé de fibres de micro-silice

Frostbeständigkeit von faserverstärktem Beton mit Flugasche-Zusatz

Sergio LAI
Civil Engineer
University of Cagliari
Cagliari, Italy

Sergio Lai, born in 1954 has a degree in Civil Engineering and for 14 years has been engaged in materials testing at the University of Cagliari (Italy). He has carried out numerous investigations on the durability of concretes, participating in various International Congresses and has published more than 25 papers on the subject.

SUMMARY

This paper presents the results of extensive laboratory investigations aimed at determining the freeze-thaw resistance of conglomerates containing silica fume and polypropylene fibres. Particular attention has been focussed on the influence of mode of preparation on freeze-thaw resistance, as well as on the prediction of such resistance on the basis of tests of short duration.

RÉSUMÉ

Cet article présente les résultats d'une longue série d'essais de laboratoire cherchant a déterminer la résistance au gel-dégel des conglomérats contenants de la micro-silice et des fibres de polypropylène. Une attention particulère a été portée aussi bien à l'influence des méthodes de préparation sur la résistance au gel-dégel qu'aux prévisions de cette résistance avec des essais de courte durée.

ZUSAMMENFASSUNG

Anhand eines Langzeitversuches wurde die Frostbeständigkeit von faserverstärktem Beton mit Flugasche-Zusatz ermittelt. Besondere Aufmerksamkeit wurde dem Einfluss der Verarbeitungsmethode sowie der Korrelation zu Kurzzeitversuchen gewidmet.

1. INTRODUCTION

Condensed silica fume, a by-product of the ferro-silicon industry, is used as a partial replacement o in addition for cement in concrete and mortar. First investigation indicated improved frost resistance (1), (2), (3). When admixed with a conglomerate, silica fume (micronized silica) acts as a filler and its pozzolanic action is enhanced. The addition of polypropylene fibres to the cement mix, serves to check the formation of cracks caused by shrinking. Superplasticizing admixtures allow to balance the larger requirement of mixing water caused by the micronized silica and polypropylene fibres.
The purpose of this paper is to study the frost resistance of concretes containing condensed silica fume and polypropylene fibres when tested in accordance with UNI 7087-72, and with ASTM C666, procedure A, modificate.

2. EXPERIMENTAL PROCEDURES

2.1 Material and proportion

The cement used was Portland 525. The fine aggregate (specific gravity: 2,70, absorption: 2,65 %, fineness modulus: 2,90) was river sand and coarse aggregate (specific gravity: 2,54, absorption: 3,58 %, fineness modulus: 6,40, maximum size: 20 mm) was crushed gravel. Superplasticizer (naphthalene-sulphonate condensed with formaldehyde) was used as admixture. Mix proportion are shown in table 1. Water cement-silica ratios of the specimens were selected as 30, 35, 40, 45 and 50 percent for all freeze-thaw tests (slow and rapid freeze-thaw test up to 30 cycles, and standard test in accordance with UNI 7087-72).
The mix designation are shown in table 2.

2.2 Preparation of specimens

Eight 100x100x400 mm prism and eight 100 mm cubes were cast from each mix. After casting, the molded specimens were covered with a plastic sheet and left in the casting room at 20° C for 24 hours.
After demolding they were cured in 20° C water for 14 days (ASTM C666, procedure A, modificate); for UNI test they were cured in 20° C climatic room for 45 days and 20° C water for another 15 days.

3. TEST METHODS

3.1 UNI 7087-72

The freeze-thaw cycle consist of:
-lowering the temperature of the specimens in air from +5° to -25° C;
-keeping temperature at -25° C;
-elevating the temperature to +5° C with the specimens in water;
-keeping the temperature at +5° C.
The elastic modulus, length and mass of the specimens are measured periodically. The test continues for 300 cycles; it can be stopped when the conglomerate undergoes either a reduction in dynamic elastic modulus of 60 %, an expansion of 0,2-0,3 % or else a mass loss of more than 3 %.

3.2 ASTM C666, PROCEDURE A MODIFICATES (RAPID F-T TEST)

This test method covers the determination of the resistance of concrete specimens when subjected to rapidly repeated cycles of freezing and thawing in water. A freezing-and-thawing cycle consist of alternately lowering the temperature of the specimens from +5° C to -18° C (3 hours) and raising it from -18° C to 5° C (1 hour). The modification consist in considering temperatures varying between +5° and -20° C with different gradients in accordance with figure 1. The relative moduli of elasticity of the test specimens, in thawed condition, are determined.

3.3 Slow F-T tests

The slow freezing-thawing tests by two cycle a day were performed in air and with temperature simulated in agreement with figure 2.

4. TEST RESULT FOR RAPID AND SLOW FREEZE-THAW

Result of the rapid freeze-thaw test up to 30 cycle are shown in figures 3-4, which illustrates the relation between the number of cycles and relative dynamic modulus of elasticity for W/C+SF=0,50 and 0,45. After freeze-thaw test up 30 cycles, relative dynamic modulus dropped to about 70-85 and 75-83 percent respectively.
Results for slow freeze-thaw test up 30 cycles is shown in figure 5, which shows the relation between the number of cycles and relative dynamic modulus of elasticity after 7 days and 28 dayd curing at water/cement-silica ratio of 45 percent. The slow freeze-thaw test is not the most suitable for prediction long term behaviour as temperature gradients are too small and temperature ranges are not very wide.

5. TEST RESULT FOR UNI 7087-72 METHOD

The freeze-thaw tests were performed for 300 cycles and some of the results are shown in figure 6. The diminution in dynamic modulus fluctuates considerably, from between 40 % (C50,0) and 20 % (C45,20). It is shown that performance in freeze-thaw cycles improves both with increasing silica fume additions and decreasing W/C+SF ratio. Along with dynamic modulus measurements, the specimens were also tested, every certain number of cycles, to determine the decline in compression properties. Figure 7 shows dynamic modulus versus compressive strength for some W/C+SF ratios, keeping SF content constant at 20 % (80 kg/cu m).

6. CONCLUSIONS

Test results are summarized as follows:

1) Concretes containing silica fume were observed to perform better in freeze-thaw cycles; in certain cases the diminution is of the order of 20 %, against 38 % observed in the controls.
2) With fast freeze-thaw cycles the reduction in dynamic elastic modulus is 20, 24 and 28 % for the conglomerates with W/C+SF of 0,5 and silica fume addi-

ns of 20, 10 and 5 % by weight of cement.

3) The C50,20 series showed, with the UNI test, a reduction after 300 cycles of 25 % compared to 20 % with the rapid test.
4) The C50,0 series showed a diminution in dynamic elastic modulus of 39 % with the UNI test compared to 26 % with the rapid test.
5) Although not all the data necessary for a statistical analysis are available (the experiments are still in progress) the results so far suggest that for the conglomerates containing silica fume and for the controls, the freeze-thaw resistance can be predicted by means of the rapid test, since the UNI test yields a diminution in dynamic modulus greater by between 25 and 55 %.

REFERENCES

1. TRAETTEBERG A., Frost Action in Mortar of Blended Cement with Silica Dust.Durability of Buiding Materials and Component, ASTM, STP-691, Philadelphia, 1980, pp.536-548.

2. CARETTE T. and MALHOTRA V.M., Mechanical Properties, Durability and Drying Shrinkage og Portland Cement Concrete Incorporating Silica Fume. ASTM Cement, Concrete and Aggregates, Vol.5, No. 1, 1983, pp.3-13.

3. YAMOTO T., EMOTO Y. and SOEDA M., Strength and Freezing-and-Thawing Resistance of Concrete Incorporating Condensed Silica Fume. Proc. 2nd International Conference on Fly-Ash, Silica Fume, Slag and Natural Pozzolans in Concrete, Madrid, Spain, SP 91-54, 1986, pp.1095-1118.

4. LAI S., Sulla messa a punto di un conglomerato fibroso con microsilica resistente ai cicli di gelo-disgelo. Atti delle Giornate AICAP, Napoli, Italy, 4-6 Maggio 1989.

5. LAI S., On the use of Silica Fume, Polypropylene Fibres and Superplasticizers in the preparation of Highly Durable Concretes. Proc. of 2nd NCB International Seminar on Cement and Building Materials, New Delhi, 30 Jan.-3 Feb.1989.

W/C+SF	Slump	Unit Weight (kg/cu m)					
	(cm)	W	C	S	G	SF	Superplast.
.30-.35						20	
.40-.45	10	variab.	400	700	998	40	variable
.50						80	

Table 1 Mix proportion

	W/C+SF	SF	Fibres
C30,0	.30	0	0
C30,5	.30	20	1
C30,10	.30	40	1
C30,20	.30	80	1
.....	...	..	.
C50,0	.50	0	0
C50,5	.50	20	1
C50,10	.50	40	1
C50,20	.50	80	1

Table 2 Mix designation

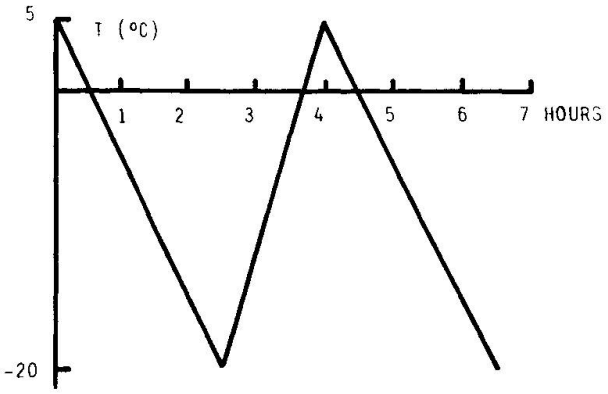

Fig.1 Rapid F-T test (gradients)

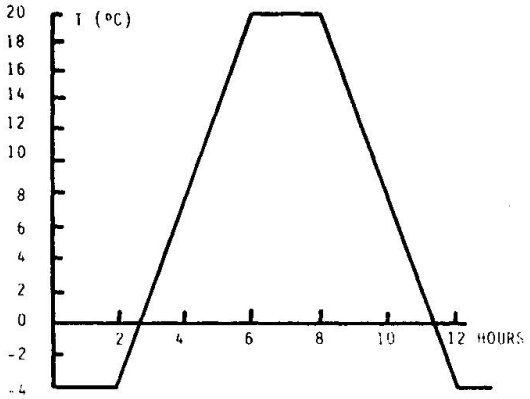

Fig.2 Slow F-T test (gradients)

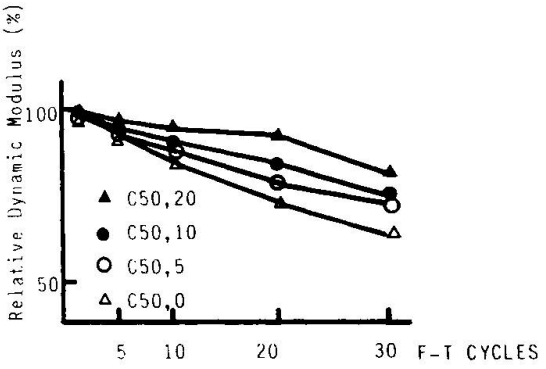

Fig.3 F-T cycle and relative dynamic modulus (W/C+SF=.50)

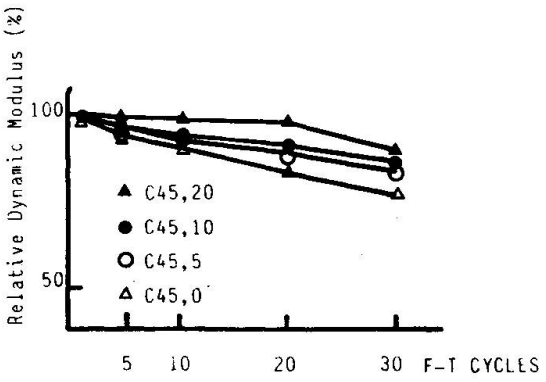

Fig.4 F-T cycle and relative modulus (W/C+SF=.45)

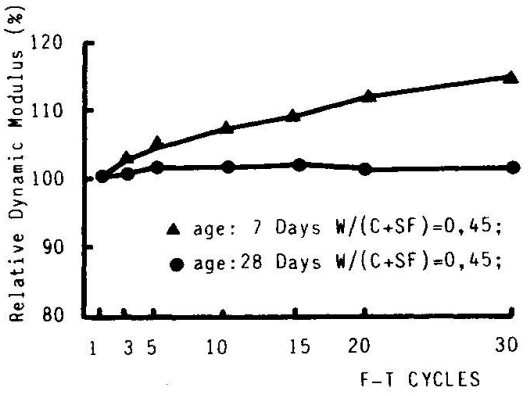

Fig.5 F-T cycle and relative dynamic modulus (slow test)

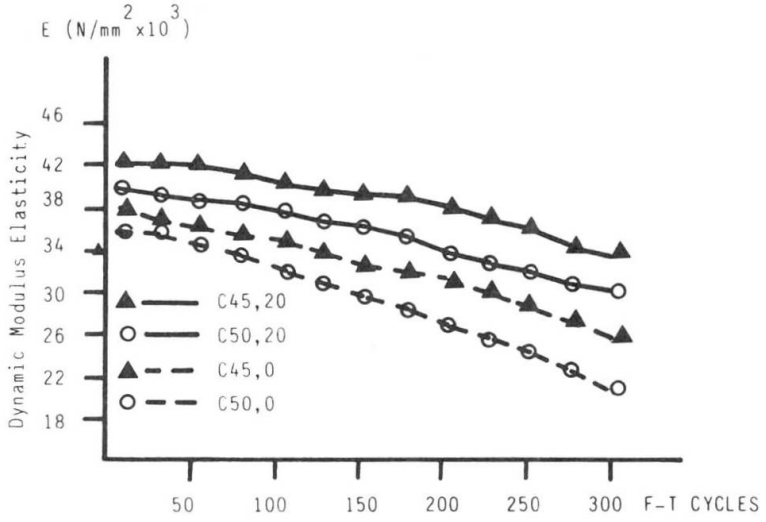

Fig.6 F-T cycle and relative dynamic modulus of elasticity

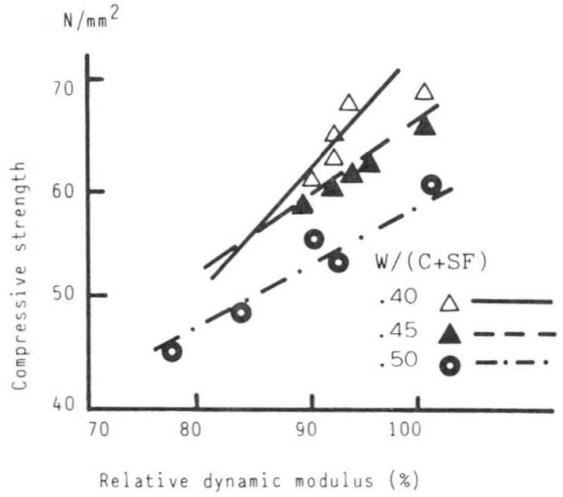

Fig.7 The relation between dynamic modulus and compressive strength

Fig.8 Distribution of fibers in hardened concrete

Creep and Durability of Wood-Joist Floor Systems

Fluage et durabilité du système de poutres dans les planchers en bois

Kriechen und Dauerhaftigkeit von Holzträgerdeckensystemen

I. Robert KLIGER
Research Ass.,
Chalmers Univ. of Technology
Göteborg, Sweden

Robert Kliger, born 1950, graduated from Chalmers University of Technology, Göteborg, Sweden, with a M. Sc. in civil engineering. For three years he was head of design at a company marketing timber-framed houses.
Robert Kliger is currently active in research into various problems related to timber structures.

SUMMARY

Experimental work is presented on the creep properties and durability of both the component parts and complete wood-joist floor structures consisting of wood, wood based materials and steel sheet. The discussion of the use of this type of structure has been limited to floors used above foundations with a crawl space in wooden houses.

RÉSUMÉ

Le travail expérimental démontre les caractéristiques de fluage et de durabilité aussi bien des éléments constitutifs que du système de poutres dans les planchers composés en bois, en matériaux à base de bois et en tôle. La discussion sur l'usage d'une telle construction est limitée au plancher qui est situé sur la fondation avec espace intermédiaire, dans des maisons en bois.

ZUSAMMENFASSUNG

Eine experimentelle Arbeit wird beschrieben, in welcher die Kriecheigenschaften und die Dauerhaftigkeit von Teilmaterialien und von ganzen Holzdeckenkonstruktionen (aus Holz, Holzwerkstoff und Stahlblech) untersucht werden. Die Diskussion der Verwendung dieses Konstruktionstyps wird auf Decken über einem Kriechkeller beschränkt.

1. INTRODUCTION

1.1 Foundations with crawl space in wooden buildings

The conventional crawl-space basement has foundation walls made of materials, such as lightweight concrete blocks, often resting on concrete base foundations. The floors are usually made of prefabricated elements made of either wood and wood-based materials or lightweight concrete. The distance between the ground and the underside of the floor structure is small, but should be a minimum of two feet (∿ 600 mm) to permit inspection.
Climatic studies of cold crawl spaces with an airtight, well-insulated floor structure and ventilated by the outside air have revealed that the relative humidity can be as high as 85-95% [1], especially in the summer, even if all the sources of moisture such as damp and water leakage are eliminated. This is due to the fact that warm outside air with a temperature of about 17°C or higher and a relative humidity of about 70% is chilled in the basement by the ground which is still cold from the winter. The relative humidity will therefore increase and it is then possible for wood and wood-based materials to mould or even rot, despite the degree of ventilation. For this reason a design using steel sheet with a zinc oxide coating on the underside of the floor structure could be advantageous.

1.2 Design of wooden floors

The design of floors is traditionally based on the assumption that the dead load and the applied load are carried entirely by the joists and that the effect of the sheeting on the behaviour of the floor system is negligible. The stresses, moments and deflections are calculated using simple beam equations in which possible composite action is ignored.

1.3 Stressed-skin panels

A stressed-skin panel can be an example of a wood-joist floor system where the interactions between joists and sheeting are included in the design. The advantage of using these panels is the high ratio between strength and weight and the fact that the choice of materials can be optimised with regard to structural, functional och durability requirements.

1.4 Aims and scope

In this paper the application of stressed-skin panels as a prefabricated element above the crawl space is discussed only for "cold" basements, i.e. basements which are not heated and are only ventilated by the outside air.
The main aim of this paper is to study the design and creep characteristics of stressed-skin panels containing wooden joists, chipboard and steel sheet. A simple theoretical model which takes account of the slip modulus between the component parts is used to compute the initial deflection and predict creep. In order to verify the model, four stressed-skin panels were constructed and subjected to long-term loading. The creep properties of the component parts and joints were studied in order clearly to define these properties which were to be used as input for theoretical calculations using the above-mentioned model. The limitations which applied to all the tests were that the sustained load should correspond to a low stress level and that all the tests should be carried out in a constant climate (20°C and 65% RH).

2. LONG-TERM STRENGTH AND DURABILITY OF COMPONENT PARTS AND ADHESIVE JOINTS

2.1 Aims

The experiments on component parts and adhesive joints were conducted primarily to produce information about the strength and creep properties of materials *matched* with those used to build four stressed-skin panels. This information was then used as input to a simple computer program based on a modified theory of elasticity for built-up structures.

2.2 Tests on component parts

The experimental studies included the long-term bending and shear characteristics of wooden beams (stringers in stressed-skin panels), the compression characteristics of chipboard (the compression flange in stressed-skin panels) and the shear properties of glued joints between wood and chipboard and wood and steel. In order to compare long-term deformation for different materials and joints loaded in different modes and varying stress levels, the results were expressed in values of relative creep, ϕ, i.e. creep deflection (deformation) related to an initial deflection. All the relative creep data taken from measurements during some 670 hours (4 weeks) was then fitted to two different mathematical expressions in order to predict creep after 1,000 and 10,000 hours. The power function (Eq.1) probably fits a regression curve, which represents the available creep data, as well as any other mode, even if it tends to overestimate creep after a long time [2].

$$\phi = \beta_0 + \beta_1 \, t^{\beta_2} \qquad (1)$$

where relative creep $\phi = \delta_t/\delta_0$ and δ_0 is the "initial deflection " (deformation) obtained after one minute ± 5 seconds (after the application of the load), which is the time corresponding to t = 0.
β_0, β_1 and β_2 are constants, t is the time (in hours).

The results of these tests show that the relative creep values were higher at the lowest stress level for both wooden beams loaded in bending and chipboard loaded in compression.

Three different types of adhesive (polyurethane, PVA with isocyanate hardener and elastomeric silicone), which join wood to wood and wood to steel, were tested in shear to obtain the short-term strength and deformation. However, in these tests the two PVA and silicone adhesives were chosen for purely scientific purposes, namely as examples of virtually rigid and somewhat flexible joints. The duration of load effect for the different types of adhesive used in timber joints showed that the shear strength decreases the least for resorcinol, followed by polyurethane and PVA with isocyanate hardener [3]. The type of adhesive, as well as the state of the metal surface, are important parameters for the *durability* of a bonded steel joint. Sandblasting the metal surface has the best effect on the durability of steel joints. The rate of degradation in steel joints exposed to humid environments is dependent on the temperature, on the water concentration in the glue- or bond-line and on the type of coating on the steel sheet surface glued to the timber [4]. An accelerated long-term test on joints between wood and steel sheet with polyurethane adhesive [5] revealed that joints did not fail during 8,000 hours' exposure to a shear stress of 0.8 MPa at 100% relative humidity and 50°C. These joints had an ultimate shear stress of 4.3 - 6.5 MPa at a temperature of 20°C.

3. DEFLECTION AND CREEP OF STRESSED SKIN-PANELS

Four specimens (Fig.1) were subjected to a 4-point constant load for nine months. The level of the concentrated loads corresponded to stresses smaller than or equal to the permissible stresses according to the Swedish Building Code SBN 80 [6]. The tests were carried out in a constant climate (20°C and 65% RH).

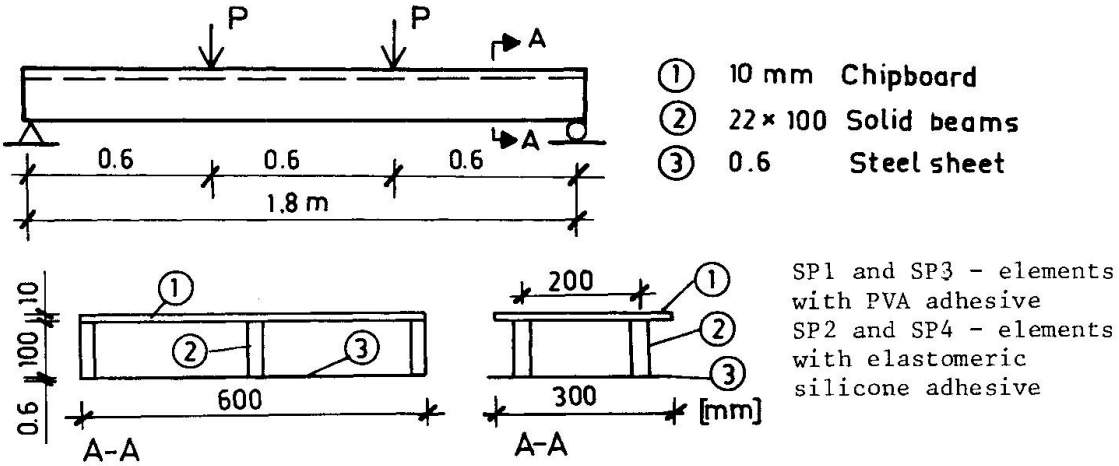

Fig. 1 Loading arrangement and cross-section of stressed-skin panels

The theoretical magnification factor for the mid-span deflections of stressed-skin panels, which includes the effects of interlayer slip, was calculated by using the solution of a differential equation [7] and based on the assumption that the slip modulus is the same in the entire joint and that no variation exists between the joints. In the case of the stressed-skin panels tested here different slip moduli were found for different interlayer joints. This difference was taken into account by calculating the magnification factor for the first two layers (inverted T-beams) and modifying the bending stiffness of these layers. The calculation was then repeated by regarding the first two built-up layers as one unit (rigidly connected) when adding the third layer. This procedure was embodied in a simple computer program.

The creep and creep rate of elements are described by different parameters which are included in the power function, Eq.1, for the creep of each of the component parts and joints. Using the sensitivity analysis of the parameters in the creep functions for each of the submaterials and allowing each of the stiffness variables of interest to change due to creep, it was possible to study the influence of these variables on deflection and creep. When using rigid glued joints with a low tendency to creep, the creep of the entire specimen was similar to that obtained due to combined creep in the stringers and the compression flange.

The creep curves show good agreement between the measured and predicted results for all the specimens which were tested (Fig.2). We must bear in mind the large scatter typical of the input data for wood-based materials and glued joints.

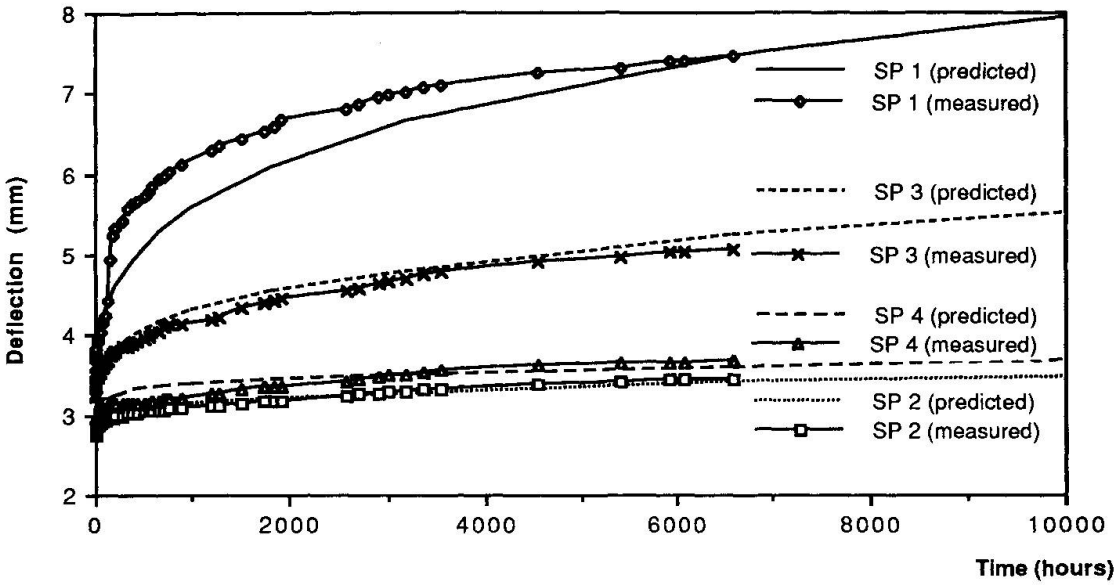

Fig.2 Comparison between theoretically obtained creep curves and the experimentally measured deflections

4. PRACTICAL EXPERIENCE OF THIS TYPE OF STRUCTURE

In order to produce cheap houses with low energy consumption, eighteen houses were built in Täby (Sweden) during the winter of 1984-85. In these houses the floor structure above the crawl-space basement consisted of simply-supported prefabricated elements (stressed-skin panels). Supports made of pressure-impregnated ground plates were placed at the long exterior walls of each house (span of 7.6 metres). The floor elements consisted of 22 mm chipboard on the compression side, 400-mm I-beams with a spacing of 600 mm as stringers and 0.6 mm steel sheet (plywood was used in one house as a reference) on the tension side. In four of these houses the moisture content was measured for one year [8]. The results of these measurements showed that the highest moisture content inside the elements was 14% on the compression side (corresponds to 62% RH) and 17% on the tension side (corresponds to 70% RH). Although the floor structure had a relatively long span, it did not show unacceptable deformation during the test period. Some condensation was discovered in the crawl space during the summer; this was predicted, but no condensation occurred inside the structural floor elements.

5. CONCLUSIONS AND SUGGESTIONS FOR IMPROVEMENTS

It appears to be extremely advantageous to use thin steel sheet as a tension flange in order to reduce deflections and creep in wood-joist floor systems. Specimens with fairly stiff glued joints (PVA adhesive) would show a 20% increase in initial deflection and a 10% increase in creep deflection after 10,000 hours if 12 mm plywood were used instead of 0.6 mm steel sheet in the tension flange. The experimental work discussed here shows that it should be possible to use the same technique to predict the long-term deformation of stressed-skin panels exposed to a varying load or varying climate, provided that one has data for the corresponding properties of the component materials and joints. The durability of steel-to-wood joints exposed to high relative humidity is a very important design consideration. One way of improving the design of this type of structure would be to add extra insulation to the underside of the steel sheet, thus in-

creasing the temperature of the steel surface (this would prevent condensation forming). The best way of protecting timber structures from the harmful influence of moisture is to use a "correct" design. This involves creating an appropriate climate (RH lower than 70%) around timber and timber-based materials. A perforated steel ground plate could be used to support a wood-joist floor system above a crawl-space basement instead of a pressure-impregnated one which could mould in the high humidity which occurs in such areas.

REFERENCES

1. ELMROTH A., Kryprumsgrundläggning (Crawl-space basements). National Swedish Building Research R12:1975 (in Swedish).

2. KLIGER I.R., Determination of creep data for component parts of stressed-skin panels. Proc. CIB-W18/IUFRO S5.02, Paper 19-9-5, 1986.

3. LUNDGREN K., Ny konstruktionslimning. BFR Rapport R85:1985 (in Swedish).

4. KINLOCH A.J., Durability of structural adhesives. Applied Sci. Publ. Ltd. London, 1983.

5. DOLK Å., JANSSON J-F., Accelererad långtidsprovning av polyuretanlim för bärande konstruktioner av trämaterial och stålkomponenter. Träteknik-Centrum P:16, 1984 (in Swedish).

6. The Swedish Building Code. SBN 80. Statens Planverk 1980 (in Swedish).

7. KLIGER I.R., Experimental study of stressed-skin panels under long-term loading. Proc. IUFRO S5.02, Turku, Finland 1988.

8. LINDSKOOG A., ROOS R., Studie av fuktproblem i högisolerade träkonstruktioner. Träteknik-Centrum Rapport P 8702014, 1987 (in Swedish).

Long-Term Properties of Arapree

Comportement à long terme du matériau composite arapree

Langzeiteigenschaften des Verbundwerkstoffes Arapree

Arie GERRITSE
Civil Engineer
Hollandsche Beton Groep nv.
Rijswijk, The Netherlands

Jürgen WERNER
Civil Engineer
Akzo nv.
Wuppertal, F. Rep. of Germany

Leon GROENEWEGEN
Civil Engineer
Hollandsche Beton Groep nv.
Rijswijk, The Netherlands

Arie Gerritse, born in 1929, graduated in Civil Engineering at Rotterdam Technical College, the Netherlands. He is a staff member of the R&D department of Hollandsche Beton Groep (HBG), an international contractor based in the Netherlands, supervising since 1984 the Akzo/HBG development project on the practical use of aramides in concrete.

Jürgen Werner, born in 1939, obtained his Civil Engineering degree at the Technical University of Braunschweig (Fed. Rep. of Germany) in 1966. He is an Akzo project manager in the field of application of fibre reinforced materials in civil engineering.

Leon Groenewegen, born in 1961, obtained his Civil Engineering degree at the Technical University of Delft (the Netherlands) in 1986. He is currently a research engineer at the R&D department of HBG.

SUMMARY

Arapree is a composite made up of aramide fibres and an epoxy resin. It is used as a prestressing material in concrete structures. Apart from some general information on Arapree and its short term properties, the durability aspects are discussed. The paper ends with some impressions of two projects in which Arapree has been applied.

RÉSUMÉ

L'arapree est composé de fibres d'aramide et de résine époxy. Il est utilisé comme matériau de précontrainte dans des structures en béton. Après une information générale sur l'arapree, son comportement à court et long terme est discuté. Enfin deux projets sont décrits, au cours desquels l'arapree a été employé.

ZUSAMMENFASSUNG

Arapree ist ein Verbundmaterial aus Aramidfasern und einem Epoxyharz. Es wird als Vorspannmaterial in Betonkonstruktionen gebraucht. Neben einigen allgemeinen Informationen über Arapree und seine Kurzzeiteigenschaften werden die Langzeitaspekte diskutiert. Am Schluss werden zwei Projekte besprochen, in denen Arapree angewandt wurde.

1. Introduction

In the past few years interesting developments have emerged in the field of non-metallic tensile elements. More and more successful applications of such new materials are reported [1], [2], [3], [4].
The use of these materials will become common practice to structural engineers in the near future. This development necessitates the need for reliable data for these non-metallic elements especially with respect to their long-term behaviour.
In this paper the main long-term properties of Arapree, one of these new materials, will be discussed. The phenomena associated with these properties are well known since they must also be taken into consideration for materials like steel and concrete. However, other -less familiar- characteristics, such as stress-rupture behaviour can be decisive in designing constructions with these new materials. A thorough understanding of the characteristics will be needed for structural engineers who are faced with the problem of assessing constructions in which such new materials are applied.
The products belonging to this new generation of non-metallic tensile elements are based on high strength fibres like glass, carbon and aramid. In this paper the discussion on long-term properties is limited to an overview of the most important characteristics of Arapree, a composite made up of an epoxy resin and Twaron, the aramid fibre produced by Akzo.

2. General information Arapree

Arapree is the result of an ongoing research program of the Dutch/German chemical company Akzo and the Dutch contractor HBG. Arapree is produced as endless elements composed of bundles of non-twisted Twaron-fibres. The elements are produced by passing the fibres through eyelets and combs and subsequently impregnating the bundles with an epoxy resin. To ensure a good bond of the elements with concrete the surface of the elements is provided with a pattern of nobs.
An essential step in the production process is the impregnation of the Twaron bundles. A number of reasons have lead to the decision to impregnate the bundles with resin:

- By impregnating the bundles with an epoxy resin shear stresses fibre to fibre can and will be transmitted in the anchorage zone and in the vicinity of an incidental fibre rupture.

- Transmission of shear stresses of the bundle to the concrete regulated by tuning the surface structure.

- Handling of the elements

- Improvement of the resistance to extreme alkaline and acid environments.

- UV-protection. If applied in concrete this aspect can be neglected. Only in case of external prestressing this might be significant, but can be prevented by the use of additives to the resin deterioration.

- Optimal use of fibre strength. Thanks to the ability of the resin to transfer shear stresses the effect of fibre rupture is limited to a small area.

In table 1 the presently available types of Arapree are summarised.

TABLE 1: Available types of Arapree

Shape rectangular round	Cross-section [mm²] [mm]	Number of filaments	Fibre-cross-section [Twaron HM] [mm²]
rectangular	0,5*20	30 000	3,3
	1,4*20	100 000	11,1
	2,8*20	200 000	22,2
	5,6*20	400 000	44,4
round	2,5	20 000	2,2
	5	100 000	11,1
	7	200 000	22,2

Figure 1 shows a picture of a rectangular Arapree-strip and an Arapree-wedge anchor that is used as a temporary anchorage device. In concrete elements the prestressing force in the elements is transmitted to the concrete by bond.
In figure 2 the stress strain relation of Arapree is compared with common reinforcing and prestressing steel.

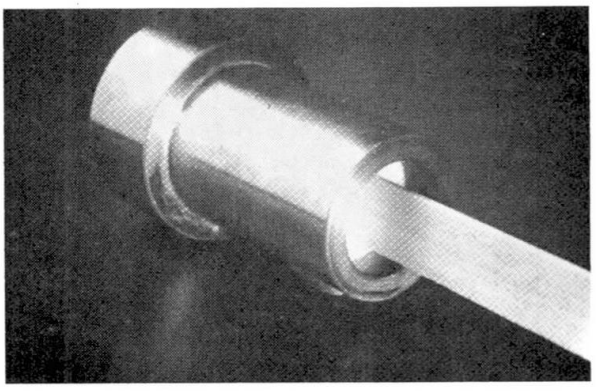

figure 1

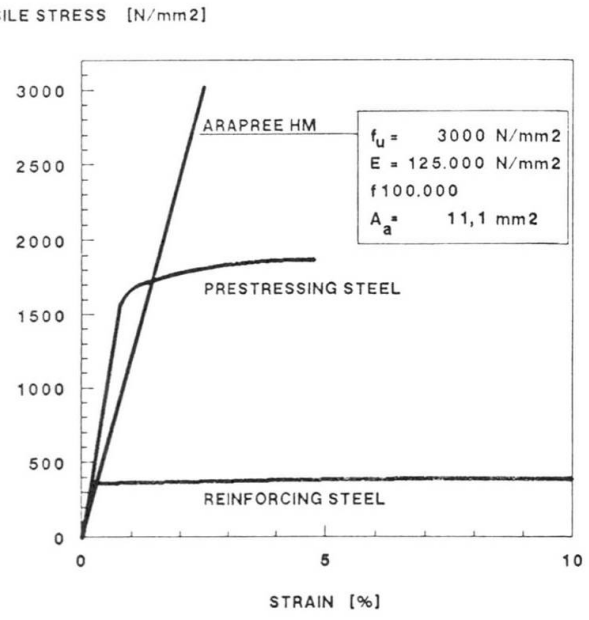

figure 2

The most significant short term mechanical properties of Arapree are given in table 2.

TABLE 2: Short-term properties of Arapree

Properties	Values	Dimension
Arapree bar-strip		
axial tensile strength	3000 (**)	N/mm² (*)
modulus of elasticity	125-130 (***)	kN/mm² (*)
failure strain	2.4	%
density	1250	kg/m³
transverse compressive strength	ca. 150	N/mm²
interlaminar shear strength	ca. 45	N/mm²
poisson ratio	0.38	-

*) Values related to the effective fibre cross-section.
**) Characteristic value: 2800 N/mm².
***) Modulus based on measurements in the range between 10 % to 50 % of the ultimate strength.

3. Durability

Apart from properties like an extremely high strength and considerably high stiffness of these new materials, the most interesting characteristics generating the interest of structural engineers have reference to the long-term behaviour.
Tensile elements based on aramid are non-corrosive, exhibit an excellent resistance to chlorides, are insensitive to electromagnetic currents and prove to have an outstanding fatigue behaviour. In case of reinforcing or prestressing steel all of these characteristics generally lead to requirements to ensure the durability. If aramid is applied there will be no need for such measures.
However, the stress-rupture behaviour and the sensitivity of glass- and - to a lesser degree - aramid fibres to an alkaline environment will give rise to new requirements. This is illustrated in figure 3.
The stress-rupture line given in figure 3 represents the relation between the stress in a tensile element and the time that passes before the material fails under a specific sustained stress-level. It is therefore a different property than the 'long-term-strength', which can be defined by the maximum constant load which can be present over a (very) long period. The long-term strength is also presented in figure 3. It can be seen that the residual strength of an unloaded strip after 100 years exposition in an alkaline environment like concrete is about 85 % of the short term strength. This value has been obtained by means of an extrapolation using the Arrhenius principle, that decribes a relation between the residual strength, temperature and time. Tests at elevated tempatures thus give indications about the residual strength level under normal circumstances.

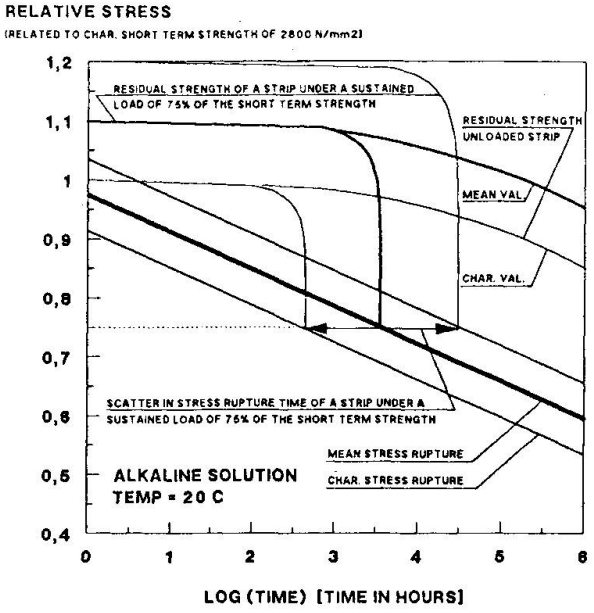

figure 3

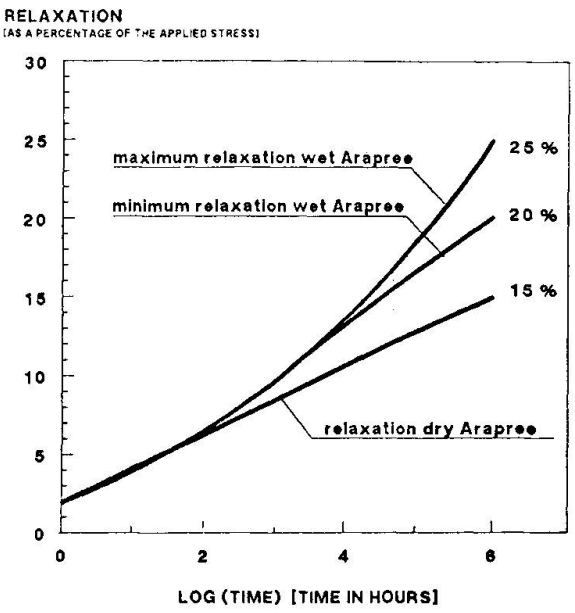

figure 4

The residual strength of a loaded strip hardly depreciates until just before stress rupture. This is illustrated in figure 3 by the residual strength of a strip to which a sustained load of 75 % of its short term strength was applied.

In assessing the structural safety one should estimate the final prestressing level, taking into account all losses caused by concrete deformations and relaxation of Arapree (figure 4). This value must be compared with the characteristic stress-rupture curve taking into consideration a partial factor for Arapree that has been set at 1.15 .
More information about Arapree is given in [5],[6].

4. Arapree in practice

Two projects have already realised in which Arapree was used as prestressing material. An impression of these projects is given in figure 5 and 6. In both cases relatively small prestressed (pretensioned) concrete elements have been produced. This first application of Arapree (1988) concerns concrete posts in a traffic noise barrier along a motorway near Rotterdam (figure 5). Ninety elements of about 4.5 m were prestressed with Arapree.
The second application of Arapree is illustrated in figure 5. Ten concrete hollow core floor slabs with a span of ca. 6 m were prestressed with Arapree (1988/1989). In both cases no additional steel reinforcement was used. The aim was to produce non-magnetic durable pretensioned elements without any steel.

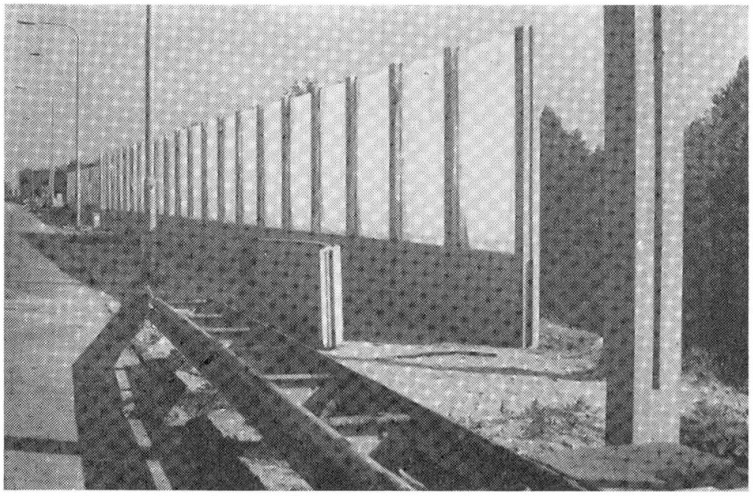

figure 5.

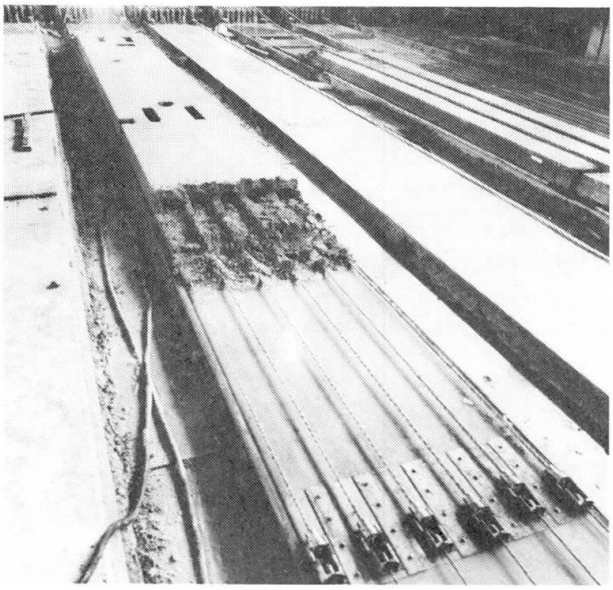

figure 6.

5. References

1: FUJISAKI T., MATSUZAKI Y., SEKIJIMA K., OKAMURA K.; New Materials for Reinforced Concrete in place of Reinforced Steel Bars; IABSE-symposium, Paris Versailles 1987.

2: Dr. WOLFF; Prestressing of Heavy Structures; Ecole Nationale des Ponts et Chaussées, Les Materiaux Nouveau pour la Precontrainte et le Renforcements d'Ouvrages d'Art; Paris, 25-26 october 1988.

3: OKUDA K.; Pitch-based Carbon Fibres; Seminar on the Future of Advanced Composite Materials, May 1987.

4: BURGOYNE C.J. e.a.; Proceedings of the Symposium on Parafil Ropes; Imperial College of Science and Technology, London 1988.

5: GERRITSE A., SCHÜRHOFF H.J.; Prestressing with Aramid Tendons. Technical Contribution to FIP 10-th Congress, Nee Delhi, 1986.

6: GERRITSE A., WERNER J.; Arapree, The Prestressing Element composed of Resin Bonded Twaron Fibres, HBG-Akzo brochure, september 1988.

Proper Use of High-Alumina Cement Concrete

Utilisation correcte d'un béton avec un ciment à haute teneur en aluminates

Korrekte Verwendung eines Betons mit Hochtonerdezement

Kesete GABREKIDAN
Professor
Garyounis University
Benghazi, Libya

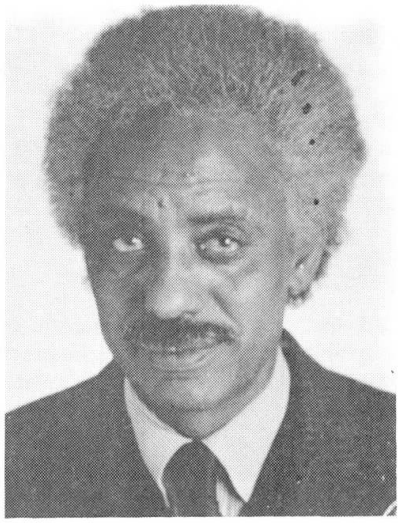

Kesete Gabrekidan, born in 1937 obtained his first degree in Civil Engineering, Addis Ababa University Ethiopia, M. Sc. University of Cincinatti U.S.A. and PhD, University of Bradford, UK. He was involved in special railway-highway bridge design for Atkins & Partners and was senior structural engineer for George Wimpeys Laboratories, UK and for a long period of time on the Addis Ababa University staff.

SUMMARY

After a two year period of storage, the reduction in HACC (High-Alumina Cement Concrete) compressive strength, indicated zero and 50% for normal and dry curing conditions respectively. Full conversion after 7 days hot water storage produces a 25% strength reduction. Under normal curing conditions, the flexural strength developed increased at a curing temperature of 22.5 °C as compared to the standard 18 °C. Shrinkage in HACC is of the same order as that of PCC (Portland Cement Concrete) for similar storage periods, while swelling is independent of storage temperature. In slow converted specimens, creep is dependent on the mineralogy or morphology of the hydrates, while full conversion leads to the same order of creep as PCC.

RÉSUMÉ

Après un temps de stockage de deux ans, la réduction de résistance à la compression du béton HACC a atteint zéro et 50% pour des conditions de conservation du béton normales, respectivement à sec. Un changement complet après 7 jours de stockage en eau chaude donne une réduction de résistance de 25%. Dans des conditions normales de conservation la résistance à la flexion qui se développe a augmenté à une température de conservation de 22.5 °C, comparée à la température normale de 18 °C. Le retrait dans le béton HACC est du même ordre que celui observé dans le béton CP pour un même temps de stockage, alors que le gonflement n'est pas affecté par la température de stockage. Pour les spécimens à changement lent, le fluage dépend de la minéralogie ou morphologie des hydrates alors qu'un changement complet mène au même ordre de fluage que le béton CP.

ZUSAMMENFASSUNG

Nach einer Lagerungszeit von zwei Jahren , erwies sich der Abfall der Druckfestigkeit von Hochtonerdezement als Null und jeweils 50% für normale wie trockene Erhärtungsbedingungen. Vollständige Umwandlung nach 7 Tagen Warmwasserlagerung erbringt eine 25%ige Festigkeitsreduktion. Unter normalen Erhärtungsbedingungen nahm bei einer Erhärtungstemperatur von 22.5 °C im Vergleich zu der Standardtemperatur von 18 °C die entwickelte Biegefestigkeit zu. Bei ähnlichen Lagerungszeiträumen erfolgt Schrumpfung des Hochtonerdezements in gleichem Umfang wie für Portlandzementbeton, während die Quellung von der Lagerungstemperatur unabhängig ist. Bei langsam erstarrenden Proben ist die Kriechdehnung von der Mineralogie oder Morphologie der hydraulischen Bindemittel abhängig, während das vollständige Erstarren zu gleichen Kriechdehnungen wie bei Portlandzementbeton führt.

1. INTRODUCTION

High-alumina cement is produced by heating a mixture of limestone and bauxite to fusing, which quickly attains a very high strength and is in its original form sulphate resistant. At hydration meta-stable aluminates are found at normal temperature and humidity crystalizing in hexagonal form which in turn transforms into a stable cubic compound. Such chemical transformation, depending on intensity of temperature and humidity, induce reduction in volume of gel and increase porosity, termed as "conversion", resulting in strength reduction.(1)
Research that went into high-alumina cement (HAC) was rather unimpressive, to say the least, and consequently code provision accorded by CP114, CP116 and CP110 to HAC in buildings was rather unsatisfactory and misleading. The highlight of this, among other things, was the collapse of two beams of the roof over the swimming pool of Sir John Cass Red Coat School at Stepney, London.(2). Consequently, the part relating to HAC in CP110 was deleted in 1974. With this realization the author conducted intensive studies from 1975 onwards on the subject with special emphasis to prestressed concrete out of which a portion is hereby presented.

2 CONCRETING AND INSTRUMENTATIONS

Short and long-term studies of standard tests running to maximum two and a half years on cylinders, cubes and flexural prismatic beams were made using destructive and non destructive tests. To simulate different environmental conditions, the following curing storages were procured: normal curing (21.5°C and 90-95%RH), dry curing (18°C and 45%RH) and hot-water curing (45°C and 100%RH). One day after cast in an open laboratory area (temperature varying from 7°C to 27°C) the specimens were carried to respective storage regimes.
A 100mm x 100mm x 1000mm prismatic beam steel moulds, fabricated at the School of Civil and Structural Engineering Dept., University of Bradford, UK, were prepared for making shrinkage and/or swell and creep specimens. Shrinkage and creep rigs, fitted with electrical and mechanical measuring devices to avoid instrumentation breakdown, were also designed and fabricated to suit storage conditions.
A mix design, 1:1.6:3, with free W/C ratio of 0.35, aggregate cement ratio of 4.6, compaction factor of 0.78 and cement content of 4100 n/m^3 of concrete was employed throughout the experimental period. The overall grading of aggregates, as suggested by Newman (3), conformed to zone No 2. d.t.a. tests were run periodically to determine the degree of conversion for the various storage regimes. Petrological analysis on sands, for possible presence of soluble alkalis, and spot checks on British brand HAC chemical composition were also performed.

3 TEST-RESULT ANALYSIS AND CONCLUSIONS

3.1 Compressive strength.

The 24-hour strength was nearly the same for all concrete cast, with mean strength of 82.8N/mm^2. Fig.1 indicates the strength - storage time curves for all regimes.

3.1.1 Normal storage: specimens stored in wet room, with indicated ambient conditions, reveal an increase in strength development except in a situation where slow conversion

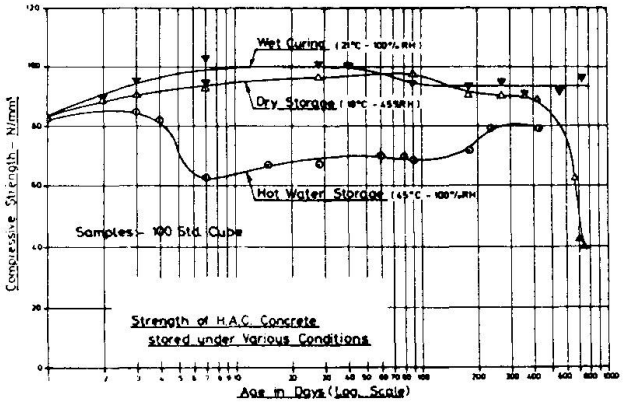

FIG. 1

takes place the fall is followed by strength recovery emanating from rehydration of the unhydrated cement. Such phenomenon persists for a length of time until the chemical reaction is complete. That is to say a cyclic behaviour, characterised by sag and hop; dominates until the hexagonal aluminates (CAH_{10}) complete transformation into the more stable cubic aluminates (C_3AH_6) is restored. It follows that such sluggish conversion does not lend itself to appreciable reduction in strength; evidently not lower than the 24-hour strength.

3.1.2 Hot water storage: specimens stored in hot-water tanks indicate slight increase in strength up to 3 to 4 days and a rapid fall is recorded after 7-8 days. Full conversion time can be estimated using Fig.2, curing temperature versus time required for specimens to reach full conversion. The curve is (Fig.1) then picks up strength gradually, a clear indication of rehydration followed by conversion of the fresh hydrated cement. The maximum observed loss of strength is in the range of 25% of the 24 hour strength. Hence steam curing could offer the best solution if HAC is employed in buildings for tropical climate.

FIG. 2

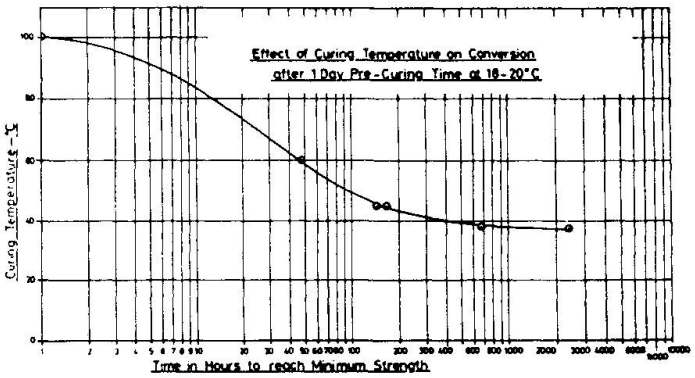

3.1.3 Dry storage: Specimens stored in dry conditions, Fig 1, received the most damage. After 400-day storage in dry room rapid deterioration without sign of strength recovery is observed. After 750 days the compressive strength was reduced to 50% of the 24 hour strength. Deterioration of high-alumina cement concrete, as some researchers claim, cannot always be attributed to conversion. In this particular case, after one day curing in an open laboratory area, specimens were stored in dry room. It is expected that, with the harsh mix the specimens received and denied of the proper curing for the crystals to mature, strength development to full capacity would be far remote. It is also possible, due to severe specimen exposure they may have lost some of the water of hydration vital to matured crystal formation. Destructive tests showed that bond between paste matrix and gravel was exceedingly weak with subsequent loss in strength. The degree of conversion obtained for these specimens also supports that conversion alone had little to play in the deterioration.

3.2 Flexural strength of Standard Prismatic Beams.

Fig.3 shows flexural strength versus time curves for all storage regimes. These curves are similar in shape as that given by Fig.1. The significant change occurs for normal storage condition in which strength development is more pronounced than the remaining storage regimes. This leads to the conclusion that normal curing temperature for HACC can best be established at about 22°C in lieu of the accepted standard of 18°C.
The trend of the curve for normal storage for indirect tensile strength, other things being equal, has a diminishing character than the 24-hour strength. This is contrary to the flexural strength development under similar storage conditions. However such reduction of strength does not raise alarm as there is appreciable strength reserve for design purposes. It is is also interesting to note that the mean Poisons' ratio falls
in the range of 0.15.

3.3 Shrinkage

To assist, compare and contrast, Fig.4 is prepared based on total length. When specimens are stored at low relative humidity, 45%, the shrinkage time curve is smooth and continuous up to 295 days; similar shape as in Fig.1 for the same storage regime. Strength reduction is followed by shrinkage reduction as indicated in Fig.4. Such behaviour affords the following explanations:

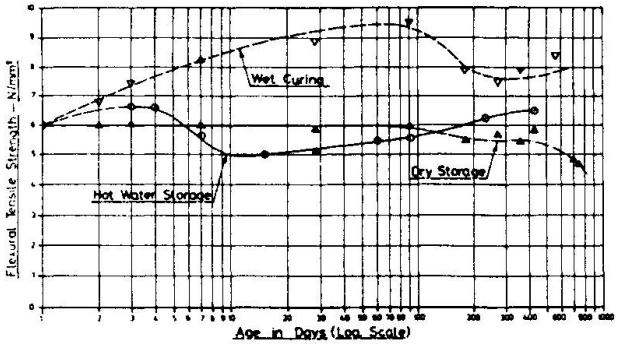

Flexural Strength of H.A.C. Concrete stored under Various Conditions

FIG. 3

1. In the absence of proper curing to achieve crystal maturity, the bond between paste matrix and gravel is weakened thereby partly relieving the restrain; offered by gravel in the shrinkage mechanism.

2. The occurence of conversion, depending on exposure conditions, allows similar mechanism as that of item 1. It can safely be concluded that, unlike Portland cement concrete (PCC) where conversion prevails or proper curing is denied for crystals to mature, shrinkage is not only retarded by also reduced by some margin. The maximum shrinkage value obtained in this research project after 500 days storage was in the vicinity of 350×10^{-6}. If we assume 66 to 85% of the 20 year shrinkage occurs in one year, this will yield 413×10^{-6} in 20 year period comparable to PCC.

FIG. 4

3.4 Swell

Consider for instance specimens stored in hot water tanks (Fig.4). The diminution of strength (Fig.1) is met to some extent by corresponding increase in swelling. As the strength recovery gradually takes charge swelling starts to retard. Second cycle of conversion will induce corresponding increase in swelling until the reaction ceases and the curve levels. The same reasoning is afforded to normal curing depending on rate of conversion. In general it can be concluded that while conversion reduces on one hand the net value of shrinkage, it promotes swelling on the other. The magnitude of swelling is irrespective of storage temperature and stands in the vicinity of 450×10^{-6}; greater than shrinkage value which runs contrary to L'Hermite's' research data on PCC.

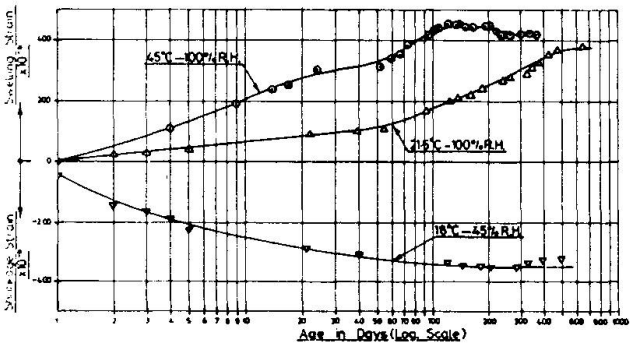

Shrinkage-Time Relationship for Samples stored under Various Conditions

3.5 Creep

Unlike PC, the subject of creep in HAC is the most neglected area of research. A limited amount of research investigations(4) had been published. Glanville showed that the age of loading, other things being equal, has large effect on creep; slower start at earlier stage and an increasing trend at latter stage. This was also confirmed by the author for dry storage conditions.

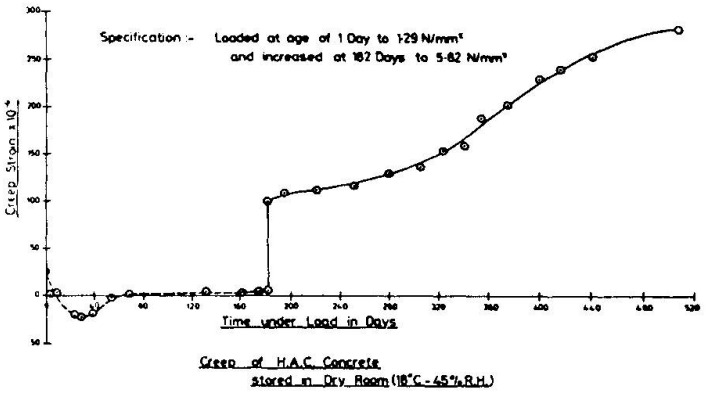

FIG. 5

3.5.1 Dry storage (Fig.5): The specimen was loaded to 13640N (1.29N/mm^2) until the age of 182 days. The curve in Fig.5 shows that creep becomes lower than the elastic deformation confirming Glanville's findings. At the age of 182 days, the sustained load was brought to 61340N (5.82 n/mm^2). The rate of creep progress is again sluggish up to 250 to 280 days and from there on creep increased at higher rate. After 400 days, creep deformation tends to achieve final value.

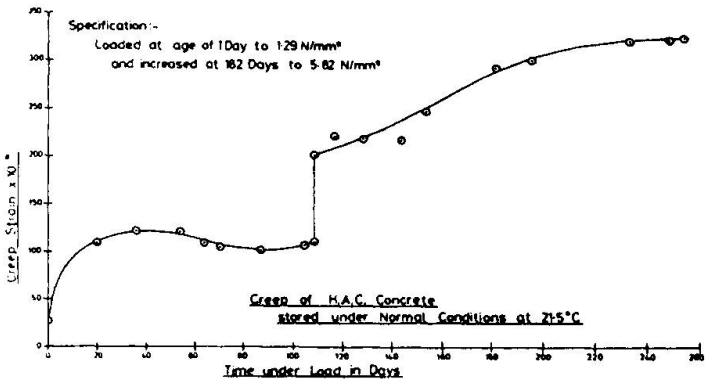

FIG. 6

3.5.2 Normal storage (Fig.6): specimens in this storage conditions were loaded to 13640N after one day cast and increased to 61340N at the age of 110 days. There appears a tendency for creep in dry storage to be less than in wet condition confirming Glanville's findings that the behaviour is organismically different from PCC. After 240 days, a slow increasing trend is observed.

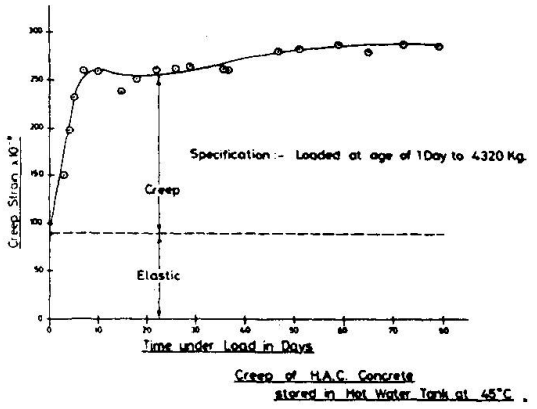

FIG. 7

3.5.3 Hot water storage (Fig.7): specimens were loaded to 43200N at the age of one day. The curve is more uniform than those discussed earlier admitting similarities to PCC creep behaviour.In other words full conversion from meta-stable compound (CA H10) to the stable compound (C_3AH_6) alters the behaviour in the creep-time curve. It follows that while porosity is a function of strength diminution, creep is dependent on the mineralogy or morphology of the hydrates formed. On the other hand at slow conversion HAC is organismically different from creep behaviour of PC while accelerated full conversion, before loading at best, offers similar behaviour as that of PC.

4 REFERENCES

1. Midgley, H.G., "Mineralogy of set HAC", transactions, British Ceramic Society, Vol.66, No4, 1967, pp 161-187.
2. Department of Environment, "HACC in Buildings", BRA 11068/2, 2nd January 1975, 3pp.
3. Newman, K., "Design of concrete mixes with HAC", R/c Rev., vol.5, No 5, March 1960, pp269-294.
4. Glanville, A.M., Glanville, Etal, "Creep or flow of concrete underload", S.I.R., London, Building research Technical Papers Nos 12 and 21, 1930 and 39, pp 39 and 34.

Role of Cement in Sulphate Attack of Reactive Aggregate Mortars

Rôle du ciment dans l'attaque de mortiers à aggrégats réactifs par les sulfates

Rolle des Zementes beim Sulfatangriff auf reaktive Mörtel

A. de SOUSA COUTINHO
Civil Engineer
LNEC
Lisbon, Portugal

Sousa Coutinho, born 1919, obtained his civil engineering degree at the Technical University of Lisbon, and is now Senior Research Officer and Head of the Building Materials Department of the National Laboratory for Civil Engineering.

Arlindo GONÇALVES
Civil Engineer
LNEC
Lisbon, Portugal

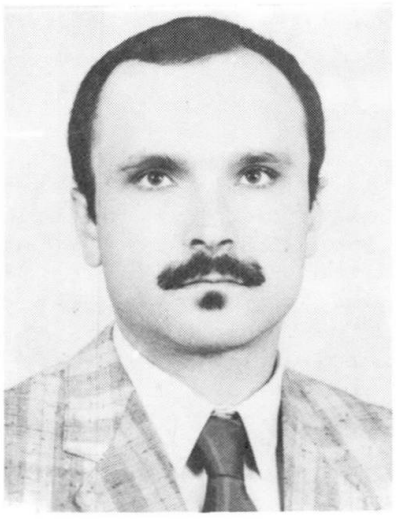

A. Gonçalves, born 1953, obtained his civil engineering degree at the Technical University of Lisbon, and is now Research Officer of the Concrete and Binders Division of the National Laboratory for Civill Engineering.

SUMMARY

This paper presents results of the influence of cement type on the durability of mortars made with sulphate reactive aggregates in a calcium hydroxide saturated medium, and kept under sea water after different curing periods. The observations, some of them over a period up to 20 years have enabled the authors to classify the resistance of the different cement types to sea water attack, when reactive aggregates are used.

RÉSUMÉ

On présente des résultats concernant l'influence du type de ciment sur la durabilité des mortiers préparés avec des agrégats réactifs aux sulfates dans un milieu saturé d'hydroxyde de calcium, et maintenus immergés dans l'eau de mer après différents temps de cure. L'observation, qui en quelques cas s'est prolongée pendant 20 ans a permis de classer la résistance des différents types de ciment à l'attaque de l'eau de mer lorsqu'on utilise des agrégats réactifs.

ZUSAMMENFASSUNG

Dieser Beitrag behandelt den Einfluss der Zementart auf die Beständigkeit des Mörtels mit sulfatreaktiven Zuschlagstoffen in einem mit Kalkhydroxid gesättigten Medium. Die untersuchten Bauelemente wurden dem Meerwasser ausgesetzt. Es wurden verschiedene Behandlunsperioden mit Beobachtungszeiten bis zu über 20 Jahren durchgeführt. Es war möglich, die verschiedenen Widerstände der untersuchten Zemente und der reaktiven Zuschlagstoffe bezüglich der Angriffigkeit des Meerwassers festzustellen.

1. INTRODUCTION

All research in the area of sulphate attack is based on formation of ettringite as a result of reaction between sulphates and C_3A present in portland cements. The ettringite formation can, however, take place without the presence of C_3A, if the reactive alumina for the formation of ettringite is provided by the aggregate [1]. When an aggregate contains kaolinized feldspar, the alumina from the aggregate reacts with sulphates, forming ettringite. The ettringite formed will be expansive as long as the reaction of alumina with sulphate takes place in a medium oversaturated with calcium hydroxide [2].

A concrete dock structure of Leixões Harbour, in the north of Portugal, built in 1940, suffered large expansions and cracking 6 months after the original installation. It was not until 15 years later that a proper explanation for the failure could be found in reactions involving sea water and the weathered feldspar of the aggregate.

With the same aggregates used in that structure, a study was undertaken to compare the resistance of different types of cements to the formation of expansive ettringite, on mortar prisms maintained under sea water in laboratory, after previous curing which varied from 2 days to 1 year. The specimens were subjected to visual inspection for detecting fissures and to length change measurements. The correlation between the Fratini test results and the behaviour of the mixes of portland cement and pozzolan are also discussed.

2. EXPERIMENTAL

The chemical analysis and some physical characteristics of cements and pozzolanas used are described in tables 1 and 2. There are no elements about the portland cement type V, according to ASTM, with exception to C_3A content that was 4.5%. The pozzolanic cement used was a ferric-pozzlanic one, from Italy. The compressive and flexural strengths were determined using prisms with 4 cm x 4 cm x 16 cm; the strength of pozzolanas was measured in pastes of standard consistency with 1 part of lime and 3 parts of pozzolan, by mass.

The pozzolana named Cape Verde is a natural one, existing in the Republic of Cape Verde. Kaoline and diatomite were activated by calcination at 850°C.

The granite, composition of which is presented in table 3, was sieved between 0.8 and 0.4 mm, the grading that has already shown to produce the most rapid alteration of the mortars.

The mortars consisted of 1 part of cementious material, 5 parts of crushed weathered granite sand and 1 part of water, by mass. When using pozzolanas, the cementious material was composed of portland cement and different percentages of pozzolana, varying from 0% to 50%. The mortars were hand mixed and the prisms with 4 cm x 4 cm x 16 cm were also hand consolidated. For each condition, 2 prisms were molded.

The prisms were kept in the molds, in a fog room, for 48 h, and then were either immediately immersed in small plastic tanks filled with sea water, or they were air-cured in the laboratory for 7 d, 28 d, 90 d and 360 d, before immersion. As sea water was encrusting, the protective layer of calcium carbonate was frequently

removed. In the same way, as the pH of the water went up quickly after the contact with the prisms, specially when the prisms were not air-cured, the sea water was also replaced. All the procedures are fully described in an earlier publication [3].

The Fratini test [4] was carried out on pozzolanic cement and on mixes of portland cement and pozzolana.

Cements	SiO_2	Al_3O_3	Fe_2O_3	CaO	MgO	SO_3	K_2O	Na_2O	I.loss
Portland	20.0	6.9	3.5	62.9	2.4	2.1	0.7	0.0	1.5
High alumina	5.5	40.4	16.0	36.6	0.6	Vest.	---	---	0.9
Pozzolanic	29.2	17.0		44.1	2.0	1.1	0.9		5.0
Natural	22.2	6.0	2.6	53.3	3.2	3.6	---	----	7.5
Slag	28.1	7.3	2.1	52.0	4.1	2.3	0.8	0.2	1.6

Pozzolanas	SiO_2	Al_3O_3	Fe_2O_3	CaO	MgO	SO_3	K_2O	Na_2O	I.loss
Cape Verde	49.5	20.2	2.3	1.9	1.7	0.3	5.2	6.2	12.8
Kaoline	52.3	33.2	1.3	0.0	Vest.	0.0	3.6	1.1	8.2
Diatomite	81.0	3.1	4.8	0.5	0.0	0.9	0.4	0.8	10.0

Table 1 Chemical analyses of cements and pozzolanas

Cements and Pozzolanas	45 μm sieve residue %	Surface area Blaine cm^2/g	Mortar or paste strength, MPa			
			Compressive 7 d	28 d	Flexural 7 d	28 d
Portland	----	4270	25.2	35.4	5.3	6.9
High alumina	----	3250	65.5	69.6	6.7	7.4
Pozzolanic	21.1	4430	6.7	19.5	2.0	4.4
Natural	----	4930	4.1	7.5	1.3	2.3
Slag		3800	20.7	33.8	5.2	7.9
Cape Verde	48.0	4270	4.6	10.3	2.0	3.8
Kaoline	15.3	10472	0.6	7.7	0.3	3.6
Diatomite	10.1	23100	2.5	12.6	1.0	3.0

Table 2 Physical characteristics of cements and pozzolanas

Constituents (% by mass)				
Plagioclase	Alkaline feldspar	Quartz	Muscovite	Other minerals
36.6	20.4	31.5	13.0	0.7

Table 3 Composition of weathered granite

3. RESULTS AND DISCUSSION

Results and their discussion will be mainly based on the number of prisms not disrupted, once it was observed that the measured expansion was not a good reference: some prisms cracked under little expansion, others did not crack under high expansion levels.

3.1 Cements

Table 4 presents, for each cement, the number of prisms not disrupted, as a function of the curing time, as well as the time of disruption of the others, that is, the time when a visible crack was recorded.

As shown, the best performance was achieved with natural cement, followed by the pozzolanic one from Italy. According to the theory set out in an earlier publication [2], expansive sulphoaluminate forms only in the presence of calcium hydroxide oversaturated solutions. Therefore, natural cement, with a composition close to that of hydraulic lime, without C_3S and C_3A, does not originate that kind of solutions and so expansive ettringite. The pozzolanic reaction explains the performance of the pozzolanic cement.

The most surprising results were obtained with high alumina cement, usually considered as resistant to sulphate attack. The results are yet more surprising, because other prisms made with not weathered granite evidenced fissuration earlier. It is difficult to find an explanation; maybe this cement does not work well with aggregates of acid nature. Curing time did not change the performance of the cement owing to absence of lime to be hydrated.

Slag cement seems to have excellent performance, on account of results until 7 years, which are compared in fig. 1 with those of a mix of portland cement and 50% of pozzolana, by mass, which showed very good behaviour, as will be seen later. In the two cases the prisms were immersed in sea water 48 h after casting.

3.2 Mixes of portland cement and pozzolana

Table 5 shows, in the same way, the number of prisms disrupted and time until disruption, depending on time of curing and percentage of pozzolana added to cement.

Increasing the percentage of pozzolana, the durability of mortars is also increased: with 40% or 50% of pozzolana, total protection from sulphate attack is obtained, even with 48 h curing. Nevertheless, with other less reactive pozzolanas, the curing time may have to be increased in order to get similar results.

Diatomite was the best pozzolana used, maybe owing to its great surface area. One of the prisms made with the pozzolana of Cape Verde, cured for 7 d, cracked after 6 years approximately, which is thought to be an exceptional result.

3.3 Curing time

The idea behind the consideration of different times of curing was determining the minimum period of cement hydration or pozzolanic reaction to obtain the necessary chemical resistance. As shown in tables 4 and 5, this period depends on the type of cement or on the percentage of pozzolana: it is possible to get good results with only 48 h curing, though increase to 7 or 28 d is always beneficial.

The most salient aspect was total protection obtained when the cure had a duration of 1 year, even for portland cement. As a matter of fact, after 6 months all prisms were completely carbonated, without free calcium hydroxide, which avoided the formation of expansive ettringite. At 7 d, 28 d and 90 d, the depth of carbonation was 2 mm, 7 mm and 14 mm, respectively.

Cements	Prisms not disrupted					Time of disruption, years				
	48 h	7 d	28 d	90 d	360 d	48 h	7 d	28 d	90 d	360 d
Portland	0	0	0	0	2	0.4	2.2	1.2	6.0	>22
High alumina	0	0	0	0	0	4.4	4.3	4.0	2.1	3.1
Pozzolanic	0	0	2	2	2	5.7	6.2	>22	>22	>21
Natural	0	0	2	2	2	12.4	16.3	>22	>22	>21
Slag	2*	-	-	-	-	>7.0	---	---	---	---
Type V	0	-	-	-	-	0.8	---	---	---	---

Table 4 Behaviour of cement mortar prisms as a function of curing time

Pozzolanas	Time of curing	Prisms not disrupted					Time of disruption, years				
		10%	20%	30%	40%	50%	10%	20%	30%	40%	50%
Cape Verde	48 h	0	0	0	1	2	0.9	2.9	5.9	8.9	>23
	7 d	0	0	2	2	1*	3.8	5.2	>23	>23	6.6*
	28 d	0	0	0	2	2	4.0	5.2	5.9	>23	>23
	90 d	0	2	2	2	2	7.2	>23	>23	>23	>23
	360 d	2	2	2	2	2	>22	>22	>22	>22	>22
Kaoline	48 h	0	0	0	2	2	0.5	0.5	13.2	>18	>18
Diatomite	48 h	0	0	2	2	2	1.5	4.2	>17	>17	>18

Table 5 Behaviour of cement and pozzolana mortar prisms as a function of the percentage of pozzolan

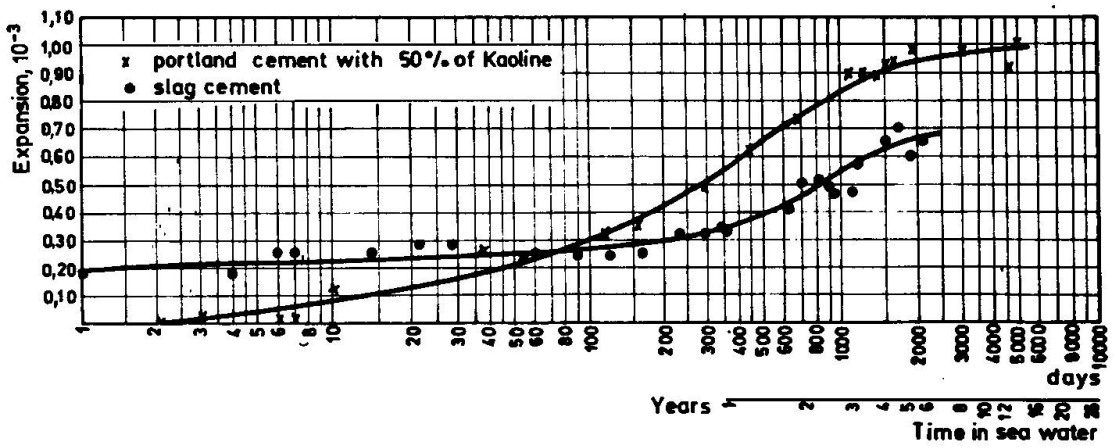

Fig. 1 Expansion of prisms made of two cementious materials

3.4 Fratini test

The Fratini test results were not conclusive to foresee the behaviour of the mixes of cement and pozzolana. Clearly pozzolanic mixes, according to this test, did not show good performance with short curing time. It is believed that the pastes for test should be kept at the same temperature of mortars and tested at the age of their contact with the aggressive medium, so that correlation can be possible. In the standard test the pastes are kept at 40°C for 7 d, which gave rise to an acceleration of the pozzolanic reaction.

4. CONCLUSIONS

The cement that exhibited better performance was the natural one, followed by the ferric-pozzolanic cement: a curing period of 28 d gives total protection against sulphate attack, with this kind of aggregates. With a short cure, 48 h, only slag cement seems to give this protection. High alumina and type V cements did not show good performance.

With an adequate percentage of pozzolan in the mix with portland cement, it is possible to get total protection, even with only 48 h of cure. In the pozzolanas tested, this percentage varied from 30% to 50%.

A curing period of 48 h may be enough for total protection, but increasing it is always advantageous.

The Fratini test does not give information about the behaviour of mixes of portland cement and pozzolana: clearly pozzolanic mixes did not provide total protection with the shorter curing period.

REFERENCES

1. COUTINHO, A. S., Influence de la Nature Minèralogique de l'Agrègat sur la Dècomposition des Mortiers et Bètons de Ciment Portland Exposès à l'Eau de Mer. Cahiers de la Recherche, nº27, Ed. Eyrolles, Paris, 1968.

2. COUTINHO, A. S., Aspects of Sulfate Attack on Concrete. Cement, Concrete and Aggregates, vol. 1, nº 1, 1979.

3. COUTINHO, A. S., Studies on the Resistance of Cements and Pozzolanas to Sea Water Attack. Ed. by LNEC, in Portuguese, Lisbon, 1982.

4. FRATINI, N., Controllo Chimico dei Cementi Pozolanici. An. di Chim., vol. 44, September 1954.